

The Synthesis of Tripnictide Macrocycles based on a Benzannulated Core

By Julia Johnstone

UMI Number: U584671

All rights reserved

INFORMATION TO ALL USERS

The quality of this reproduction is dependent upon the quality of the copy submitted.

In the unlikely event that the author did not send a complete manuscript and there are missing pages, these will be noted. Also, if material had to be removed, a note will indicate the deletion.



UMI U584671

Published by ProQuest LLC 2013. Copyright in the Dissertation held by the Author.
Microform Edition © ProQuest LLC.

All rights reserved. This work is protected against
unauthorized copying under Title 17, United States Code.



ProQuest LLC
789 East Eisenhower Parkway
P.O. Box 1346
Ann Arbor, MI 48106-1346

Abstract

This thesis focuses on the synthesis of novel tripnictide macrocycles facilitated by a relatively unexplored dehydrofluorinative synthetic methodology involving the formation of a P-C bond and concomitant removal of HF from precursor complexes containing ortho-fluorophenyl phosphines and adjacent primary phosphines.

The first example of a template ($\text{CpFe}^+/\text{Cp}^*\text{Fe}^-$) synthesised triarsenic macrocycle has been isolated in excellent yields along with its analogous tribenzannulated triphosphorus counterpart. Similar dibenzannulated and monobenzannulated tripnictide macrocycles have also been prepared.

An expansion of this mechanism has allowed the synthesis of mixed donor macrocycles that previous to this research were unknown.

The same synthetic procedure has been adapted to facilitate the synthesis of novel bimetallic complexes incorporating both phosphorus and arsenic donors.

Acknowledgements

I would like to thank Pete for his advice and supervision over the last three years (and the trip to Corfu!).

This thesis wouldn't have been possible without the help, advice and infinite patience of Woody, Gimp for introducing me to 'proper' chemistry, Boycey for his endless companionship at the pub, Dongmei for her kindness, Thomas for his supervision albeit brief, Ben, Adam, Wenjian, Eli, Becky, Peter, Rajika and Natalie for their hard work in contributing to the lab., Dan for losing so gracefully at pool!, Markus and Mark for their good humour, Marcus for his firefighting abilities and the people who have made this Ph.D. worth doing, for their support and friendship as well as Sam despite my endless problems who was always there to lend advice.

I'd also like to thank the technical staff especially Rob for coaxing the NMR machine into action and rescuing swallowed samples, John for having to continually fill out accident reports about me, Steve and Robin for their tireless work in stores, and Sue for organising Pete's desk. Many thanks must also go to Ricky for all of the amazing glassblowing that he's done over the last few years, Sham for his often futile and unappreciated work on the mass spec. machine and Al. for fixing pumps and being so entertaining especially while teaching me how to weld.

For advice about the endless (seemingly) ways to synthesise oxazolines I'd like to thank Mark Elliott for his advice, and for helping with both NMR's and supplies of chemicals Simon.

Finally, none of this would have been possible without all of my friends and family, Just. for encouragement and many welcome trips to the pub., Farah and Rajinder for their friendship, Iain, Gran and Mum for their love and support and Bob for his inspiration and love, I couldn't have written this without his wit (debatable!) and dedication to making me write this up.

This thesis is dedicated to my Dad who I loved so much, I only wish he was here to read it, I hope he would be proud.

Thomas William Johnstone

7 August 1943 – 14 July 1997

Contents Page

Chapter	Description	Page Number
	Declaration	i
	Abstract	ii
	Acknowledgements	iii
	Contents Page	iv
	<u>Introduction</u>	1
1	General Phosphine Chemistry	2
1	Macrocyclic Ligands	9
1	What makes Macrocycles so Robust?	12
1	Why are Triphosphorus Macrocyclic Ligands of Interest?	16
1	Aim of this Research	18
1	Previously Known Tridentate Phosphorus and Arsenic Macrocycles	19
1	Synthesis of Triphosphorus and Triarsenic Macrocycles	20
1	Macrocyclic Constituents	24
1	Demetallation	28
1	References	31
	<u>Benzannulated, Dibenzannulated and Tribenzannulated Macrocycles</u>	33
2	Introduction	34
2	Results and Discussion	36
2	Variable Temperature NMR Spectroscopy	53
2	Crystal Structures	56
2	Electrochemical Studies	63
2	Conclusions	65
2	Experimental	68
2	References	90
	<u>Bimetallic Complexes</u>	91
3	Introduction	92

3	Results and Discussion	97
3	Conclusions	101
3	Dimacrocylic Preparation	102
3	References	111
	Appendix	112

Chapter 1

Introduction

Introduction

Reducing the energy requirements of industrial processes could make a major contribution to the efficient use of the world's limited petrochemical and fossil fuel resources. This objective is being pursued by the development of molecular catalysts, often involving metal-phosphine complexes, to carry out extremely efficacious and specific chemical transformations.

There has been considerable interest in the chemistry of metal-phosphorus compounds, because of their ability to stabilise unusual co-ordination environments and oxidation states of transition metals. The control that these abilities allow over the co-ordination sphere of the metal, with the consequent influences on reactivity that result, may be of use in applications such as homogeneous catalysis.

Phosphine ligands also allow the manipulation of the electronic environment and reactivity patterns of metal complexes. This is especially important for the promised, and sometimes proven, versatile co-ordination chemistry and catalytic activity of these complexes. By developing synthetically more flexible strategies to make chelating agents bearing tertiary phosphine donors it is possible to expand their chemical capabilities. Phosphorus(III) ligands are extensively used in organic syntheses, organometallic chemistry and catalysis.

Macrocycles with rigid, non-collapsible unsaturated carbon backbones have attracted great interest in the past few years due to their novel properties and potential applications in synthesis and catalysis (*e.g.* asymmetric hydrogenation).

As well as their potential as precursors to homogeneous catalysis, triphosphorus macrocycles can act as neutral, tridentate, six electron donor ligands. The phosphorus groups within the macrocycle can be easily manipulated and the constituents of the macrocycle can be adjusted to alter the metal ions' reactivity.

General Phosphine Chemistry

Phosphines as Ligands

Tertiary phosphines are one of the few series of ligands in which both the steric and the electronic properties of the ligands can be changed in a systematic and predictable way by varying the nature of R. Tertiary phosphines stabilise a wide

form a σ -bond (Figure 1.1). Phosphines are also good π -acids which means that they readily accept electron density into the P-C σ^* -orbitals via a back bonding interaction (Figure 1.1). The π -acidity of phosphines increases from alkyl < aryl < alkoxy due to the ligands increasing electrophilicity.

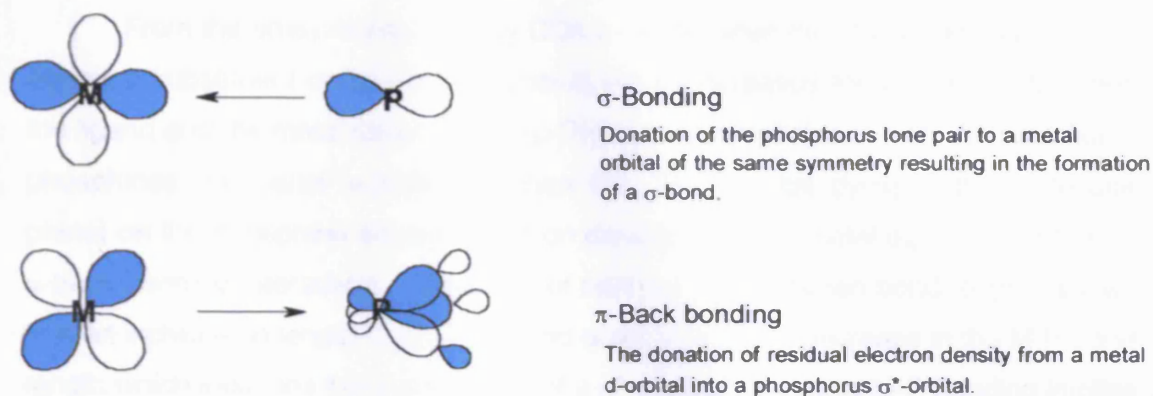


Figure 1.1 Metal phosphine bonding.

Phosphines are one of the most widely used ligands in coordination chemistry. The fine tuning of the properties of transition metal complexes can be achieved by varying the nature of the phosphine. Introduction of functional groups close to the phosphorus atom change the donor properties of the phosphorus ligand, for both steric and electronic reasons and accordingly change their co-ordinating ability towards metal centres.¹ Phosphines act as traditional Lewis bases (donating electrons to a metal) or ligands in transition metal complexes. The strongest bonds exist between phosphines with the highest Lewis basicity and metals with the highest Lewis acidity.

By comparison between various complexes containing phosphines (PH_2R , where $\text{R} = \text{H}, \text{CN}, \text{F}, \text{NH}_2, \text{OH}$) coordinated to Pt (along with two PH_3 ligands) it has been shown that the σ -type ligand to metal donation is strong because of the large overlap in participating orbitals. The stabilising effect of this donation can be diminished by repulsive interactions between filled orbitals on the ligand and occupied orbitals located on the metal. Charge decomposition analysis²(CDA) allows a detailed study of bonding between ligands and metals within complexes. It takes into account information about donation, back-donation and repulsive interactions through parameters including the mixing of filled orbitals of the ligand with both the filled (repulsive) and unfilled (attractive) orbitals of the metal containing fragment and the mixing of the unfilled orbitals of the ligand with both the filled (attractive) and

filled (repulsive) and unfilled (attractive) orbitals of the metal containing fragment and the mixing of the unfilled orbitals of the ligand with both the filled (attractive) and unfilled (residual term) orbitals of the metal containing fragment. CDA has already been proven to be a valuable tool in the analysis of ligand-metal interactions³ although it has not been extended to encompass macrocyclic ligands to date.

From the analysis provided by CDA it can be seen that the introduction of a π -donating substituent on to the phosphorus centre increases the interaction between the ligand and the metal fragment ($\text{NH}_2 > \text{OH} > \text{F}$) with respect to $\text{R} = \text{H}$. All substituted phosphines are better π -acceptors than PH_3 , a σ^* -orbital (lying in the molecular plane) on the phosphine accepts electron density from the metal d_{xy} orbital to form a π -back bonding interaction. The study of relationships between bond lengths shows that an increase in length of the P-R bond gives a resulting decrease in the M-P bond length which indicates the involvement of a σ^* -orbital.⁴ Stronger M-P bonding implies more M-P π -bonding which populates the σ^* orbital in the P-R bond and therefore weakens the bond. Backbonding can be studied for individual phosphine ligands by synthesising complexes with carbonyl ligands trans to this phosphine ligand. The infra red stretching frequency of the carbonyl groups indicates the co-ordination environment of the phosphine ligand involved. As the phosphine ligand becomes a better σ -donor and π -acceptor the ligands trans to them have longer (and typically weaker) bonds to the metal. In consideration of the suitability of a phosphine ligand, their Lewis basicity is a useful property to manipulate in the design of a suitable ligand.

The bonding in simple complexes and especially the effects of ligand substituents on both σ -donation and π -backbonding is difficult to predict, the substituents on phosphines in particular have a great effect on the metal-ligand interactions.

The quantitative analysis of ligand effects (QALE), utilises four properties to determine the stereoelectronic parameters of phosphorus ligands namely, the donor capacity of the ligand χ_d , Tolman's cone angle θ , the aryl effect parameter E_{ar} and the π -acidity parameter π_p , which can be used to give a better idea as to the type of bonding between a phosphorus containing ligand and the metal fragment.⁵ The electronic environment around the metal atom is influenced by the σ -basicity and the π -acidity of the phosphorus ligands. In bonding with transition metals, the back bonding to the P-C σ^* -orbitals⁶ produces a synergistic increase in its σ -basicity. Forward σ -donation and π -back donation both increase the s-electron density at the metal nucleus and as the back bonding increases, more d-electron density is driven

from the metal to the ligand orbitals which makes oxidation more difficult. Therefore oxidation potentials increase with increasing π -backbonding.⁷ More electronegative and arylated R functions will lower the energy of the P-C σ^* -orbitals and facilitate back donation.

R-Group	Ligand σ -donation kJ/mol	Metal-Ligand π -backbonding kJ/mol	σ -donation/ π -backbonding	Filled orbital interaction kJ/mol	Residual term kJ/mol
H	0.38	0.23	1.67	-0.52	0.02
CN	0.35	0.29	1.2	-0.53	0.02
F	0.46	0.34	1.35	-0.36	-0.04
NH ₂	0.49	0.27	1.78	-0.44	0.01
OH	0.47	0.3	1.53	-0.45	0

Table 1.1 The effect of the R-group functionality on metal-ligand bonding.

Bite Angle Effects

There are several factors that must be taken into account when looking at bite angles, the Tolman parameters (θ the cone angle, and χ the electronic parameter),⁸ are used to assess the steric and electronic properties in monodentate phosphine ligands. For phosphine ligands the larger the cone angle the faster ligand dissociation becomes.⁹ Figure 1.2 illustrates Tolmans cone angle for P(CH₃)₃.

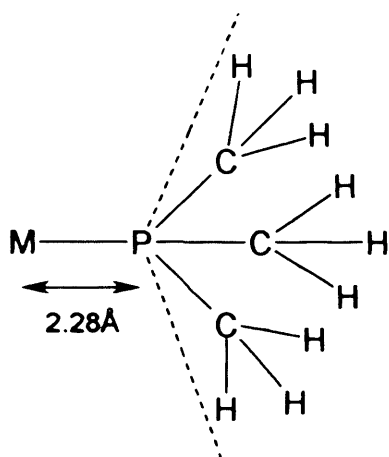


Figure 1.2 Illustration of Tolmans cone angle for trimethylphosphine.

The effect of bite angles and their influence upon catalysis and the coordination environment within metal complexes has led to their investigation in catalytic reactions. The bite angles of phosphine ligands play an important role for diphosphines in determining the selectivity and rate of catalytic reactions. The regioselectivity of rhodium catalysed hydroformylation reactions are governed by steric factors¹⁰ and the rate is influenced by the electronic influence of the bite angle. Specific effects are difficult to assess unless the nature of the mechanism and selectivity limitations of the reactions are known.

Other parameters that can be defined for diphosphines include the solid angle ($\Omega = \text{Size of area on sphere}/r^2$, the angle that seen from the centre of a sphere includes a given area on the surface of that sphere), the pocket angle, repulsive energy (electron repulsions) and the accessible molecular surface area (the area at the Van der Waals surface which can be touched by another molecule, and the location of the centre of the touching molecule), which give an idea about the steric properties of the ligands. The steric bite angle effect is related to the steric interaction between the diphosphine and the metal ion. This can be altered by changing the nature of the backbone while keeping the phosphorus substituents the same. The steric interactions can alter the energy of both the transition states and the catalytic resting state, which may affect the activity or selectivity of the catalytic system. The electronic bite angle effect is associated with electronic changes in the catalytic centre that happen as a result of altering the nature of the backbone. Evidence of this relationship can be seen in nickel catalysed hydrocyanation where ligands which favour tetrahedral co-ordination are less catalytically active than those which favour square planar co-ordination.¹¹

The bite angle determines metal hybridisation (due to its' relationship to the orientation of the bonding orbitals within the ligand) and as a consequence metal orbital energies and reactivity. This can cause a change in the stability of reaction intermediates.

The steric bulk of the ligand is important with respect to macrocyclic ligands. The same parameters as for bite angles, with the same effects, can be investigated. The steric bulk of the phosphorus macrocycle may affect the stability of reaction intermediates, by affecting the steric congestion around the metal centre. This favours less sterically demanding transition states possibly promoting new reactivity. New coordination environments can be created by varying the nature of the backbones within the macrocyclic ligand.

Uses of Phosphorus Ligands in Catalysis

Phosphine ligands have been shown to stabilise metals in low oxidation state complexes and with unusual geometries. They support reactive complexes in a variety of applications.

Catalysis is a kinetic phenomenon meaning that the activity of a catalytic system may depend on a small component of the catalyst. Determining the mechanistic steps in a catalytic system may lead to an ability to manipulate components of the catalyst in order to make it more active. Alternatively the active species can be adjusted to probe the effects of (for example) different R groups on a phosphorus ligand within a catalytic system.

In catalytic reactions the catalysis usually takes place via substrate coordination, rearrangement and finally product dissociation. The catalyst works by lowering the energy barrier for the formation of the transition state.

Some common homogeneous catalytic reactions involve alkene isomerization, alkene hydrogenation and alkene hydroformylation (alkene → aldehyde or ketone).

Phosphorus ligands are used extensively in catalysis. Phosphines are commonly found as spectator ligands in many catalytic reactions; an example being Wilkinson's catalyst $[\text{RhCl}(\text{PPh}_3)_3]$ which is used in alkene hydrogenation (Figure 1.3). Spectator ligands in a catalytic complex are not directly involved in any catalytic process, even where they remain associated with the transition metal centre. Their effect is electronic and steric in nature and acts mainly to affect the selectivity and activity of the catalytic system. The catalytic activity of the system (both metal ion and ligands which participate in the catalytic reaction) can therefore be altered, by

adjusting the properties of the spectator ligands. The maximum electronic effect between participating ligands and spectator ligands can be seen when they are *trans* to each other (due to the *trans* position affording maximum ligand interaction through ligand orbitals.).¹²

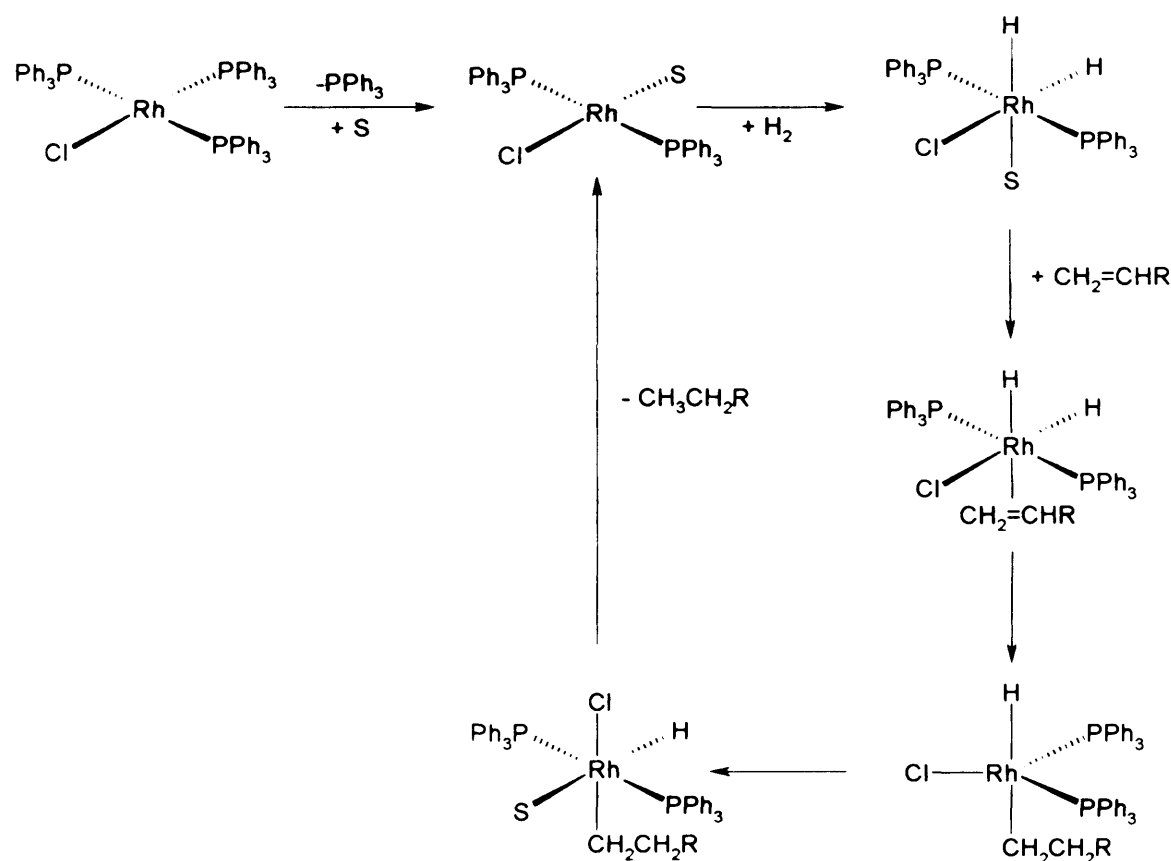


Figure 1.3, Wilkinson's catalyst where S represents a solvent molecule.

The nature of the phosphine ligand in Wilkinson's catalyst is important, some phosphines result in the formation of inactive dihydride complexes, however some of these intermediate complexes can be synthesised *in-situ*. The catalytic mechanism is more complicated than the simplified reaction scheme drawn.¹³ Wilkinson's catalyst limits isomerisation. The hydrogenation rates depend on the ease of binding of the alkenes to the metal complex, more weakly bound alkenes hydrogenate more slowly. Iridium analogues of Wilkinson's catalyst have been synthesised but have proven to be ineffectual due to the failure of their dihydrides to lose phosphine, which is due to the increased M-L bond strength. Wilkinson's catalyst selectively hydrogenates primary alkenes over secondary alkenes, it is unable to hydrogenate tertiary alkenes. Phosphine ligands have also been shown to be active in alkene polymerisation.¹⁴

Triphosphorus macrocycles have been shown to be alkene polymerisation catalysts.¹⁵ Currently triphosphorus macrocycles exhibit low activity for this application although there is a wide potential for the development of these systems.

Currently most ethylene polymerisation catalysts are based on cyclopentadienyl complexes of electropositive metals. Triphosphorus macrocycles could act as an alternative to these Cp ligands because they are six electron facially capping tridentate donating ligands and therefore analogous to cyclopentadienyl ligands in this respect. They could also exhibit a greater ability to tune their steric and electronic nature. Triphosphorus macrocycles would also form very stable complexes which are a necessity in catalytic reactions to avoid catalyst degradation.

Macrocyclic Ligands

Macrocyclic ligands are polydentate ligands containing donor atoms within (or attached to) a cyclic backbone. Macrocyclic ligands contain at least three donor atoms and the macrocyclic ring (incorporating donor atoms unless they are externally attached to the ring) contains a minimum of nine atoms.¹⁶ This definition includes most cyclic, polydentate ligands, which can incorporate a metal ion into a central binding cavity. When tridentate macrocyclic ligands are of a suitable size in relation to the metal ion to which they are bound, they adopt a facially capping co-ordination mode leaving three mutually *cis* coordination sites in octahedral complexes.

Bonding between the Metal ion and the Macrocycle

The bonding between the metal ion and the macrocycle depends on the nature of the metal and the nature of the donor. It also depends on the size of the macrocyclic ring and the size of the metal ion in relation to the ring.

The Nature of Donors and Metal ions

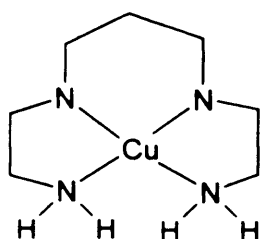
A good match with metal ions and their ligands can be made by comparing their electron donating/accepting abilities. Another way to discuss this is through the terms hard and soft. Hard ligands are those which bond almost solely through their σ -interaction between the ligand and the metal, examples include amine ligands. Hard ligands prefer to bond with high oxidation state metals, which by their nature are short of electron density. Soft ligands such as phosphines can not only donate using a σ -bond, but they can also accept electron density from the metal into vacant

σ^* -orbitals. Soft donor ligands are therefore more suited to low oxidation state metals which have superfluous electron density to back bond with the ligand.

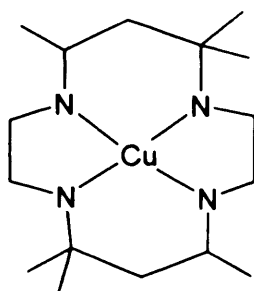
An example of this is the lack of early transition metal complexes containing phosphine ligands (with respect to late transition metal complexes) because of their seeming incompatibility in terms of the iron being a hard oxophilic metal and the phosphine donors being soft in nature. A solution to incompatibilities between metals and donors is to use chelating ligands as the chelate effect makes them more stable. Many bidentate phosphines bound to an early transition metal have been synthesised.¹⁷ The next obvious step was the use of macrocycles to further enhance the stability noted for bidentate phosphines.¹⁵

Macrocyclic ligands can be further divided into subclasses depending on the nature of the donor ligand. Firstly, cyclic compounds incorporating a number of ether functions as donors (commonly called crown ethers), and secondly, systems containing nitrogen, sulphur, phosphorus or arsenic donors. These macrocycles often form very stable complexes with transition metals. Macrocycles containing nitrogen and sulphur donors such as 1,4,7-triazacyclononane (TACN) and 1,4,7-trithiacyclononane¹⁸ have been studied in detail due to their ease of synthesis. In comparison phosphorus and arsenic containing macrocycles are rare due to synthetic difficulties encountered during their preparation.

Unusual properties can be associated with many cyclic ligand complexes, including increased stability, which can be illustrated by comparing dissociation rates for macrocyclic and related non-macrocyclic complexes.



Non-macrocyclic Ligand
 $t_{1/2}$ in 6.1M HCl, 298K
Minutes



Macrocyclic Ligand
 $t_{1/2}$ in 6.1M HCl at 298K
22 Days

Macrocycles bestow additional stability to the metal complexes that they form due to enhanced kinetic stability and thermodynamic inertness. Therefore metal ions involved in these complexes are held strongly within the macrocyclic cavity formed in comparison to acyclic systems. These ligands, as with many other systems, invoke

novel chemical properties on to the metal ion they are bound to, and the resulting complex formed resulting from the nature of the metal-ligand bonding.

The properties of macrocycles especially those involved in biological systems (such as in haemoglobin, vitamin B₁₂ and chlorophyll) and in catalytic applications indicate the potential of macrocyclic chemistry within the future of medicine, biochemistry and industry. Macrocyclic ligands could prove invaluable in catalytic applications as they provide a framework for highly selective catalysis under mild conditions of temperature and pressure.^{19,20} This is partially due to the occupation of mutually *cis* co-ordination sites by the macrocycle, which in turn forces the remaining reaction sites to also be mutually *cis*. Another essential feature of asymmetric catalysis is steric rigidity in the incorporated ligand

Tridentate macrocyclic ligands are similar in their co-ordination to isoelectronic cyclopentadienyl ligands. They are facially capping ligands, occupying three mutually *cis* co-ordination sites and they donate six electrons to the metal centre, therefore analogies between the behaviour of cyclopentadienyl metal complexes, and in particular their applications in organometallic synthesis can be extended, theoretically to macrocyclic metal complexes.

Macrocyclic complex properties can be varied to suit a particular function. With more s-hybridisation within the donor atom (for example by changing a phosphorus donor for an arsenic donor), overlap between the metal-ligand orbitals increases causing a resulting decrease in the metal-donor atom bond length. Reduction of M-L bond lengths causes the distances between the donor atoms to be smaller and the macrocyclic cavity to decrease in size. However the smaller effective covalent radius of the donor atom (caused by the increased s-hybridisation) means that the reduction in hole size is minimised.

Macrocycles can promote the formation of less common co-ordination geometries, because there is increased macrocyclic ring strain on their co-ordination to metal complexes which may enhance unusual bonding modes. Co-ordination geometry and complex reactivity can be altered by varying the size of the ligand backbone, the chelate bite angle²⁸ or the nature of the substituent groups.²⁸

Due to their cyclic nature, macrocycles have additional stereochemical constraints than related open chain polydentate species. In addition, macrocycles are able to adapt to imperfect bonding opportunities, when a metal ion is too large to fit inside the macrocyclic cavity formed or electronically mismatched, the metal ion can be displaced outside of the macrocyclic plane (when the macrocycle is sterically rigid), or the macrocycle can become distorted in order to optimally accommodate the metal ion (the entatic state). Partially as a result of the adaptable nature of

macrocyclic ligands they can adopt unexpected donor atom-metal ion bond lengths and unusual angular relationships between co-existing donor-metal bonds in relation to similar open chain systems. These can cause unusual properties, such as a preference for low spin Ni(II) in the presence of three high field phosphorus ligands, resulting from the unique macrocyclic structure which restricts the freedom of the phosphorus donors in the $[\text{Ni}(12[\text{ane}]\text{P}_3\text{Et}_3)\text{Br}]^+$ complex.²¹ There is much current interest in linear triphosphine complexes and acyclic systems containing hemilabile ligands,^{22,23,24} both systems show new and unusual chemical properties (including the stabilisation of reactive intermediates).

Types of Macrocycles

There are two main types of macrocycles, firstly crown ether based with oxygen donor atoms which prefer alkali/alkaline metal ions and secondly, macrocycles with nitrogen, sulphur, phosphorus and arsenic donors which form stable complexes with transition and heavy metal ions.^{25,26} Within this thesis phosphorus and arsenic macrocycles are investigated.

What Makes Macrocycles so Robust?

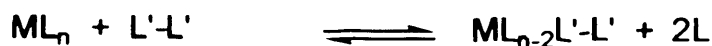
The aim in synthesising novel triphosphorus and arsenic macrocycles is to explore their novel chemistry which is expected to be unusual as a result of their stability and structure.

The Chelate Effect

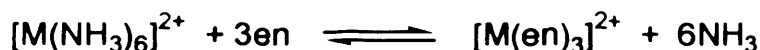
The stability of any complex type increases as the number of chelate rings (rings involving the metal ion and two donor atoms) increases due to the chelate effect (in effect more donor atoms give more stability). By using chelating instead of two monodentate ligands, the second donor atom for the chelate system will be in greater proximity to the metal ion resulting in a more favourable co-ordination environment (when one arm of the chelate is joined, the other will already be in the metals outer co-ordination sphere).²⁷ By increasing the chelate effect the metal-ligand interaction becomes stronger which in turn makes the complex thermodynamically more robust.

The chelate effect is mainly entropic in origin. To make the entropy of a reaction more positive (and therefore the reaction more favourable in terms of ΔG°) disorder must increase in the system. Disorder in a chemical reaction is measured

by the number of moles of reactants at the start of the reaction and the number of moles of products at the end. If there are more moles of products then the reaction is entropically favourable.



For example:



4 moles reactants

7 moles products

The complexes on each side of the equilibrium have 6 M-N bonds meaning that ΔH is not significantly altered. The chelate effect is energetically driven by the desire to create disorder. When the metal involved in this reaction is nickel, the entropy for this reaction is 86.5 kJ mol^{-1} . The formation constant for $[Ni(NH_3)_6]^{2+}$ is $\log_{10}\beta$ 8.7 and $[Ni(en)_3]^{2+}$ $\log_{10}\beta$ 18.1.

Enthalpy has a small part to play in the chelate effect, if the chelating ligand is of the same type then the enthalpy differences between the bonding at the start of the reaction and at the end is minimal.

The chelate effect can be studied by looking at the formation constants (β), which show the affinity of a metal ion for a ligand.

Ligand	Equilibrium Expression	$\log_{10}\beta$ for Co^{2+} Complex
Ammonia	$[Co(NH_3)_6]^{2+} / [Co^{2+}][NH_3]^6$	4.4
Ethylene diamine	$[Co(C_2H_6NH_2)_3]^{2+} / [Co^{2+}][NH_3]^3$	14.1
Ethylene diamine tetraacetic acid	$[Co(EDTA)]^{2-} / [Co^{2+}][EDTA]$	16.3

The formation constants reflect the stability of the complexes, their relative stabilities are influenced by the increasing positive entropy of their formation reactions. The chelate effect is a result of enthalpic and entropic contributions which make the driving force of a reaction (ΔG°) more negative.

$$\Delta G^\circ = -RT \log_{10}\beta$$

$$\Delta G^\circ = \Delta H - T\Delta S$$

The Macrocyclic Effect

Even when the co-ordination geometry for a metal ion is ideal, the macrocyclic complex will often have enhanced thermodynamic and kinetic stability, the combination of which are referred to as the macrocyclic effect. The macrocyclic effect is an extension of the chelate effect with an additional stability, which depends on the nature of both the macrocyclic ligand and the metal with which it is bonding. The separate contributions to the macrocyclic effect change individually for each system so the macrocyclic effect cannot be given a description that equally applies to all macrocyclic systems. The change of free energy (ΔG°) always favours the formation of a macrocyclic complex. The macrocyclic effect may also sufficiently stabilise more reactive phosphines to broaden the range of ligand systems that can be investigated and exploited.

Thermodynamic Contribution to the Macrocyclic Effect

The thermodynamic contribution to the macrocyclic effect involves both enthalpic and entropic contributions. The enthalpic contributions are a result of many factors including the nature of the bond between the donor atom and the metal, the ligands involved within the macrocyclic system, changes in ligand conformation upon complexation and the compatibility of the metal ion and the macrocyclic cavity, all of which affect the stability of the metal ion-ligand interaction. Macrocycles should (in relation to their linear analogues) be less soluble, due to their compact nature and the lack of terminal groups, which often provide greater solubility to ligand systems. The cavity size in particular affects the properties of any metal complexes formed between macrocycles and metal fragments. In uncomplexed ligands the cavity size may vary due to ring expansion and contraction caused by the nature of the ligand. Co-ordination to a metal centre may induce distortions in the macrocyclic ring resulting in an increase in ligand strain energy, balanced by the stability provided by the complexation.²⁸ Cavity size is influenced by the number of atoms within the macrocyclic ring, the balance between the dictates of the metal ion and the macrocyclic ligand (which may invoke unusual coordination geometries), and the nature of the donor atoms incorporated within the macrocyclic ligand. Macrocycles have steric constraints depending on ring size and the number and nature of various chelate rings formed on co-ordination. The chelation of the macrocycle affects the position of donor atoms both with respect to other donor atoms and the metal ion. It also affects the co-ordination modes and conformations of the co-ordinated macrocycle. With rigid backbones the possibilities of ring expansion and contraction

are severely limited. In such complexes M-L distances far from normal are often observed. For sterically rigid rings, folding is energetically unfavourable with respect to the displacement of the metal fragment from the donor plane of the ring (necessary for dissociation reactions). Complexes formed by macrocyclic ligands have properties which reflect the compatibility of the macrocyclic cavity size with the electronic and steric requirements of the metal.

Entropic effects towards the thermodynamic contribution to the macrocyclic effect are similar in their nature. Changes in the number of species present (which affect β), the translational entropy (ligand rigidity) within the macrocycle and the entropic effects of solubility all contribute to the overall entropic contribution to the macrocyclic effect. The cyclic nature of macrocyclic ligands means that during complexation they undergo less conformational change leading to less loss of disorder and more positive configurational entropy.

Kinetic Contributions to the Macrocyclic Effect

The kinetics and mechanism of macrocyclic formation are closely associated with the structural features of the macrocyclic ligand and the metal ion involved in complex formation.

The formation of a macrocycle, especially on its templated complexes, is often controlled by the solvent exchange rate of the solvated metal ion used. The cyclisation of macrocyclic ligands may be dependant on the nature of the solvent, steric or electrochemical effects, which may influence the rate determining step of a reaction and hence whether it is feasible.

The other important kinetic aspect of macrocyclic complexes are the dissociation kinetics. This is especially important when it is considered that the template approach is the one utilised in this research. The macrocycle must therefore be able to be separated from the template before further chemistry can be investigated. Dissociation pathways can take a number of different routes. Other reagents may assist, a second metal ion can scavenge the ligand as it dissociates or adding another strongly co-ordinating ligand (such as cyanide or EDTA) which will bind strongly to vacated co-ordination sites may make macrocyclic dissociation more favourable. The dissociation of a macrocycle from its metal ion can be extremely slow (in the order of 20 years for some complexes)²⁸ even in the presence of strong acid. Even complexes involving normally labile metals may become inert with complexation to a tightly bound cyclic ligand due to the slow dissociation kinetics. If a macrocycle is bound too tightly to the metal ion it is co-ordinated to, it may be too difficult to remove it from its' template. However if the complex is too labile then it

may decompose before taking part in the catalytic reaction, or other reactions of interest.

Macrocyclic complexes are kinetically stable with respect to the loss of the metal ion (e.g. to remove Ni^{2+} from a tetraazamacrocycle involves a prolonged reaction with potassium cyanide).²⁹ The kinetic stability of macrocyclic ligands is partially due to the snug fit of the metal ion within the macrocyclic framework, this provides a partial explanation as to the increasing lability of larger macrocyclic ring sizes. Larger, more flexible rings are easier to dissociate from their metal ions and result in a reduced macrocyclic effect.

Macrocyclic Catalysis

Manganese and iron complexes of N,N',N''-trimethyl-1,4,7-triazacyclononane catalyse oxidation reactions although their vacant co-ordination sites often lead to the formation of dimers.³⁰ Monomeric macrocyclic complexes which are more resistant to oxidative hydrolysis and yet still able to participate in catalytic reactions (with an available site for the binding of the metal ion to an oxidant,) include cross bridged tetraazamacrocycles. Iron(II) and manganese(II) complexes are excellent to use as oxidation catalysts due to their stability in aqueous conditions and the easy accessibility to higher oxidation states.³¹

Why are Triphosphorus Macrocyclic Ligands of Interest?

Over the last decade, triazacyclononane³² and trithiacyclononane³³ have been used as versatile tridentate facially capping ligands in many areas of macrocyclic co-ordination chemistry. Interest more recently has been concentrated towards the development and study of triphosphorus macrocycles. The 12[ane],³⁴ 11[ane],³⁵ 10[ane]³⁶ and 9[ane]³⁷ triphosphorus macrocycles have been stereoselectively prepared, to act as facially capping, neutral, κ^3 , six electron ligands on $[(\text{C}_5\text{R}_5)\text{Fe}(\text{L})_3]^+$ templates. Further chemistry of the 12[ane] triphosphorus macrocycle has been investigated particularly with regard to catalytic applications including alkene polymerisation and ROMP (ring opening metathesis polymerisation) this type of catalytic application is illustrated in Figure 1.4.

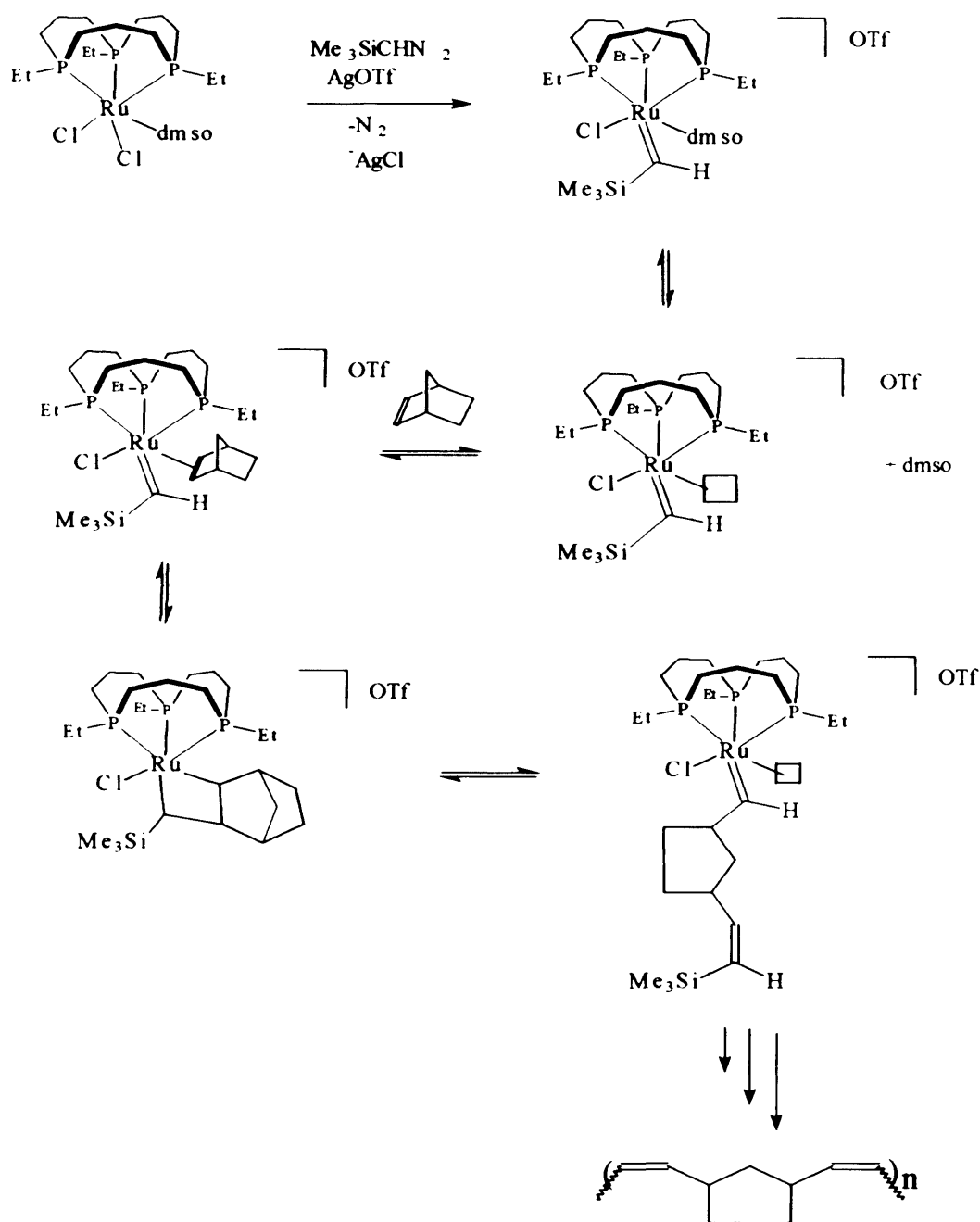


Figure 1.4 Illustration of the uses of triphosphorus macrocycles in ROMP (ring opening metathesis polymerisation).

The rigidity of phosphorus and arsenic macrocyclic ligands can be varied, increased rigidity means that once the macrocycles have been made they are less flexible and they would be expected to strongly retain their facially capping orientation, but it also increases the steric strain within the ring making them harder to synthesise.

Aim of this Research

Within this thesis the potential influences macrocyclic phosphines may have on the behaviour of co-ordinated metals are investigated. The macrocyclic co-ordination effect may aid the stabilisation of classes of compounds in unusual electronic and co-ordination states such as the stabilisation of low oxidation states for d- and f-block metals, these complexes will allow the study of the fundamental properties and reactivity of the novel complexes. Macrocyclic tripnictide ligands are expected to have substantially reduced lability in comparison to alternative ligands with three tertiary monodentate phosphine ligands. They also allow the retention of mutually *cis* reactive sites which are necessary to many types of catalytic reaction. The tripnictide ligands that we aim to synthesise will be analogous to related face capping ligands such as cyclopentadienyl (Cp) and tris-pyrazolylborate (Tp).

We aim to build on work previously established for macrocycles with larger ring sizes, to synthesise smaller conformationally rigid macrocyclic rings in order to further increase the unfavourability of ligand freedom and the consequent M-L bond breakage which leads to macrocyclic dissociation.

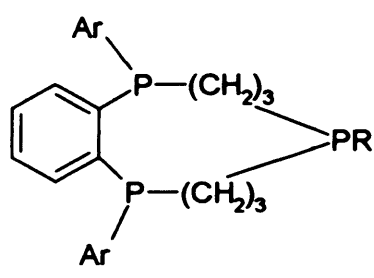
Macrocycles will show new chemical behaviour in comparison to monodentate phosphines (due to the macrocyclic effect), their enhanced stability can lead to new classes of metal complexes. Macrocycles should also (in the same way as Cp) stabilise reaction intermediates in many different catalytic processes (such as alkene polymerisation and ROMP).

Triphosphorus and triarsenic macrocycles are rare ligands to work with primarily due to a lack of suitable synthetic procedures and the sensitivity to air and moisture of the bidentate and monodentate phosphines required prior to cyclisation. Very few examples have been investigated in the literature so we aim to expand this area of tripnictide macrocyclic chemistry and investigate the new macrocyclic complexes formed. This thesis reports the synthesis and characterisation of new macrocyclic complexes incorporating phosphorus and arsenic donors and details the new synthetic methodologies developed in order to allow this. The novel macrocycles we have prepared are robust, rigid, versatile, facially capping, six electron donor ligands.

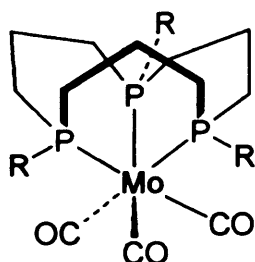
Previously Known Tridentate Phosphorus and Arsenic Macrocycles

The first tripnictide (grp 15) macrocycles were made by Evan P. Kyba.^{38,39} Some early 14[ane] examples were synthesised using a high dilution method.⁴⁶ There are two different methods that can be used to synthesise macrocycles: high dilution (as used by Kyba in the synthesis of the first 11-membered triarsenic macrocycle);⁴⁰ or template synthesis in which a metal entity (e.g. FeCp^+) is used as a building block during the construction of the macrocyclic framework. The 12[ane] triphosphorus macrocycle was made using the template method in which the macrocycle cyclisation was achieved *via* a radical catalysed coupling of P-H groups with allylic carbons (hydrophosphination). Previous studies in the Edwards group have been directed towards developing a synthetic strategy for making the 11[ane], 10[ane] and 9[ane] triphosphorus macrocycles. This was based on the intramolecular cyclisation of a co-ordinated diphosphine and monophosphine *via* a pseudo Michael type addition. We have subsequently developed an alternative cyclisation pathway involving reactive fluorophenyl moieties.

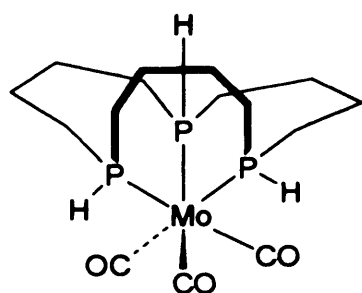
Some examples of previously known macrocycles are the following (x[ane] refers to x number of atoms in the macrocyclic ring including donor atoms).



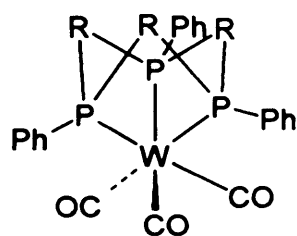
11[ane]⁴⁰



12[ane]



15[ane]⁴¹



45[ane]⁴²



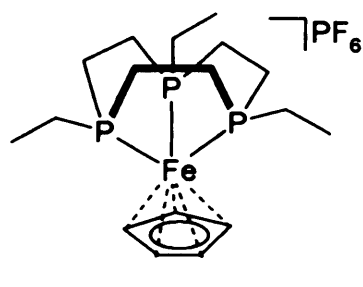


Figure 1.5 Previously made triphosphorus macrocycles with varying ring sizes.

Mixed Donor Macrocycles

The synthesis of mixed donor macrocycles is exciting due to their potentially hemilabile nature and the opportunity they offer to explore the more subtle control of metal properties at the metal centre.⁴⁴ Examples of mixed phosphorus nitrogen macrocycles of varying sizes are common as are mixed nitrogen sulphur macrocycles. Examples of macrocycles containing both phosphorus and arsenic donors have been previously reported by Kyba (see reaction scheme figure 1.6).^{45,46}

Synthesis of Triphosphorus and Triarsenic Macrocycles

As alluded to above there are currently two methods for the synthesis of tridentate macrocycles, high dilution methods and templated synthesis.

High Dilution Synthesis

High dilution synthesis does not use a metal ion template, it involves the cyclisation of diphosphine and monophosphine precursors under high dilution conditions to limit unwanted side reactions. Unfortunately, as there is no stereochemical control during the synthesis of macrocycles using this methodology, a mixture of stereoisomers is formed. The stereoisomers can be separated using column chromatography, however the resulting yield of individual isomers are poor. High dilution methodology is not environmentally friendly and can be expensive (due to the large volumes of solvents required) and polymerisation of the starting materials cannot be fully prevented, which contributes to the low yield. This methodology can also lead to problems in manipulating large volumes of solvents.

The only current example of a triarsenic macrocycle is the 11[ane]⁴⁶ synthesised and stereoselectively isolated by Kyba after a high dilution synthesis (Figure 1.6).

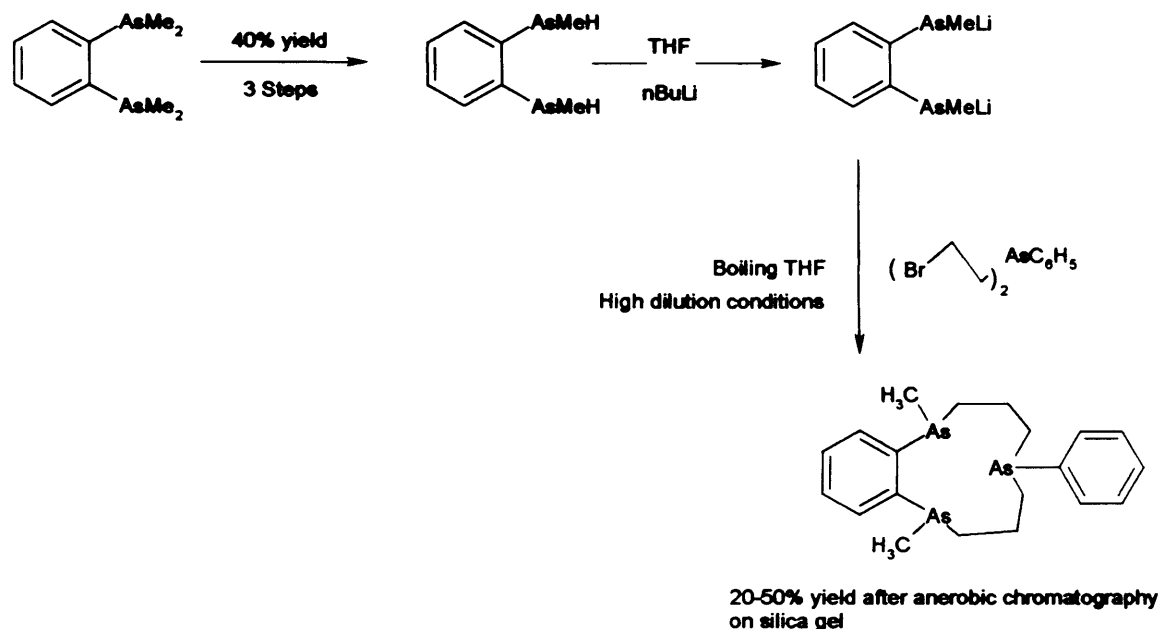


Figure 1.6 An illustration of the synthesis of the first triarsenic macrocycle, synthesised by Kyba using high dilution methodology.

Entropy is the dominant factor in the synthesis of large ring compounds. The energy involved is related to the probability of the two ends of the macrocyclic precursors coming into close enough proximity to react with each other. Unless there are special secondary interactions within the chain or a highly pre-organised or rigid system is used, the likelihood of the two ends meeting is low. It is far more likely that the reactive group will meet another reactive group on a different precursor. The result of this entropic constraint is the formation of polymeric species, which is a significant alternative pathway to the formation of the desired macrocycle. By using a non-templated synthesis it is necessary to use high dilution conditions to prevent two reactive moieties from meeting. By using a template to synthesise the precursor complex, the reactive groups are brought into much closer proximity and therefore exhibit a much higher degree of pre-organisation.

High dilution synthesis becomes more difficult for smaller ring sizes as polymerisation is more prominent.⁴⁷

Templated Synthesis

The introduction of a metal template to stereoselectively co-ordinate both the diphosphine and the monophosphine prior to cyclisation introduces kinetic control and reduces the entropic barrier to macrocyclic formation (it directs the steric course of the reaction by holding the donor atoms in position).⁴⁸ The first macrocycle to be synthesised using a template method was (Figure 1.7) by Curtis⁴⁹ in 1960.

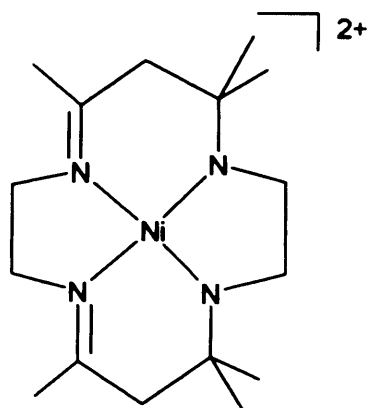


Figure 1.7 The first template synthesised macrocycle.⁴⁹

For the synthesis of the 9[ane]P₃ macrocycle (Figure 1.8) a $[(\eta^5\text{-C}_5\text{R}_5)\text{Fe}(\text{CO})_2(\text{CH}_3\text{CN})]^+$ template has been found to be effective and from this template $[(\eta^5\text{-C}_5\text{H}_5)\text{FePH}(\text{C}_2\text{H}_4)\text{PH}(\text{C}_2\text{H}_4)\text{P}(\text{C}_2\text{H}_3)(\text{C}_2\text{H}_4)]\text{PF}_6$ has been synthesised according to the methodology developed by the Edwards group. A single facially capping stereoisomer is formed and the metal template minimises intermolecular reactivity resulting in side polymerisation reactions. The template can be removed for the 12[ane] triphosphorus macrocycle in high yields.⁵⁰ The 9[ane] triphosphorus macrocycle has also been removed as a trioxide although as yet, attempts to reduce the trioxide to the free tritertiary phosphine have failed.⁵¹

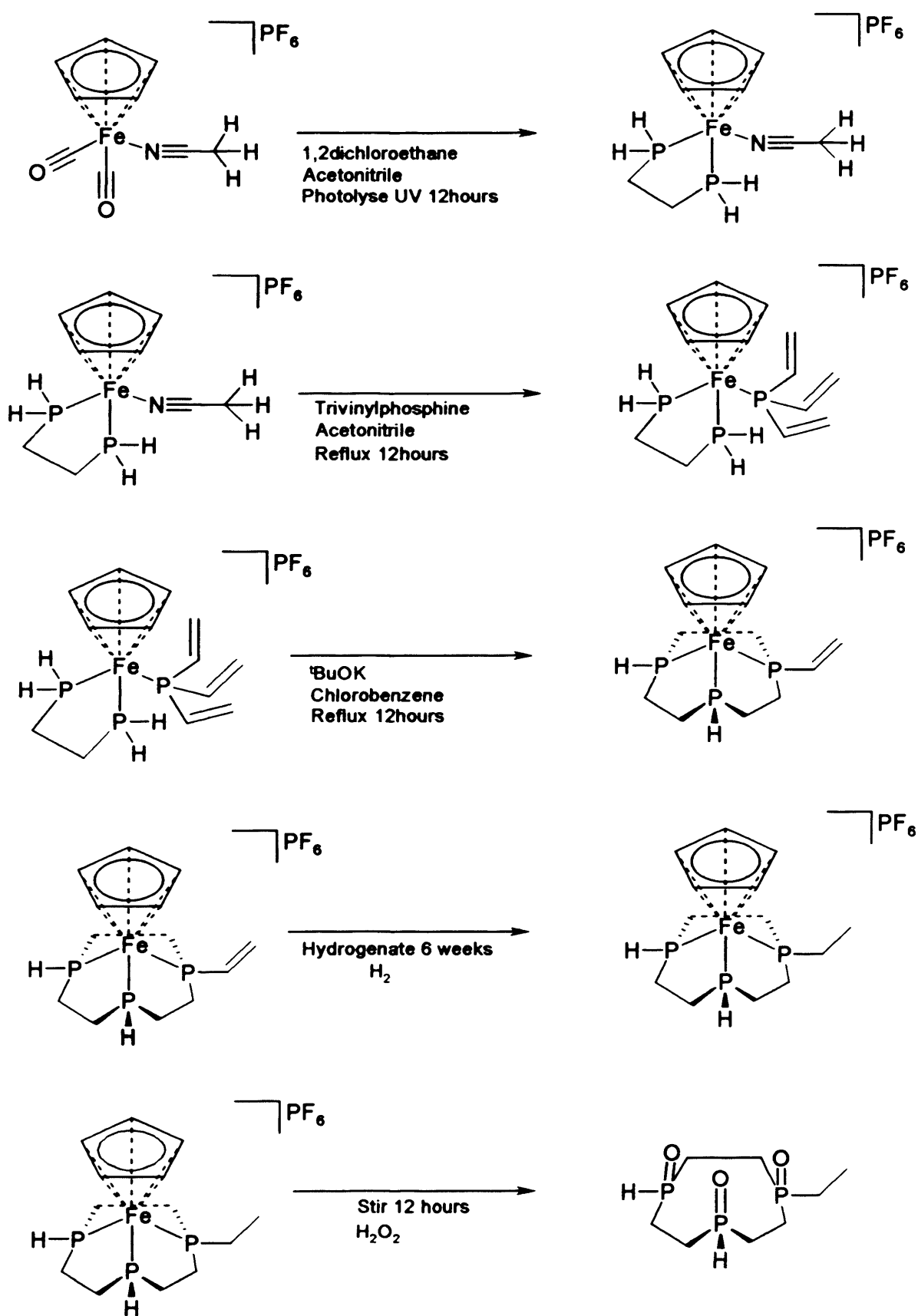


Figure 1.8 Synthesis of triphosphorus macrocycles by template methodology.

This reaction scheme illustrates the current template method for the synthesis of triphosphorus macrocycles. The monobenzannulated triphosphorus macrocycle has also been synthesised using the same reaction conditions with the substitution of 1,2 bisphosphinoethane for 1,2 bisphosphinobenzene.⁵² Templated synthesis is an important method of stereochemically controlling the orientation of the lone pairs on the phosphorus atoms. By template synthesis, the tripnictide macrocycle would retain its facially capping nature. This should also be the case even when the macrocycle is removed from the metal template especially if a mild liberation method is employed.

Without a specific stereoisomer being formed the isomers have to be separated (through chromatography) to give a much lower yield of macrocycle. The inversion barriers for phosphorus are relatively high which restricts rotation upon complexation ($\Delta G^\circ=124-149\text{kJmol}^{-1}$).⁵³ The restricted rotation limits the utility of the *syn-anti* stereochemistries and makes a stereospecific route desirable for the formation of facially capping ligands.

Macrocyclic Constituents

The chemistry of the triphosphorus macrocyclic complexes synthesised can be manipulated in different ways to affect their chemical properties and to make them more synthetically viable in terms of yield and ease of synthesis. The variability of macrocyclic complexes can be extended from the backbone of the macrocyclic ligand, to the metal ion, to the nature of donor atoms and the R-groups that they contain.

Metal Ion

A metal template must be used in the synthesis of 9[ane] macrocyclic complexes as the non-bonding angles do not allow a non-templated cyclisation.

A transition metal's ability to accommodate different ligands within its co-ordination sphere has led to their use in catalytic systems, which often involve up to three different participating groups in addition to the spectator ligands. The ability to change between co-ordination numbers is important for substitution and addition reactions. The metal has 9 bonding orbitals which can be accessed (1xs, 3xp and 5xd) providing accommodation for up to 18 electrons. Most metals have the ability to

σ bond and π back bond to ligands. A range of oxidation states should be accessible for the transition metal ion to possibly allow the complexes formed on the template to be destabilised via oxidation or reduction prior to demetallation.

The metal ion has an effect on the bonding properties within the complex and its inherent stability. Research for 9-membered macrocyclic complexes has concentrated on Fe^{2+} metal ion templates, which in combination with Cp ligands provide a stable template on which to synthesise macrocyclic phosphines. The use of an Fe(II) metal ion in combination with a six electron ligand such as Cp, and the six electrons also donated from the precursor ligands form a very stable 18 electron complex.

The metal template gives the donor atoms a high degree of pre-organisation prior to cyclisation.

Template Ligand

Ideal Requirements of a Template Ligand for Macrocyclic Cyclisation

For a ligand to be utilised effectively as a template it needs to have the following properties:

- It needs to have 6 electrons to donate.
- It needs to form octahedral complexes with a *fac* geometry in order to force the other constituents to bind in a mutually *fac* orientation.
- It needs to be inert under macrocyclic cyclisation conditions.
- It needs to enable the co-ordination of a range of precursor phosphines and arsines.

The cyclopentadienyl group (Cp) is one of the most important template ligands because it is firmly bound to the metal centre and generally inert to nucleophilic and electrophilic reagents (*i.e* it is stable in cyclisation conditions). It is a rigorously *fac* ligand co-ordinated to an iron (II) cation (CpFeL_3^+) and allows sequential replacement of L by bidentate and monodentate phosphines, the iron (II) has a d^6 electron configuration making it inert. The Cp functionality can be adjusted in order to provide a more sterically demanding template to aid cyclisation (by increasing the proximity of the mono- and di-phosphines), the steric effects of adding groups to the Cp template also affects ΔG° for the rotation of other ligands about their bonds.

The nature of the Cp function affects the solubility and reactivity of the complexes formed which is important, both in relation to the ability to remove the template from the macrocyclic ligand, and the solubility of the precursors and intermediates during cyclisations, as well as influencing the ring closing reaction. The type of Cp functionality used affects the oxidation potential of the complex formed according to its electron donating ability and the effect this has on the metal ion. The steric effects that additional groups on the Cp have affect the bonding between the metal and the macrocycle, with the more electron donating Cp* resulting in more backbonding to the phosphine ligands, the deficit is made up by increased σ -donation from the phosphine ligands.⁵⁴

Many Cp derivatives have been investigated recently including pentamethyl cyclopentadienyl (Cp*), trimethylsilyl cyclopentadienyl and bis-trimethylsilyl cyclopentadienyl all of which have proven difficult to remove from the cyclised macrocycle.⁵⁵ The necessity of the Cp ligand has been well illustrated by attempts to make the 9[ane] triethyl macrocycle using a $\text{Cr}(\text{CO})_3(\text{CH}_3\text{CN})_3$ template, this proved unsuccessful, due to the lack of compression of the P-P non-bonded distances, which are forced together as a result of the more bulky Cp substituent. The shorter M-P bond length in the iron(II) template in comparison to the chromium (II) template decreases the distance between the phosphine donors increasing the likelihood of cyclisation.

Previous studies on 9[ane] triphosphorus macrocyclic complexes of iron have shown that the ligand has proved to be difficult to remove even under forcing reaction conditions. We have expanded our area of macrocyclic synthesis by including alternatives to Cp ligands, including 1,2-dicarboclovocarborane ligands and trisoxazoline ligands, both of which are isoelectronic with Cp ligands although the synthesis of tripnictide macrocycles on these templates has remained elusive. The different nature of the ligands may promote different stabilities for each of the reaction intermediates, which could in turn be utilised to invoke different reactivities for the alternative template ligand complexes.

Synthetic Precursors

The choice of synthetic phosphine precursors for the macrocyclic ligand has an important effect on the chemistry involved within the cyclisation and the resulting conditions that are most favourable to direct the formation of the macrocycle. Previously (as illustrated in scheme 1.6) cyclisations have involved pseudo Michael type additions. The initial co-ordination of a bidentate diphosphine ligand, which can

have either a 1,2-phenyl backbone, or an ethandiyl backbone is followed by coordination of a monodentate trivinyl phosphine or arsine and the cyclisation reaction is base catalysed (e.g. with triethylamine). As the bidentate phosphine changes in nature from ethandiyl to 1,2-phenyl, the electronics and sterics of the ligand are both affected. The increased rigidity of the 1,2-phenyl backbone makes the macrocycle more stable and a more rigid, facially capping ligand, it is also less labile to macrocyclic dissociation due to the lack of flexibility of the backbone. Both the nature of the diphosphine and the monophosphine affect the solubility and the stability of the macrocyclic complex and its precursors (which is discussed in Chapter 2).

Chiral Macrocycles

Chiral macrocycles are a valuable tool because they may act as ligands for asymmetric catalysts allowing the enantiomeric configuration of products to be controlled by the catalyst. One important characteristic of successful asymmetric catalysis is that the steric rigidity of the ligand is essential. Therefore, within the macrocycle the choice of backbone functionality has an effect on the efficiency of asymmetric catalysis. The macrocycle must have the correct stereochemical conformation in addition to steric rigidity to be an effective catalyst. To be a successful asymmetric catalyst in hydrogenation the chiral phosphine must be capable of distinguishing between the enantiotopic faces of the reactant in order to synthesise a homochiral product. Chiral triphosphorus macrocycles (with P as the site of asymmetry) have been previously synthesised although the yield has been poor.⁵⁶ By synthesising chiral macrocycles with a much greater rigidity using techniques described in this thesis, modified catalytic systems could be envisaged.

If macrocycles are formed non-stereospecifically their separation is lengthy and results in a much reduced yield. Using high dilution methodology it is impossible to control the stereochemistry of the resulting macrocycle. For nitrogen based macrocycles their stereochemistry at nitrogen is not important as the inversion barriers for nitrogen are low. Phosphorus ligands have much higher inversion barriers ($\Delta G = 124-149\text{kJmol}^{-1}$) and arsenic ligands higher again ($\Delta G = 175-179\text{kJmol}^{-1}$)⁵⁷, this means that once the ligand has been formed in one stereochemical configuration inversion to change it into another configuration is difficult requiring elevated temperatures. If a *syn-anti* isomer is formed, it may bind as a bridging or bidentate ligand, but it will not bind as a tridentate ligand on to one metal centre. The *syn-syn* isomer is required to form a macrocycle that is able to bind in a tridentate fashion to a single metal centre.

Size of the Macrocyclic Ring

The size of the macrocyclic ring has a profound effect on the chemistry it exhibits: larger rings are more flexible and as a result are more easily displaced from their metal template. Ring strain (caused by non-optimal bond distances and angles being forced upon the macrocycle) is non-existent in macrocycles with over twelve atoms in their ring structures. By synthesising smaller ring macrocycles the chemistry and fundamental properties of these ligands can be investigated, they should exhibit decreased lability due to their more constrained geometry, by increasing their rigidity they will become less labile and form more robust metal-ligand complexes.

Counter Ion

For ionic complexes such as macrocyclic complexes, the counter ion may also be able to bind to the metal ion. BF_4^- is a useful anion although F^- abstraction can occur, PF_6^- and SbF_6^- are less strongly co-ordinating but as noted in this thesis unwanted side reactions involving the PF_6^- anion can occur resulting in PR_2F products which can be identified in ^{31}P NMR spectra at approximately 160ppm. BPh_4^- anions are non co-ordinating and being bulky they have a different influence on lattice energies and therefore the solubility and crystallinity of the macrocyclic complexes formed.

Demetallation

With macrocycles demetallation is often difficult due to their unfavourable dissociation kinetics and the thermodynamic stability of the macrocyclic complexes. There are several methods that can be used to demetallate macrocycles:

1. Addition of excess acid to reduce the macrocycle, often used for amine based macrocycles.
2. Introduction of competing ligands either as solvent molecules such as THF or acetonitrile, or for more strongly co-ordinated ligands EDTA^{4-} or OH^- .

3. Changing the oxidation state of the metal ion. By reducing or oxidising the metal ion its co-ordination chemistry is changed which can make it more labile.

The 9[ane] ligands which have been previously synthesised on an iron(II) template by Edwards *et al* have been difficult to demetallate resulting in only one success with the oxidation of the 9[ane] triethyl triphosphorus macrocycle (Figure 1.6). The resulting triphosphine trioxide macrocycle is difficult to reduce in large quantities preventing further study.

Another method for demetallation which has not previously been utilised is to use macrocyclic ligands with two types of donor atom in order to create hemilability. If one donor atom is easily removed from the metal template it would affect the co-ordination chemistry of the remaining co-ordinated ligands making them more susceptible to replacement by competing ligands.

Some substitution reactions have been found to be promoted by UV light. The mechanism of this photon induced reaction is thought to involve the promotion of a $d\pi$ electron into a $d\sigma$ orbital which is M-L antibonding in character therefore destabilising the complex. Possibly by trying dissociation reactions under photolytic conditions the free macrocycles could be obtained.⁵⁸ It has also been previously shown that ligand dissociations can be promoted by ultrasound as a result of high local temperatures formed by the opening and closing of small bubbles of vapour in the solvent (cavitation).⁵⁹ This could also be used to try to increase the dissociation kinetics of macrocyclic complexes.

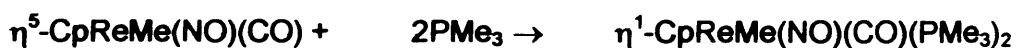
Demetallation is not promoted by using substitutionally inert d^6 octahedral complexes. The templates we currently use are all based on forming an eighteen electron complex, these complexes are stable but reduction or oxidation can be used to reduce their stability. Attempts to reduce 9[ane] triphosphorus macrocycles have proved to be unsuccessful although several methods have been utilised.

- Using alkali metals in ammonia to reduce Fe(II) to Fe(0) and resulting in the formation of cyclopentadiene, this method caused macrocyclic degradation as monitored by ^{31}P NMR.⁶⁰
- Ligand displacement from the Cp/Cp*Fe⁺ template by using KCN, this methodology required the oxidation of the iron(II) complex to iron(III) using silver (I) tetrafluoroborate in CH₂Cl₂ followed by work up to remove elemental

silver. KCN was added as an aqueous solution and competing ions were added to try to displace the macrocycle from the iron template.⁶⁰

- Oxidative cleavage has been attempted using conc. HCl and 30% H₂O₂. Pellets of sodium hydroxide were added resulting in the precipitation of a red solid however the desired trioxide could not be isolated from the reaction mixture.⁶⁰

Cp can be forced to ring slip from η^5 to η^3 or η^1 but the tendency for this to happen in Fe(II) complexes is small. An example of a successful ring slippage forming a stable complex is the phosphination of the following Cp rhenium complex.⁶¹



Existing Routes to the Liberation of Triphosphorus Macrocycles

Currently there are few successful routes to the demetallation of template cyclised triphosphorus macrocycles. The predominant method is the digestion of the metal with a cyanide salt.⁶² After synthesising 1,5,9-triphosphacyclododecane on a molybdenum tricarbonyl template, attempts to liberate the macrocycle using cyanide salts, triphenylphosphine, trifluorophosphine and trimethoxyphosphine all failed. The macrocycle was stereoselectively demetallated using bromine to oxidise Mo(0) to Mo(II) followed by digestion of the metal complex in strong base (NaOH). This novel liberation technique also works for the analogous chromium complexes.⁴³

References, Chapter 1 - Introduction

- ¹ O. Dahl, U. Henriksen, C. Trebbien; *Acta Chim. Scand. B*; **1983**; *37*; 639
- ² S. Dapprich, G. Frenking; *J. Phys. Chem.*; **1995**; *99*; 9352
- ³ G. Frenking, N. Fröhlich; *Chem. Revs*; **2000**; *100*; 717
- ⁴ N.G. Connelly; A.G. Orpen; *J. Chem. Soc., Chem. Comm.*; **1985**; 1310
- ⁵ A. L. Fernandez, M. R. Wilson, A. Prock, W.P. Giering; *Organometallics*; **2001**; *20*; 3429
- ⁶ N.G. Connelly; A.G. Orpen; *J. Chem. Soc. Chem. Commun.*; **1985**; 1310
- ⁷ E. J. S. Vichi, E. Stein; *Inorg. Chim. Acta*; **2002**; *334*; 313-317
- ⁸ C. A. Tolman; *Chem. Revs*; **1977**; *77*; 313
- ⁹ D.J. Darenbourg; *Adv. Organomet. Chem.*; **1982**; *21*; 13
- ¹⁰ Z. Freixa, P. W. N. M. Leeuwen; *J. Chem. Soc., Dalton Trans.*; **2003**, 1890
- ¹¹ M. Kranenburg, P.C. Kamer, P.W.N.M. van Leeuwen, D. Vogtand, W. Keim; *J. Chem. Soc., Chem. Commun.*; **1995**, 2177
- ¹² A. Cotton, G. Wilkinson; *Advanced Inorganic Chemistry*; Wiley Interscience; **1988**
- ¹³ B.R. James; *Homogeneous Hydrogenation*; Wiley Interscience; NY; **1973**, *Adv. Organomet. Chem. 17*; 319; **1979**
- ¹⁴ P.G. Pringle, N.A. Cooley, S.M. Green, D.F. Waas, K. Heslop, A.G. Orpen; *Organometallics*; **2001**; *20(23)*; 4769
- ¹⁵ R.J. Baker, P.C. Davies, P.G. Edwards, R.D. Farley, S.S. Linyanage, D.M. Murphy, B.S. Yong; *Eur. J. Inorg. Chem.*; **2002**; 1975
- ¹⁶ E. C. Constable; *Metals and Ligands Reactivity*; Ellis Horwood; England; **1990**; 136
- ¹⁷ M.D. Fryzuk, T.S. Haddard, D.J. Berg; *Coord. Chem. Revs*; **1990**; *99*; 137
- ¹⁸ W. Levason, G. Reid; *J. Chem. Res. S*; **2002**; 467
- ¹⁹ R.J. Baker, P.G. Edwards; *J. Chem. Soc., Dalton Trans.*; **2002**; 2960
- ²⁰ R.J. Baker, P.G. Edwards, J.G. Mora; F. Ingold, K.A. Malik; *J. Chem. Soc., Dalton Trans.*; **2002**; 3985
- ²¹ P.G. Edwards, F. Ingold, S.J. Coles, M.B. Hursthouse; *Chem. Commun.*; **1998**; 545
- ²² P.G. Edwards, P.W. Read, M.B. Hursthouse, K.M.A. Malik; *J. Chem. Soc. Dalton*; **1994**, 971
- ²³ P.G. Edwards, S.J. Chadwell, S.J. Coles, M.B. Hursthouse, A. Imran; *Polyhedron*; **1995**; *18*; 1057
- ²⁴ P.G. Edwards, S.J. Chadwell, S.J. Coles, M.B. Hursthouse; *J. Chem. Soc. Dalton*; **1995**, 3551
- ²⁵ T.J. Atkins, J.E. Richman; *J. Am. Chem. Soc.*; **1974**; *96*; 2268
- ²⁶ T.J. Atkins, W.F. Oettel, J.E. Richman; *Org. Synth.*; **1978**; *86*; 1978
- ²⁷ N.F. Curtis; *J. Chem. Soc.*; **1960**; 4409
- ²⁸ L.F. Lindoy; *The Chemistry of Macrocyclic Ligand Complexes*; Cambridge University Press; **1989**
- ²⁹ E.C. Constable; *Metal and Ligands Reactivity*; Ellis Horwood; **1990**; p153
- ³⁰ K. Wieghardt, U. Bossek, B. Nuber, J. Weiss, J. Bonvoisin, M. Corbella, S.E. Vitols, J.J. Girerd; *J. Am. Chem. Soc.*; **1988**; *110*; 7398
- ³¹ T.J. Hubin, J.M. McCormick, S.R. Collinson, N.W. Alcock, H.J. Clase, D.H. Busch; *Inorg. Chim. Acta*; **2003**; *346*; 76
- ³² T. Weyhermuller, K. Wieghardt, P. Chaudhuri; *J. Chem. Soc., Dalton Trans.*; **1998**; *24*; 4237
- ³³ A.J. Blake, Y.V. Roberts, M. Schröder; *J. Chem. Soc., Dalton Trans.*; **1996**; *9*; 1885
- ³⁴ P. G. Edwards, J.S. Fleming, S.S. Linyanage, S.J. Coles, M.B. Hursthouse, J. Chem. Soc., *Dalton Trans.*; **1996**; 1801
- ³⁵ R. Haigh; Ph.D. thesis, Cardiff University **2002**
- ³⁶ P.G. Edwards, P.D. Newman, D.E. Hibbs, *Angew. Chem. Int. Ed.*; **2000**; *39*; 2722
- ³⁷ P.G. Edwards, M.L. Whatton, R. Haigh; *Organometallics*; **2000**; *19(14)*; 2652

-
- ³⁸ E.P. Kyba, S.S.P. Chou; *J. Org. Chem.*; **1981**; *46*(5); 860
- ³⁹ E.P. Kyba, D.C. Alexander, A. Hohn; *Organometallics*; **1982**; *1*(12); 1619
- ⁴⁰ E.P. Kyba, S.T. Liu; *Inorg. Chem.*; **1985**; *24*; 1613
- ⁴¹ A.D. Norman, B.N. Diel, R.C. Haltiwanger; *J. Am. Chem. Soc.*; **1982**; *104*; 4700
- ⁴² J.A. Gladysz, E.B. Bauer, J. Ruwwe, J.M. Martin-Alvarez, T.B. Peters, J.C. Bohling, F.A. Hampel, S. Szafert, T. Liz; *Chem. Commun.*; **2000**; 2261
- ⁴³ P.G. Edwards, S.J. Coles, J.S. Fleming, M.B. Hursthouse, S.S. Liyanage; *J. Chem. Soc., Chem. Commun.*; **1996**; *35*; 4563
- ⁴⁴ E.P. Kyba, C.N. Clubb, S.B. Larson; *J. Am. Chem. Soc.*; **1985**; *107*(7); 2141
- ⁴⁵ E.P. Kyba, S.S.P. Chou; *J. Am. Chem. Soc.*; **1980**; *102*; 7012
- ⁴⁶ E.P. Kyba, S.S.P. Chou; *J. Org. Chem.*; **1981**; *46*; 860
- ⁴⁷ W. Levason, G. Reid; *J. Chem. Soc., Dalton Trans.*; **2001**; *20*; 2953
- ⁴⁸ M.C. Thompson; D.H. Busch; *J. Am. Chem. Soc.*; **1964**; *86*; 3651
- ⁴⁹ N.F. Curtis; *J. Chem. Soc.*; **1960**; 4409
- ⁵⁰ P.G. Edwards, J. Fleming, S.S. Linyage; *Inorg. Chem.*; **1996**; *35*; 4563
- ⁵¹ P.D. Newman; Cardiff University; Unpublished results
- ⁵² P.G. Edwards, M. Whatton; *Organometallics*; **2000**; *19*; 2652
- ⁵³ E.P. Kyba, C.W. Hudson, M.J. MacPhaul, A.M. John; *J. Am. Chem. Soc.*; **1977**; *99*; 8053
- ⁵⁴ D.M. Tellers, S.J. Skoog, R.G. Bergman, T.B. Gunnoe, W.D. Harman; *Organometallics*; **2000**; *19*; 2428
- ⁵⁵ P.G. Edwards, P.D. Newman; Unpublished results
- ⁵⁶ D. Li; Cardiff University; Unpublished results
- ⁵⁷ J.W.L. Martin, F.S. Stephens, K.D.V. Weerasuria, S.B. Wild; *J. Am. Chem. Soc.*; **1988**; *110*; 4346
- ⁵⁸ R.H. Crabtree; *The Organometallic Chemistry of the Transition Metals*; Wiley Interscience; **1987**; 84
- ⁵⁹ K.S. Suslick; *Adv. Organomet. Chem.*; **25**; 73; 1986
- ⁶⁰ M.L. Whatton; Ph.D. Thesis; Cardiff University; **2002**
- ⁶¹ C.P. Casey; W.D. Jones; *J. Am. Chem. Soc.*; **1980**; *102*; 6154
- ⁶² D.J. Brauer, F. Gol, S. Hietkamp, H. Peters, H. Sommer, O. Stelzer, W.S. Sheldrick; *Chem. Ber.*; **1986**; *119*; 349

Chapter 2

**Benzannulated, Dibenzannulated
and Tribenzannulated
Triphosphorus and Triarsenic
Macrocycles**

Benzannulated, Dibenzannulated and Tribenzannulated Triphosphine Macrocycles

Introduction

Macrocycles having rigid unsaturated hydrocarbon backbones have attracted great interest recently due to their novel properties and potential applications particularly in catalysis. Macrocycles with arylene and ethynylene backbones have demonstrated synthetic versatility and the ability to form ordered frameworks. Macrocycles formed in this way have an internal binding cavity because of their toroidal shape which could potentially be used as an aid to the crystallisation of these complexes. The cyclic backbone of the macrocycles can be modified in terms of the nature and function of the R-group attached to the donor atom as well as the nature and size of the ring.¹

As described in the previous chapter, current macrocyclic cyclisation methodology has centered around pseudo-Michael type additions of co-ordinated primary diphosphines with co-ordinated trialkenyl phosphines. For triphosphorus macrocycles this type of macrocyclic formation only works for a limited range of backbones, namely those involving alkenyl functionalities.

An alternative to this method needed to be evolved to provide access to the more rigid di- and tribenzannulated macrocycles. This would allow investigations to be made into the chemistry of macrocycles with benzannulated backbones and pnictide donors, providing a wider understanding into the nature of the structure and bonding within more rigid triphosphine macrocyclic complexes. The conformation within the proposed macrocycles will give the complexes extra stability and should increase the potential for metal-ligand back bonding due to the aromatic nature of the backbone.² The increased inflexibility within the system will enhance the barrier to rotation of the lone pairs in the free macrocycle. This restriction to rotation is initially caused by the increased inversion barriers present in phosphorus by comparison to nitrogen, it also increases due to the rigidity of the benzo backbones in comparison to ethyl backbones.

Investigations have therefore been carried out to study the effect of varying the rigidity of the backbones throughout the macrocycle. In order to synthesise the tri-aryl backbone macrocycles a new synthetic method was developed, which utilised fluoro-phenyl moieties attached to the bisphosphine /arsine fragment. The activation of the *ortho* C-F bond in arylfluorophenylphosphines within the co-ordination sphere

of transition metals has been previously reported^{3,4} and was utilised here in order to base activate the macrocycle and promote cyclisation.

The template methodology previously utilised in the synthesis of triphosphorus macrocycles is similar to research carried out by Gladysz⁵ which concentrated on sulphur ylides and their stable generation in cationic transition metal complexes containing unsaturated organic sulphides. This research provided an indication as to the stabilising effect of the transition metal template on co-ordinated reactive groups. By extending the nature of the ligands to phosphines, deprotonation to form a co-ordinated phosphide results in a lone pair of electrons that are able to attack at the Michael acceptor. By using a diphosphine ligand such as 1,2-bisphosphinobenzene then reacting the phosphide with a co-ordinated alkenyl group such as trivinyl phosphine, a Michael type addition can occur by the following mechanism (Figure 2.1) to form a partially cyclised product (which cannot be isolated). The reaction happens in duplicate, with the diphosphine again forming an ylide and reacting with one of the remaining vinyl groups to form the fully cyclised product. Post cyclisation, the macrocycle can be hydrogenated to change the vinyl substituent into a less reactive ethyl functionality.

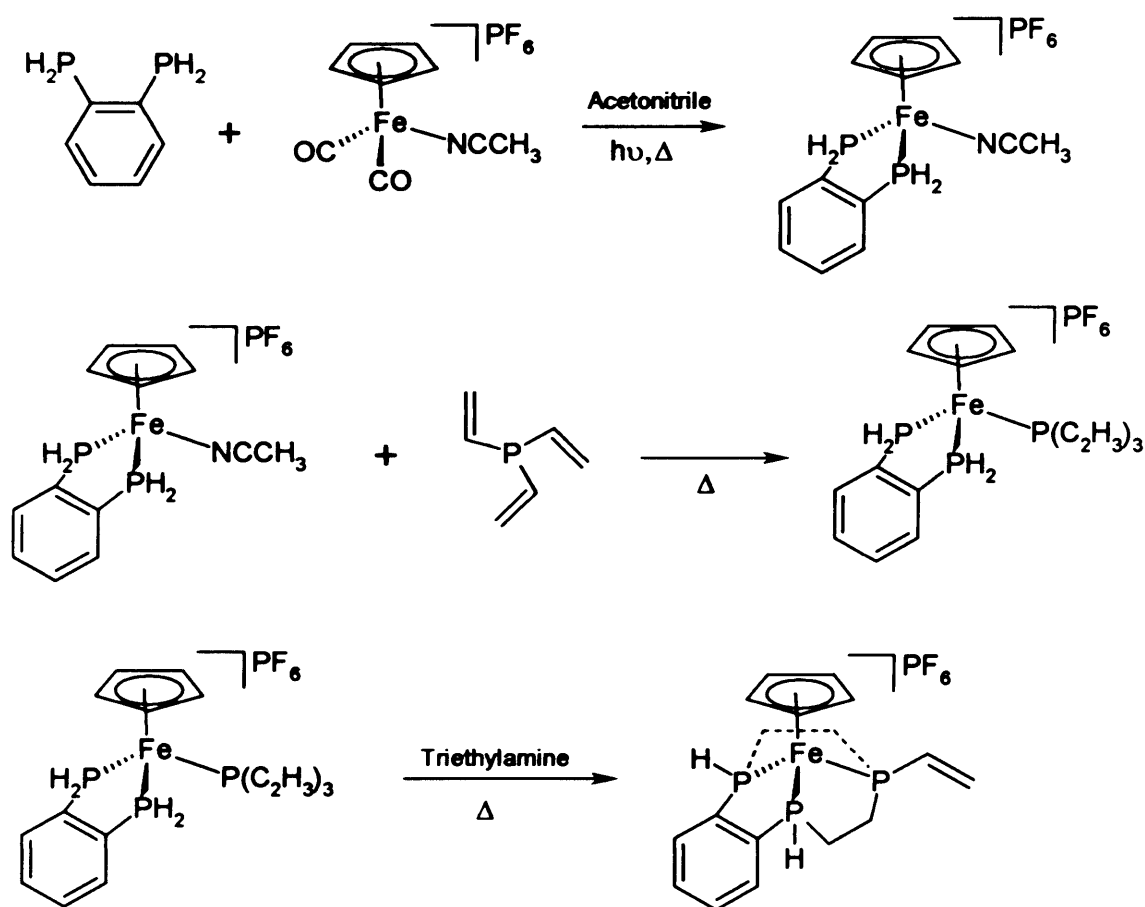


Figure 2.1 Macrocyclic synthesis from alkenyl and primary phosphine precursors.

Results and Discussion

In order to make tribenzannulated macrocycles a different strategy needed to be adopted due to the reduced reactivity (in terms of pseudo Michael type additions) of phenyl R-groups. Phenyl groups are not as reactive as ethyl groups due to their electron delocalisation which prevents the attack of the phosphorus lone pair. To alter the reactivity of the phenyl groups and make them suitable to make into 9[ane] triphosphorus macrocycles the carbon *ortho* to the phosphorus donor must be electrophilically activated. This can be achieved by the use of an electron withdrawing fluorine attached to the *ortho* carbon which will initiate nucleophilic attack as for an alkyl halide. Fluorinated phosphines are often inert within the co-ordination sphere of a metal centre⁶ with the exception of *ortho* C-F bonds in fluoroaryl phosphines. There is also a stabilised P-C₆H₄F interaction⁷ caused by fluorination of the aryl group (this is diametrically different from phenyl phosphines where the P-Ph bond is activated).⁸ Cyclisation results from the initial formation of a phosphide containing a lone pair of electrons (by catalytic base attack) followed by nucleophilic attack by the phosphorus lone pair at the *ortho* carbon resulting in the overall loss of HF. The concept of an intramolecular dehydrofluorinative P-C coupling reaction involving two functionalities, with the loss of a proton (catalytically to the base used to activate the reaction) and nucleophilic attack by the resulting phosphide at the *ortho*fluorophenyl substituent of the phosphine, provides a rational method for the synthesis of tripnictide macrocycles.⁹

The modified method to macrocyclic cyclisation utilising fluorophenyl moieties was used to prepare novel tribenzannulated and dibenzannulated triphosphorus macrocycles. Two techniques both utilising the same dehydrofluorinative coupling were used to synthesise di- and tribenzannulated macrocycles, the disconnection of the resulting macrocycle into its' constituent synthons allows a clarification of these approaches.

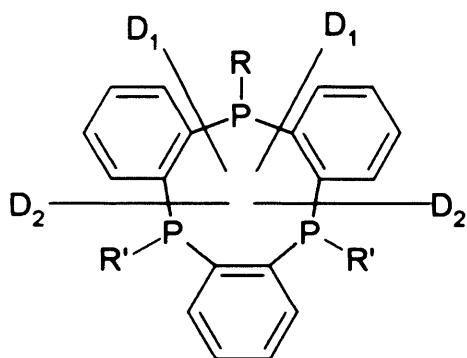


Figure 2.2 Disconnection approaches for dehydrofluorinative coupling.

- D₁ Disconnection 1, utilising the *ortho*fluorophenyl aryl rings on the bidentate pnictide
- D₂ Disconnection 2, *ortho*fluorophenyl aryl rings located on the monodentate pnictide
- R Either Ph (D₁) or C₆H₄F (D₂)
- R' Either C₆H₄F (D₁) or H (D₂)

The new procedure involves either the initial co-ordination of a bidentate pnictide ligand with four *ortho*fluorophenyl aryl groups to the metal template followed by the addition of a primary monodentate pnictide (disconnection 1), or the addition of a bidentate primary pnictide followed by the addition of tri*ortho*fluorophenylphosphine (disconnection 2).

In both examples cyclisation involves the addition of base to encourage the initial proton loss from the primary pnictide (whether bidentate or monodentate) and attack by the resulting nucleophile at the *ortho* position of the fluorophenyl ring. This mechanism previously described by Saunders⁴ uses a pentafluorophenyl moiety attached to a co-ordinated diphosphine, which on addition of catalytic quantities of base attacks the moderately acidic Cp* protons to induce C-C bond formation (Figure 2.3). In our similar system the base initiates P-C bond formation. Insufficient data has been collected to determine the nature of the base in the reaction mechanism, a stoichiometric amount of base would seem to be required to quench released HF although (as mentioned above), Saunders *et al.* have reported the use of merely a catalytic quantity.

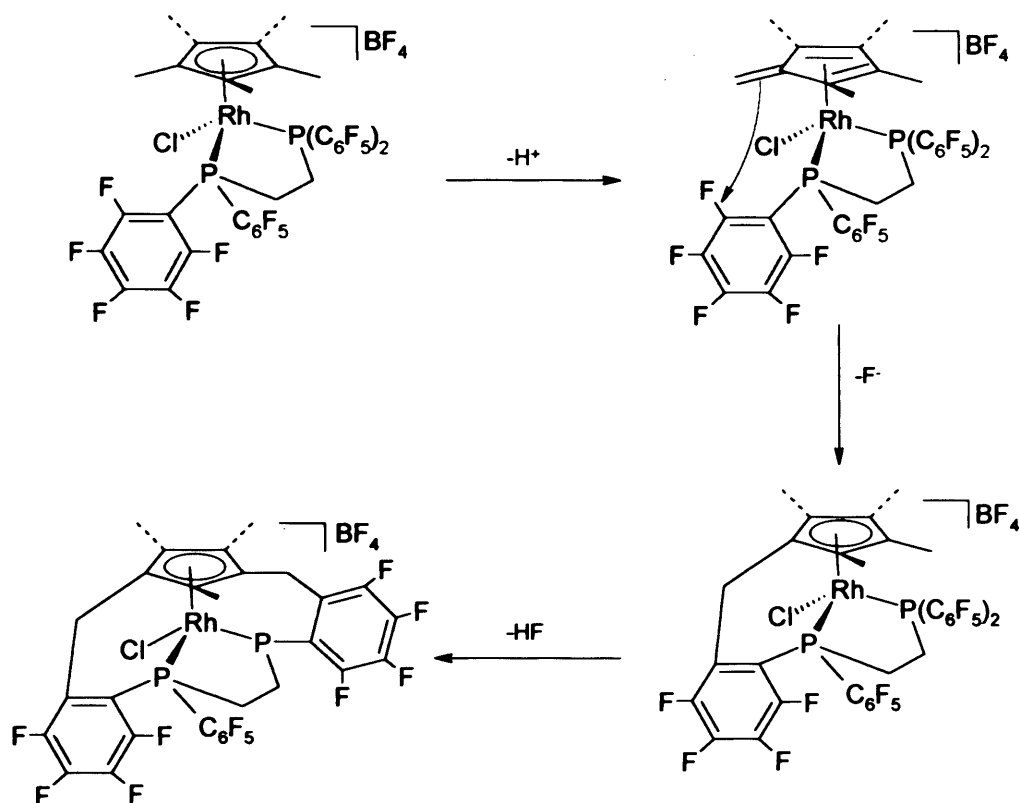


Figure 2.3 Saunders reaction scheme showing dehydrofluorinative coupling to form a C-C bond.

Additional benefits of the dehydrofluorinative mechanism include the electrostatic attraction between the nucleophilic fluoride located on the aryl ring and the electrophilic proton located on the primary phosphine which allow increased pre-organisation of the macrocycle, and the possibility that macrocyclic cyclisation could be induced on non-sterically influencing ligands. Another advantage is the ability to vary the nature of the donor atoms to form mixed donor complexes. The nature of the backbones can be varied from the less constrained ethyl backbones used in previous template synthesised triphosphorus macrocycles (which it is also possible to utilise with the dehydrofluorinative P-C coupling method) to the more rigid benzannulated backbones. Initial experiments by Albers¹⁰ confirmed the validity of this synthetic methodology in the synthesis of the dibenzannulated complex $[\text{CpFeP}(\text{C}_6\text{H}_4\text{F})(\text{C}_2\text{H}_4)\text{P}(\text{C}_6\text{H}_4\text{F})(\text{C}_6\text{H}_4)\text{P}(\text{C}_6\text{H}_5)(\text{C}_6\text{H}_4)][\text{PF}_6]$ and its full characterisation. The crystal structure of this complex admirably illustrates the increased rigidity of this macrocycle in comparison to the $[(\text{C}_5\text{H}_5)\text{FeP}(\text{C}_2\text{H}_5)(\text{C}_2\text{H}_4)\text{P}(\text{C}_2\text{H}_5)(\text{C}_2\text{H}_4)\text{P}(\text{C}_2\text{H}_5)(\text{C}_2\text{H}_4)][\text{PF}_6]$ and shows the feasibility of a new cyclisation template technique to prepare tripnictide macrocycles (Figure 2.4). The crystal structure also illustrates the twisted conformation of the ethyl

backbone. By utilising the novel dehydrofluorination strategy to cyclise tribenzannulated macrocycles a more rigid structure should be attained.

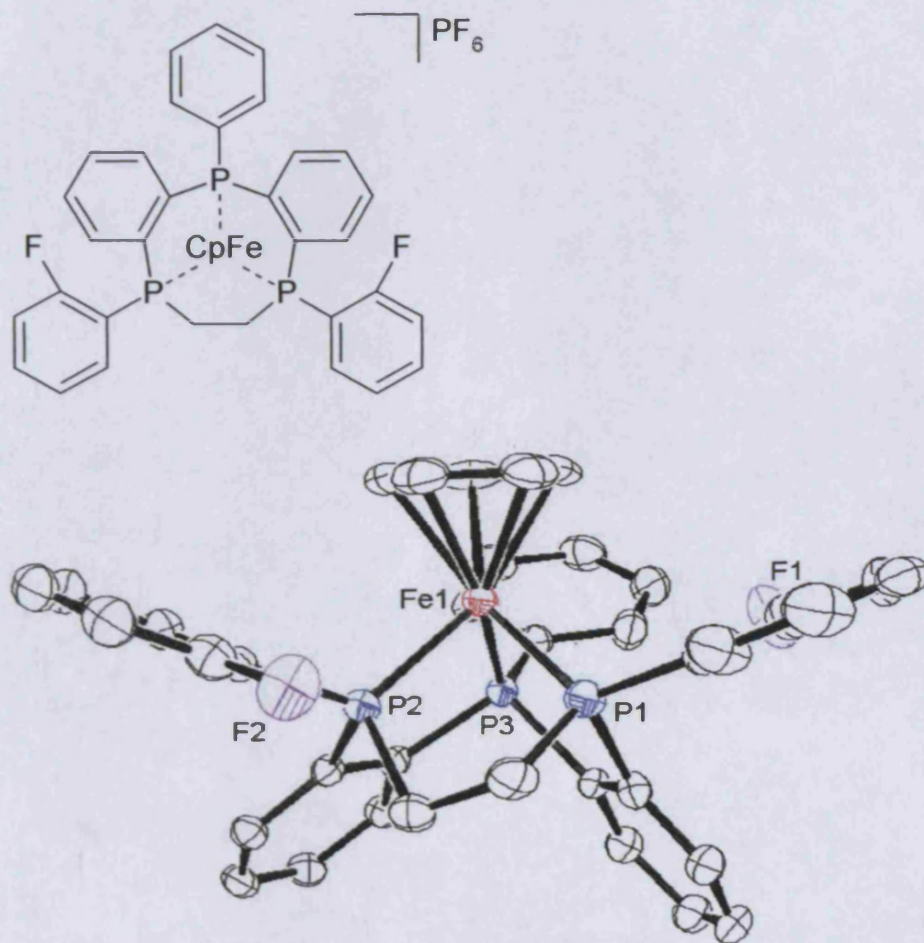


Figure 2.4 A dibenzannulated triphosphorus macrocycle synthesised by Albers by dehydrofluorinative cyclisation.¹⁰

Synthesis of Triphosphorus, Tribenzannulated Macrocycles

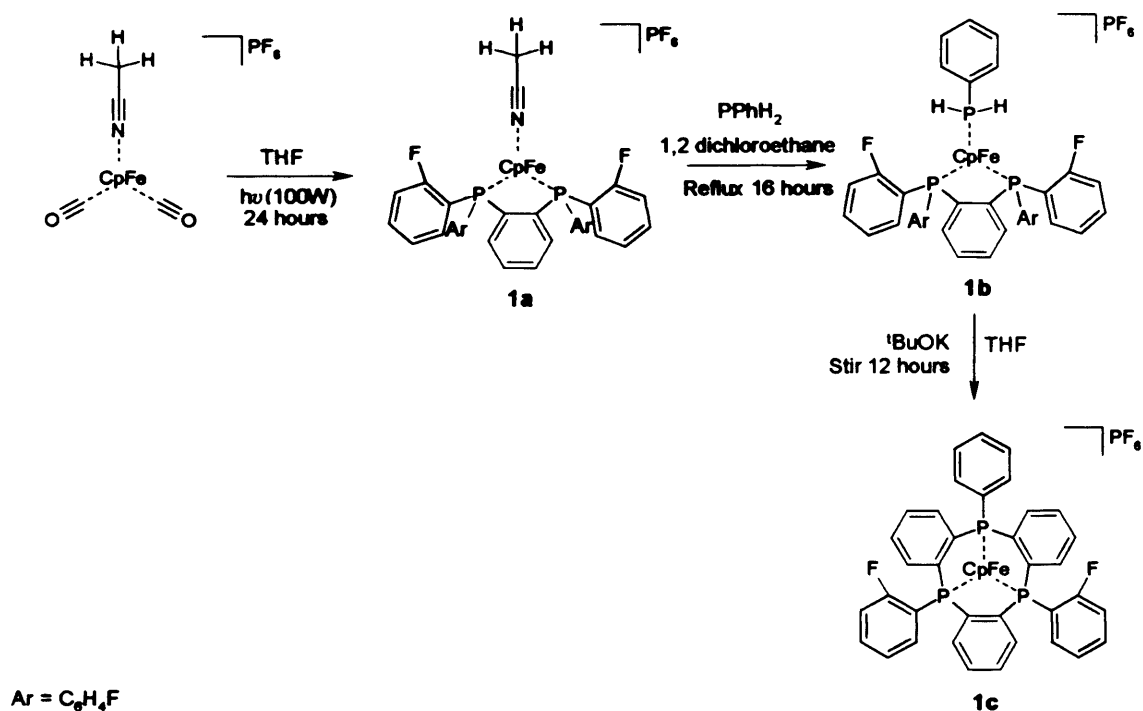


Figure 2.5, Method 1, synthesis of triphosphorus tribenzannulated macrocycles from a bidentate fluoroarylated phosphine and a monodentate primary phosphine.

The first example of a tribenzannulated triphosphorus macrocycle was synthesised according to scheme 2.5. Treatment of $[\text{CpFe}(\text{CO})_2(\text{CH}_3\text{CN})][\text{PF}_6]$ with the bidentate phosphine $(\text{C}_6\text{H}_4\text{F})_2\text{P}(\text{C}_6\text{H}_4)\text{P}(\text{C}_6\text{H}_4\text{F})_2$ gave **1a** as an air sensitive red powder in very good isolated yield (94%). The $^{31}\text{P}\{^1\text{H}\}$ NMR spectrum shows a triplet at 92.5ppm ($^3J_{\text{P-F}}$ 36.0Hz) which is shifted downfield with respect to the free ligand (-32.6ppm) and indicative of co-ordination to the metal ion. The ^1H NMR spectrum shows a broadened singlet at 3.96ppm due to the Cp fragment, in addition to the expected aromatic peaks (7.70-6.90ppm). The $^{13}\text{C}\{^1\text{H}\}$ NMR spectrum shows peaks due to the methyl protons of the acetonitrile ligand (2.8ppm), the Cp (81.5ppm) and aromatic carbons (123.2-133.9ppm). A doublet of doublets at 165.0ppm ($^1J_{\text{C-F}}$ 242.9Hz) can be assigned, whilst the $^2J_{\text{C-P}}$ interaction is not seen due to insufficient resolution of the spectra. The ^{19}F NMR spectrum shows a singlet at -98.0ppm representing the co-ordinated ligand. The CN stretch for the co-ordinated acetonitrile appears in the infrared spectrum at 2266cm^{-1} .

On addition of phenylphosphine under reflux conditions complex **1b** is formed as a yellow air sensitive powder in excellent yield after workup (93%). The $^{31}\text{P}\{^1\text{H}\}$ NMR spectrum shows an AX_2 pattern at 84.6ppm ($^3J_{\text{P-F}}$ 32.6Hz) and a further peak at

12.1ppm indicating co-ordination of the phenyl phosphine to the CpFe⁺ template. The ¹H NMR spectrum shows a doublet at 4.38ppm with ¹J_{P-H} 331.0Hz again indicating the co-ordination of the phenyl phosphine ligand. ¹⁹F NMR showed a singlet at -98.0ppm representing the co-ordinated bidentate phosphine.

Catalytic quantities of base were added to cyclise the precursor complex **1b** forming the complete macrocycle **1c** as an air stable yellow powder. Cyclisation was monitored by ³¹P{¹H} NMR spectroscopy, resonances were seen to move from a singlet at 84.6ppm to two resonances representing a ABB'XX' system at 119.6ppm (tt, ²J_{P-P}116.1Hz, ⁶J_{P-F}32.8Hz) and 127.5ppm(multiplet), the resonances are complicated by the magnetic inequivalence, yet chemical equivalence of the phosphorus atoms with *ortho*fluoroaryl groups. ¹³C{¹H} NMR data shows a doublet at 115.3 (²J_{C-F}23.1Hz) and a doublet of doublets at 163.3 (¹J_{C-F}252.7Hz) again without the ability to observe the coupling constant between C and P due to poor spectral resolution, the broadened Cp resonance is observed at 82.1ppm. At room temperature in the ¹⁹F NMR spectrum a singlet is seen at -98.4ppm, but at low temperature (83K) the peak splits into four separate peaks. The ³¹P{¹H} NMR spectrum was also taken at low temperatures (83K) in an attempt to deconvolute the multiplet observed, unfortunately although the clarity of the spectra increased no significant improvement in resolution was seen. In the mass spectrum a molecular ion peak was observed at 709.1Da/e.

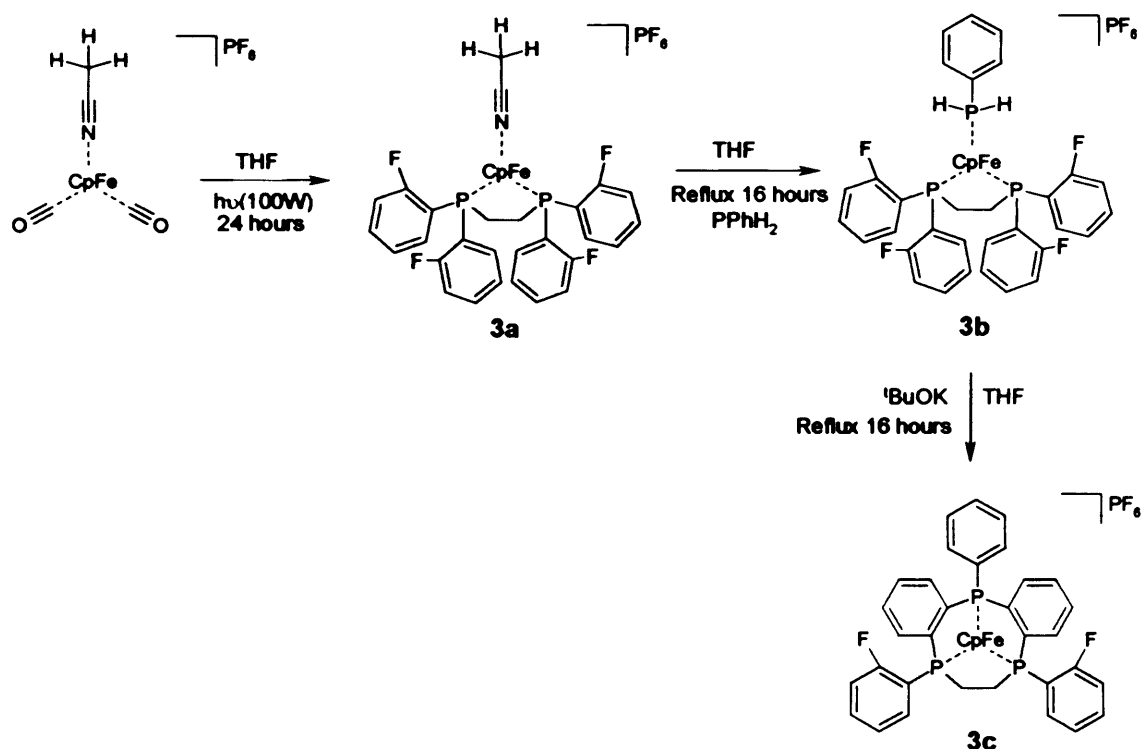


Figure 2.6, Method 1, synthesis of triphosphorus tribenzannulated macrocycles from a bidentate fluoroarylated phosphine (ethyl backbone) and a monodentate primary phosphine.

Other triphosphorus macrocycles have been synthesised using method 1 including macrocycles utilising a precursor involving *diortho*fluorophenyl bisphosphinoethane as the bidentate phosphine and phenyl phosphine as the monodentate phosphine (Figure 2.7). The Cp precursor 3b can again be characterised with peaks representing the co-ordinated diphosphine in the $^{31}\text{P}\{^1\text{H}\}$ NMR at 80.9ppm ($^3J_{\text{P-F}}$ 51.0Hz) and the monophosphine at 8.7ppm. The completely cyclised macrocycle 3c has a characteristic $^{31}\text{P}\{^1\text{H}\}$ NMR triplet at 127.7ppm ($^3J_{\text{P-P}}$ 31.0Hz) and multiplet at 123.5ppm, ^{19}F NMR shows a singlet at -103.0ppm.

The analogous Cp* tribenzannulated complex can also be synthesised (Figure 2.7). The initial precursor complex 2a [$\text{Cp}^*\text{Fe}(\text{o-C}_6\text{H}_4\text{F})_2\text{PC}_6\text{H}_4\text{P}(\text{o-C}_6\text{H}_4\text{F})_2\text{MeCN}\rangle[\text{BF}_4]$] was synthesised as a red air sensitive powder, soluble in THF, in very good yield (94%). Characteristic peaks at 1.63ppm (Cp*) and 2.19ppm (CH₃CN) are seen in the ^1H NMR along with an aromatic multiplet 6.69-7.86ppm. In the $^{13}\text{C}\{^1\text{H}\}$ NMR a characteristic doublet is seen at 115.7ppm ($^2J_{\text{C-F}}$ 23.5Hz) showing the coupling between the *meta* carbon on the *ortho*fluorophenyl ring and the fluorine atom. A doublet of doublets is seen at 165.0ppm ($^1J_{\text{C-F}}$ 242.9Hz) representing the *ortho* carbon coupling to the adjacent fluorine and the phosphorus atom. Peaks for

the acetonitrile at 3.9ppm and 118.1ppm and for the Cp* at 9.5ppm and 87.3ppm were identified. A broad singlet is seen at 90.1ppm in the $^{31}\text{P}\{^1\text{H}\}$ NMR which is believed to represent the expected triplet from phosphorus, poor resolution means that the expected P-F coupling cannot be observed. The ^{19}F NMR shows the *ortho*fluoro groups as a singlet at -99.6ppm. After the co-ordination of phenylphosphine to form an air sensitive yellow powder 2b in very good yield (92%) the $^{31}\text{P}\{^1\text{H}\}$ NMR resonance for the diphosphine moves significantly downfield to 18.7ppm, although the resolution into a triplet is again not observed. A singlet representing the co-ordinated phenylphosphine appears at 10.1ppm. The ^{19}F NMR singlet observed in the initial diphosphine complex representing the *ortho*fluoro groups moves slightly downfield to -98.2ppm.

Post cyclisation 2c is formed, the $^{31}\text{P}\{^1\text{H}\}$ NMR shows a triplet of triplets at 117.3 (tt, $^2J_{\text{P-P}}$ 102.4Hz, $^6J_{\text{P-F}}$ 35.3Hz) due to the coupling between the unique phosphine (with the attached phenyl group) and initially the two chemically equivalent phosphines (with attached *ortho*fluorophenyl groups) followed by coupling to the *ortho* fluorine spin active nuclei. A multiplet is observed 112.0-111.7ppm representing the chemically equivalent phosphines. No clear coupling is resolved in the $^{31}\text{P}\{^1\text{H}\}$ NMR spectrum due to the secondary interactions which occur as a result of the chemically equivalent phosphines being magnetically inequivalent.

The Cp* dibenzannulated triphosphorus macrocycle could not be synthesised as the addition of base resulted in immediate decomposition possibly as a result of the methyl groups attached to the Cp* attacking the labile *ortho*fluorophenyl rings.

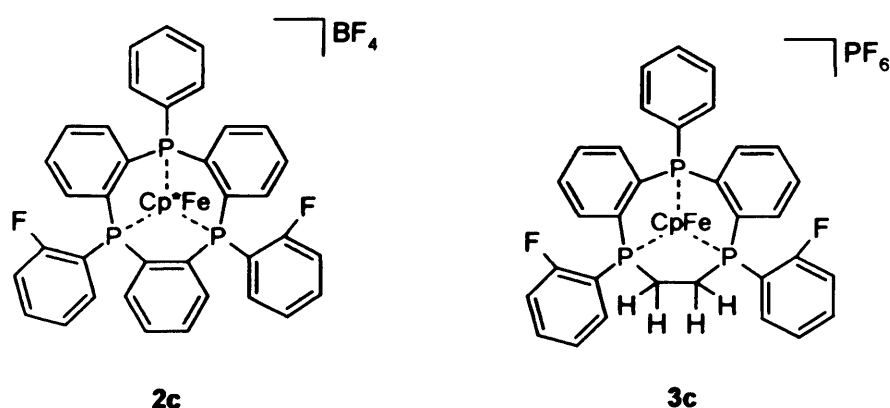


Figure 2.7 Both Cp* and ethylated triphosphorus macrocycles can be synthesised.

Synthesis of Triphosphorus, Tribenzannulated Macrocycles with Primary Diphosphines

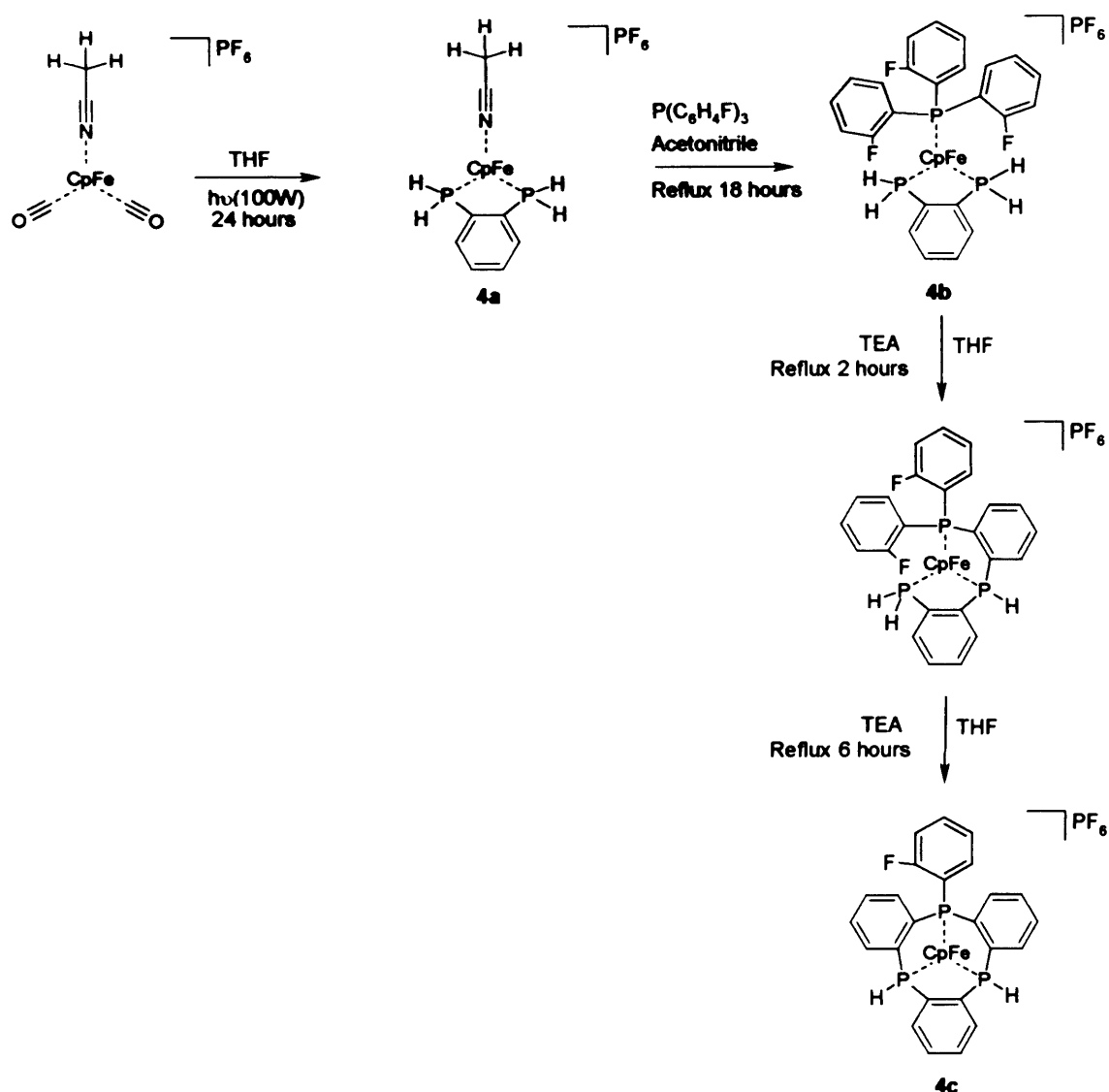


Figure 2.8, Method 2, synthesis of triphosphorus tribenzannulated macrocycles from a bidentate primary phosphine and a monodentate fluoroarylated phosphine.

In order to explore the potential of the novel dehydrofluorinative synthesis the diortho-fluorophenyl bisphosphinobenzene ligand was replaced with the primary diphosphine, bisphosphinobenzene. Phenyl phosphine was replaced with triortho-fluorophenyl phosphine followed by base cyclisation. The advantage to this methodology was the ability to use a wider range of primary diphosphine (and diarsine) ligands (Figure 2.8, Method 2).

Triortho-fluorophenyl phosphine was added to [CpFe(H₂PC₆H₄PH₂)(CH₃CN)][PF₆] (**4a**)¹¹ and refluxed to give **4b** as a yellow air sensitive powder in good yield (82%) as shown in Figure 2.8. The ³¹P{¹H} NMR

spectrum shows a singlet at 16.0ppm representing the co-ordinated bisphosphinobenzene. A broad singlet at 22.0ppm represents co-ordinated $P(C_6H_4F)_3$, the peak moves considerably downfield after co-ordination from -42.1ppm ($^3J_{P-F}$ 56.6Hz) for the free ligand. The ^{19}F NMR spectrum shows a characteristic singlet at -97.9ppm . The ^1H NMR shows a broad singlet at 3.61 due to the Cp resonance and complex multiplets from 6.94-7.39ppm which can be assigned to the aromatic protons. The $^{13}\text{C}\{^1\text{H}\}$ NMR spectrum shows a doublet of doublets at 165.0ppm ($^1J_{C-F}$ 285.3Hz) in addition to other aromatic resonances.

After the addition of an excess amount of triethylamine, the cyclisation was monitored by $^{31}\text{P}\{^1\text{H}\}$ NMR spectroscopy. After refluxing the mixture for 2 hours a triplet at 89.1ppm ($^3J_{P-F}$ 35.7Hz) was observed when the cyclisation had partially completed (*i.e.* one backbone had been formed), a complex multiplet at 66.5ppm representing the tertiary phosphine was also observed. Further loss of a fluorine atom from one of the aryl groups led to the formation of a doublet at 90.7ppm ($^3J_{P-F}$ 35.7Hz). Cyclisation was completed after 8 hours to give **4c** as a yellow air stable powder in good yield (74%) which resulted in the formation of a complex multiplet in the $^{31}\text{P}\{^1\text{H}\}$ NMR spectrum from 118.4-122.8ppm. The ^{19}F NMR spectrum showed a characteristic singlet at -101.8ppm . Resonances corresponding to aromatic protons (6.95-7.71ppm) and the Cp resonance (3.73ppm) were seen in the ^1H NMR spectrum. $^{13}\text{C}\{^1\text{H}\}$ NMR shows a doublet of doublets at 165.0ppm ($^1J_{C-F}$ 286.0Hz), as observed in the previous synthesis, the $^2J_{C-P}$ coupling constant is not resolved. The molecular ion was observed in the mass spectra at 779.6Da/e.

The Cp* tribenzannulated triphosphorus macrocycle (Figure 2.9, **5c**) can also be synthesised by the initial preparation of the Cp* iron(II) bisphosphinobenzene acetonitrile complex¹² as a red air sensitive powder, followed by the addition of tri*ortho*fluorophenyl phosphine which led to the synthesis of a yellow air sensitive powder in good yield (82%) **5b**. Characteristic Cp* resonances are seen in the ^1H NMR at 1.72ppm and in the carbon NMR spectra at 9.91ppm and 87.24ppm. Other characteristic resonances in the $^{13}\text{C}\{^1\text{H}\}$ NMR are seen at 115.2ppm (doublet, $^2J_{C-F}$ 24.0Hz) resulting from coupling between the *ortho*fluoro group and the *meta* carbon in the *ortho*fluorophenyl ring. A doublet is seen at 164.0ppm ($^1J_{C-F}$ 234.3Hz), the spectra is insufficiently resolved to observe the further splitting of this doublet into a doublet of doublets. In the $^{31}\text{P}\{^1\text{H}\}$ NMR spectrum a singlet is seen at 15.1ppm illustrating the co-ordination of the bisphosphinobenzene to the Cp* iron template, a doublet at 18.00ppm ($^3J_{P-F}$ 41.7Hz) shows the coupling between the *ortho*fluoro atom and the co-ordinating tertiary phosphine. A broad singlet at -100.8ppm in the ^{19}F NMR shows the *ortho*fluorine. After cyclisation with triethylamine a yellow air

sensitive powder is formed in a very good yield (90%) **5c**, characteristic Cp* resonances (as above) are seen in both the proton and carbon spectra.

$^{31}\text{P}\{^1\text{H}\}$ NMR resonances show a multiplet at 61.5ppm which has been assigned to the partially cyclised macrocycle, a broad singlet is seen at 115.1ppm and a multiplet from 105.2-111.3ppm is also observed with both resonances representing the fully cyclised macrocycle. The ^{19}F NMR singlet moves marginally upfield to -103.4ppm. A characteristic P-H stretch is observed in the infrared spectrum at 2310cm^{-1} .

Other triphosphorus macrocycles have been made by method 2 including macrocycles made from bisphosphinoethane as a replacement bidentate phosphine (Figure 2.9, **6c** and **7c**). The precursors can again be characterised with peaks representing the co-ordinated diphosphine in the $^{31}\text{P}\{^1\text{H}\}$ NMR at 16.0ppm and the co-ordinated monophosphine at 22.8ppm. The cyclised macrocycle **6c** has a characteristic $^{31}\text{P}\{^1\text{H}\}$ NMR broad singlet at 111.5ppm and multiplet from 105.2-105.9ppm, ^{19}F NMR shows a singlet at -101.8ppm.

Complex **7c** (Figure 2.8) is also synthesised from the corresponding bisphosphinoethane Cp* complex the reaction gave a poor yield in comparison to similar synthetic procedures (48%), characteristic Cp* data is seen in the proton and carbon spectra for all of the precursor complexes. The $^{31}\text{P}\{^1\text{H}\}$ NMR for the macrocyclic precursor **7b** shows a multiplet at 19.0ppm representing the co-ordinated tri-*ortho*fluorophenyl phosphine and a singlet at 12.3ppm representing the co-ordinated bisphosphinoethane a characteristic peak is also seen at -100.0ppm in the ^{19}F NMR spectrum. After cyclisation with triethylamine the macrocycle was isolated in poor yields (32%) as a yellow air sensitive solid **7c**. A singlet in the ^{19}F NMR appears at 102.4ppm. The $^{13}\text{C}\{^1\text{H}\}$ NMR spectrum shows a characteristic doublet of doublets at 166.2ppm ($^1J_{\text{C-F}} 248.4\text{Hz}$, $^2J_{\text{C-P}} 9.2\text{Hz}$) due to the *ortho*fluorophenyl group. The ^{31}P NMR spectrum shows multiplets between 112.3 and 117.4 representing the fully cyclised macrocycle.

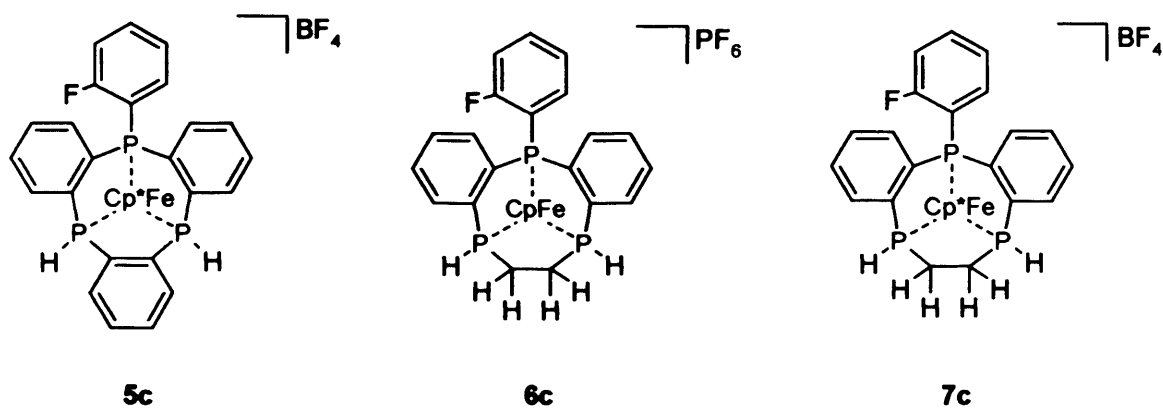


Figure 2.9

Synthesis of Triarsenic, Tribenzannulated Macrocycles

The first example of a template synthesised triarsenic macrocycle has been made in good yield by a method analogous to method 1 (Figure 2.6). *Diortho*fluorophenyl bisphosphinobenzene and phenyl phosphine were replaced by the analogous arsines. Complexes are represented in Figure 2.10 with **8a** representing the co-ordinated diarsine, **8b** the co-ordinated diarsine and monoarsine and **8c** the cyclised macrocycle.

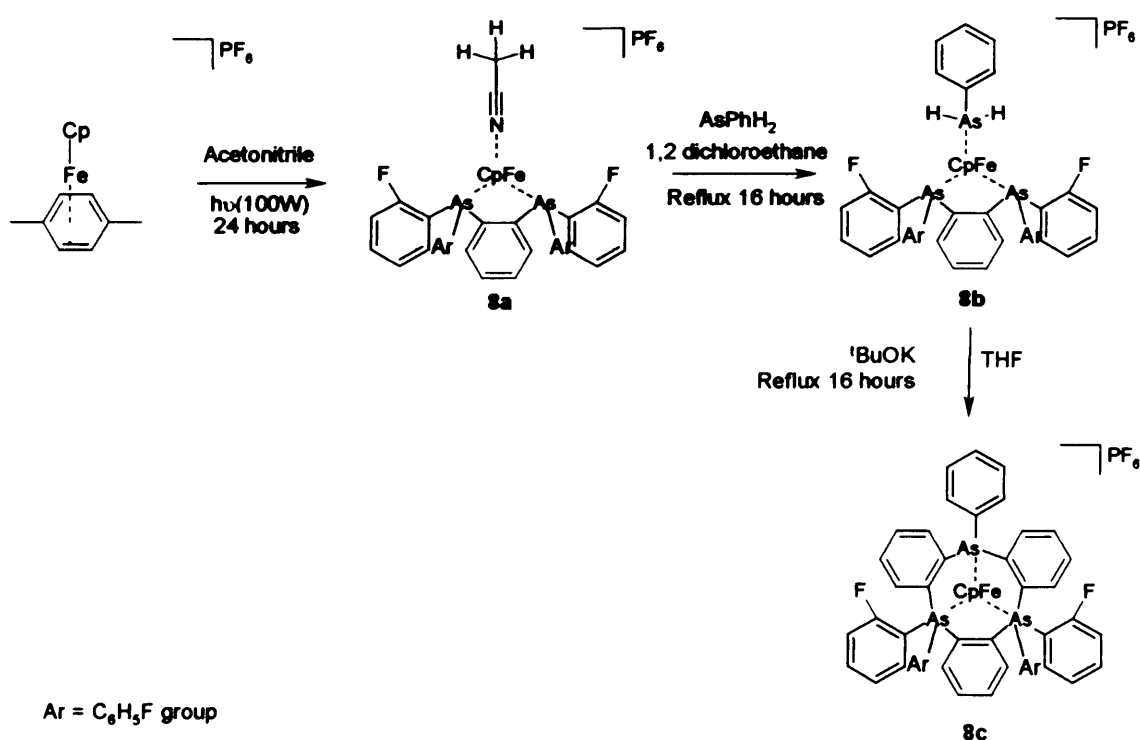


Figure 2.10, synthesis of triphosphorus tribenzannulated macrocycles from a bidentate fluoroarylated arsine and a monodentate primary arsine.

Diorthofluorophenyl bisarsinobenzene was added to $[\text{CpFe}(\text{CO})_2(\text{CH}_3\text{CN})][\text{PF}_6]$ and refluxed to form complex **8a**. The ^{19}F NMR spectrum showed a characteristic singlet at -99.8ppm . The $^{13}\text{C}\{^1\text{H}\}$ NMR spectrum showed a singlet at 2.6ppm representing the co-ordinated acetonitrile, a broad singlet for the Cp is seen at 76.4ppm . As for the phosphorus analogue a doublet with C-F coupling is seen at 115.5ppm ($^2J_{\text{C-F}}$ 24.1Hz). Another characteristic doublet for the ortho-fluorocarbon is observed at 165.0ppm ($^1J_{\text{C-F}}$ 241.9Hz). In the infrared spectrum a characteristic peak at 2262cm^{-1} shows the co-ordinated acetonitrile.

The addition of phenylarsine to complex **8a** gave complex **8b**. This complex was characterised by a upfield movement in the ^{19}F NMR spectrum to -101.5ppm for the co-ordinated diarsine ligand on addition of phenylarsine. The $^{13}\text{C}\{^1\text{H}\}$ NMR spectrum showed the characteristic doublet (assigned to the carbon bearing the fluorine) at 164.9ppm ($^1J_{\text{C-F}}$ 239.8Hz).

Refluxing **8b** with base gave rise to the formation of **8c**, the fully cyclised macrocycle. The ^{19}F NMR spectrum shows a singlet at -100.1ppm . The $^{13}\text{C}\{^1\text{H}\}$ NMR spectrum showed similar peaks to the precursor complex.

The triarsenic macrocycle is unique. It is the first time that this novel template synthesised macrocycle has been prepared. The only other example of a triarsenic macrocycle was synthesised by Kyba under high dilution conditions where he was able to obtain the non-templated macrocycle.¹³ By synthesising the macrocycle in this way the yield has been improved from 30-60% isolated yield for the high dilution methodology to 73% isolated yield for the dehydrofluorination template methodology although demetallation has yet to be successfully attempted. Final structural characterisation was carried out by crystallography, which Kyba was unable to achieve.

The reaction scheme initially completed on the CpFe^+ template was however unable to be completed on an alternative Cp^*Fe^+ template presumably due to either steric factors due to the larger size of Cp^* in comparison to Cp or electronic factors resulting from the increased electron donation from Cp^* .

In comparison to the equivalent triphosphorus example after co-ordination of the precursor dipnictide the diarsine complex was unstable in acetonitrile solution and decomposed to form the free diarsine ligand and products resulting from the decomposition of the $[\text{CpFe}(\text{CH}_3\text{CN})_3]^+$. Base cyclisation proceeded marginally more quickly for the triarsine ligand. Overall the novel synthetic technique has proved versatile for a wide variety of phosphine and arsine ligands.

Mixed Donor Macrocycles

One of the main aims of using mixed donor ligands is their hemilability. Hemilabile ligands are those which are polydentate in nature and contain two (or more) different donor atoms.¹⁴ Another characteristic of hemilabile ligands is the difference in lability between the different types of bonding groups within the ligand. Often this difference in lability results in the replacement of one bonding group but not the others, because the ligand is chelating in nature the bonding group stays close to the metal and is able to stabilise lower co-ordination reaction intermediates.

Metal complexes with hemilabile ligands are often used in catalysis due to their ability to create transient vacant co-ordination sites on the metal ion. By creating mixed donor macrocycles we hope to create macrocycles which are stable to base cyclisation yet with labile bonding groups which can be attacked by incoming ligands. This would be promoted by a strongly competing ligand and the process may encourage the whole macrocycle to dissociate from the metal template.

Continuing from the synthesis of triphosphorus and triarsenic macrocycles the expansion of the methodology to mixed donor macrocycles was the next obvious step. We attempted to synthesise (on Cp*Fe⁺ and CpFe⁺ templates) both diarsine monophosphine complexes and diphosphine monoarsine complexes. We were only able to utilise the bisarsinobenzene ligand for the CpFe⁺ template. All of the mixed donor macrocycles synthesised have been illustrated (Figure 2.11), along with characteristic data for the complete macrocycles (Table 2.1).

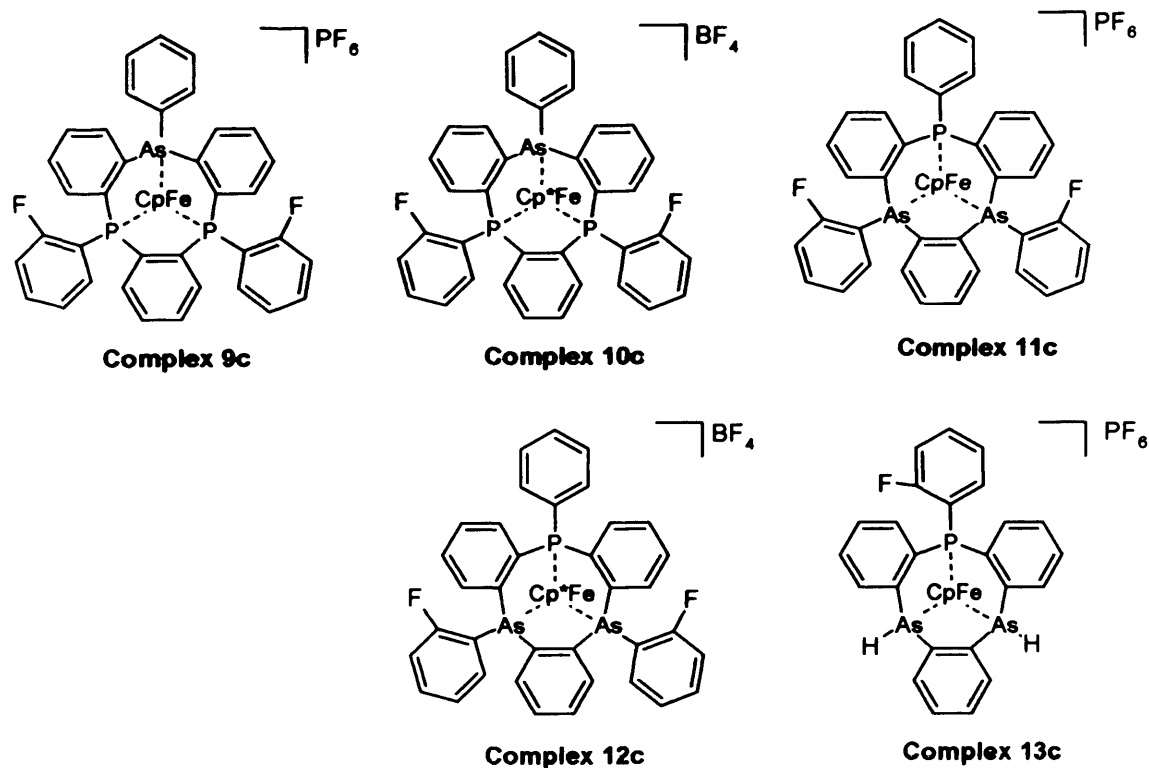
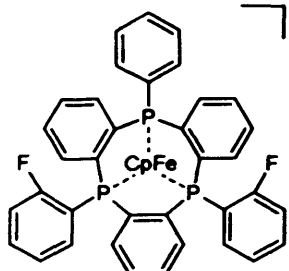
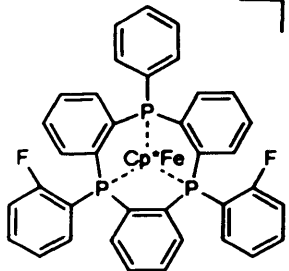
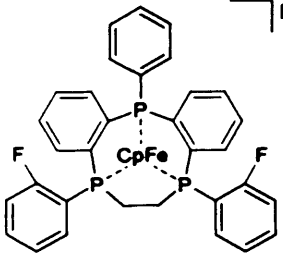
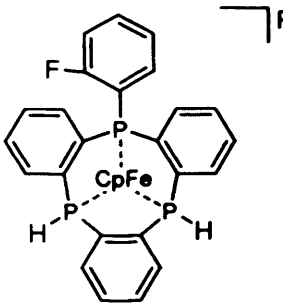
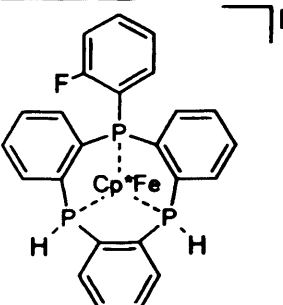
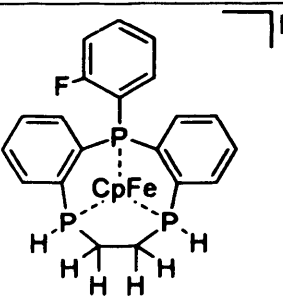
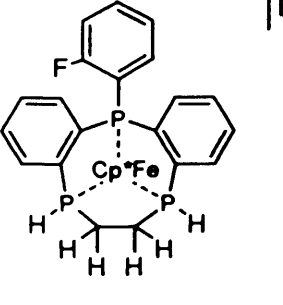
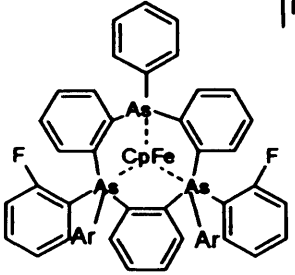
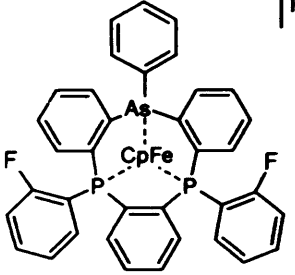
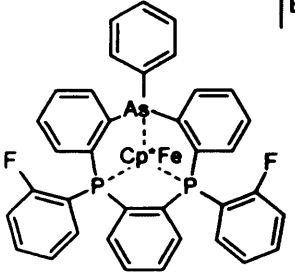
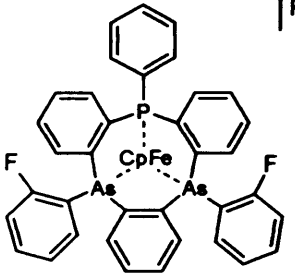
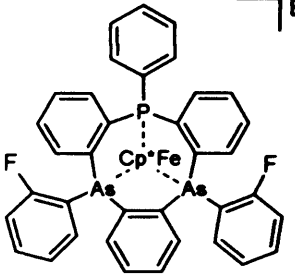


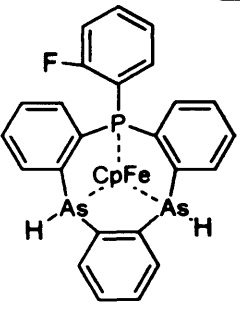
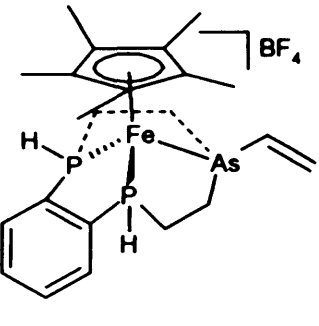
Figure 2.11 All of the mixed donor macrocycles successfully synthesised.

Table 2.1 $^{31}\text{P}\{^1\text{H}\}$ and ^{19}F NMR data for all of the macrocycles synthesised.

Complex	Number	$^{31}\text{P}\{^1\text{H}\}$ NMR Data	^{19}F NMR Data	Yield
	1c	119.6ppm (tt, $^2J_{\text{P}}$, $^6J_{\text{P}}$, $^{\rho}116.1\text{Hz}$, $^{\rho}32.8\text{Hz}$), 127.5ppm complicated multiplet	-98.1ppm (s), at 83K the singlet became a doublet of doublets - 99.2ppm ($^3J_{\text{F}}$, $^6J_{\text{F}}$, $^{\rho}100.6\text{Hz}$, $^{\rho}38.2\text{Hz}$).	78%
	2c	117.3ppm (tt, $^2J_{\text{P}}$, $^6J_{\text{P}}$, $^{\rho}102.4\text{Hz}$, $^{\rho}35.3\text{Hz}$), 112.0-111.7ppm(m)	-100.9ppm (s)	78%

	3c	127.7ppm (t, 2J_P , ρ 31.0Hz), 122.8-124.1ppm (m)	-103.0ppm (s)	62%
	4c	118.4-122.8ppm (m)	-101.8ppm (s)	74%
	5c	115.1ppm (s), 105.2-111.3ppm (m)	-103.4ppm (s)	65%
	6c	111.5ppm (s), 105.2-105.9ppm (m)	-101.8ppm (s)	90%
	7c	112.3-117.4 (m)	-102.4ppm (s)	32%

 <p>PF₆⁻ 8c</p>			<p>-100.1ppm (s, major peak), -101.5ppm (s, minor peak), at 83K the singlet became three peaks at -101.5, -101.6 and -102.4ppm.</p>	73%
 <p>PF₆⁻ 9c</p>	135.0ppm(s), 135.6ppm(s)		-102.4ppm (s)	78%
 <p>BF₄⁻ 10c</p>	130.38-132.09 (m)		-102.68 (s)	78%
 <p>PF₆⁻ 11c</p>	134.6ppm (s)		-100.1ppm (s)	73%
 <p>BF₄⁻ 12c</p>	112.0ppm (s)		-102.4ppm (s)	71%

	13c	122.0-137.9 (m)	-101.6ppm (s)	42%
	14c	106.4ppm (s)		24%

All complexes synthesised with primary arsines were much more unstable to heat than their phosphine alternatives which could at least partially explain the poor yield seen for complex 13c.

Variable Temperature NMR Spectroscopy

Variable temperature NMR spectroscopy was carried out on the tribenzannulated triphosphorus and triarsenic macrocycles to deconvolute the complicated NMR signals seen for ^{31}P NMR in these complexes. We can also observe the splitting of the unexplained ^{19}F singlet as the samples are cooled. By cooling down the NMR samples any kinetic factors causing complicated NMR signals will be reduced, this includes ring rotation about the P-R [with R representing H, Ph or (*o*-C₆H₄F)] bond. The ^{19}F signal is expected to be split by P-F coupling however this is not observed, an explanation has yet to be found.

The $^{31}\text{P}\{^1\text{H}\}$ VT NMR for the Cp tribenzannulated triphosphorus macrocycle 1c shows the triplet of triplets becoming less defined. The couplings are difficult to identify as the spectra are second order, at cooler temperatures additional resonances can be seen appearing within the doublet of triplets possibly as a result of the isolation of different rotamers which can be seen in the ^{19}F NMR spectra.

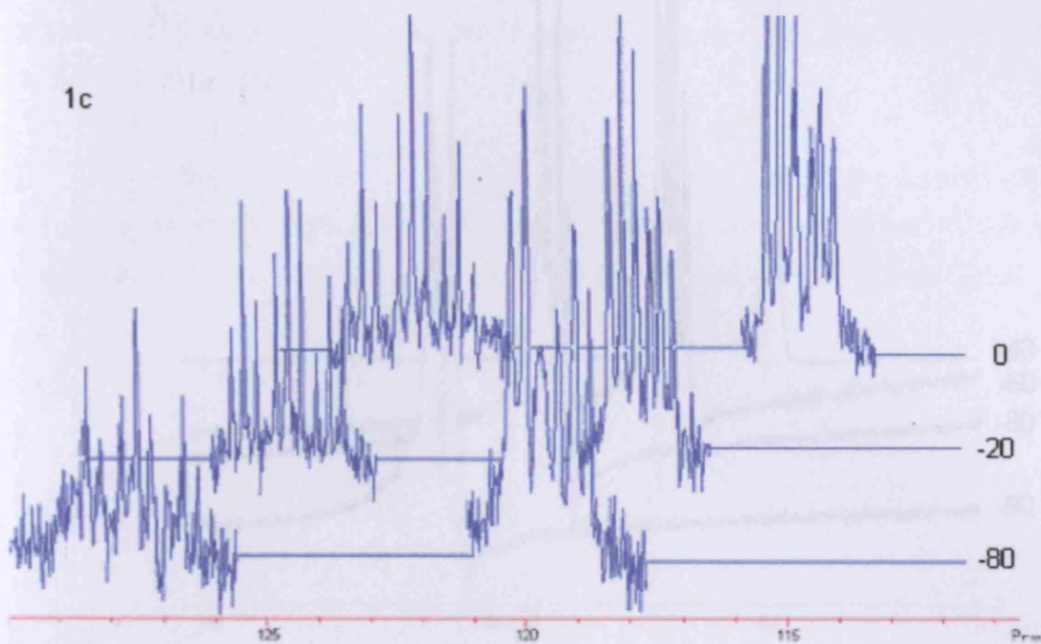


Figure 2.12, Variable temperature $^{31}\text{P}\{^1\text{H}\}$ NMR spectra for $[\text{CpFeP}(\text{C}_6\text{H}_4\text{F})(\text{C}_6\text{H}_4)\text{P}(\text{C}_6\text{H}_4\text{F})(\text{C}_6\text{H}_4)\text{P}(\text{C}_6\text{H}_5)(\text{C}_6\text{H}_4)][\text{B}(\text{C}_6\text{H}_5)]$ taken at -80°C , -20°C and 0°C .

The $^{31}\text{P}\{^1\text{H}\}$ NMR spectrum (Figure 2.12) shows a well defined triplet of triplets at 0°C representing the unique phosphorus coupled to the two chemically equivalent phosphorus atoms and then to the *ortho* fluorine atoms. The ^{19}F NMR in comparison shows no coupling to any phosphorus atoms.



Figure 2.13 Possible rotamer structures seen in the ^{31}P NMR after cooling to -80°C .

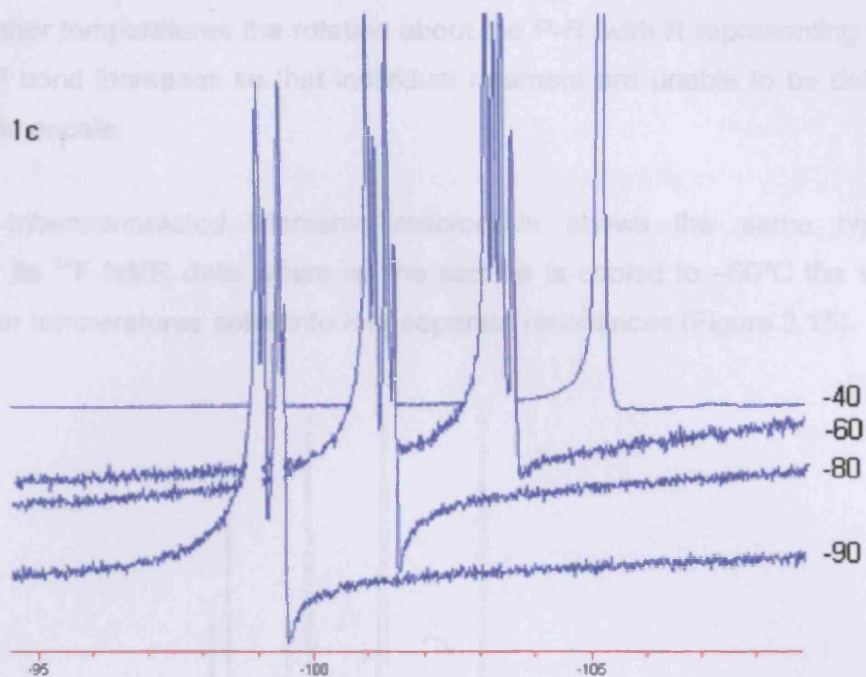


Figure 2.13, Variable temperature ^{19}F NMR spectra for $[\text{CpFeP}(\text{C}_6\text{H}_4\text{F})(\text{C}_6\text{H}_4)\text{P}(\text{C}_6\text{H}_4\text{F})(\text{C}_6\text{H}_4)\text{P}(\text{C}_6\text{H}_5)(\text{C}_6\text{H}_4)][\text{B}(\text{C}_6\text{H}_5)]$ taken at -90°C , -80°C , -60°C and -40°C .

The ^{19}F NMR variable temperature spectra (Figure 2.13) shows the appearance of four peaks, the nature of these peaks cannot be conclusively determined but may be formed as a result of the isolation of different rotamers within the macrocyclic structure (Figure 2.14).

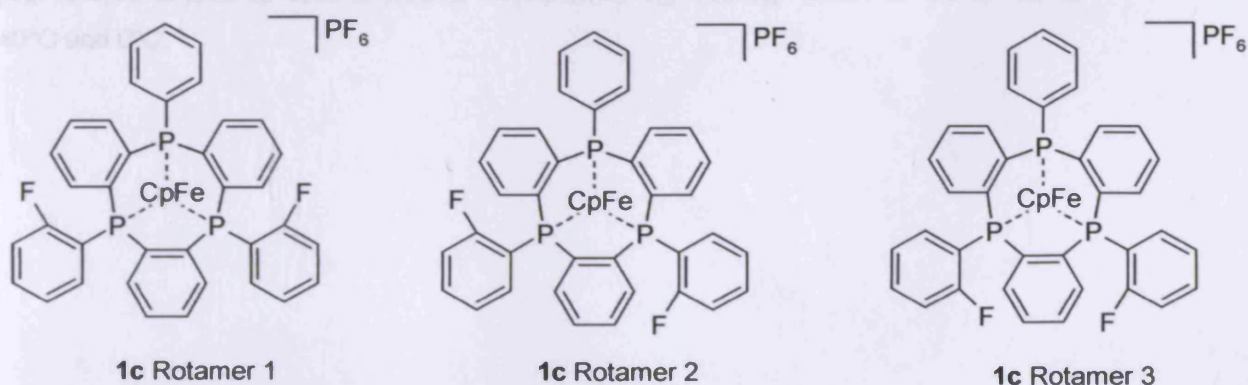


Figure 2.14 Possible rotamer structures seen in the ^{19}F NMR after cooling to -60°C

At higher temperatures the rotation about the P-R [with R representing H, Ph or (*o*-C₆H₄F)] bond increases so that individual rotamers are unable to be detected on an NMR timescale.

The tribenzannulated triarsenic macrocycle shows the same type of behaviour in its ¹⁹F NMR data where as the sample is cooled to -60°C the singlet seen at higher temperatures splits into four separate resonances (Figure 2.15).

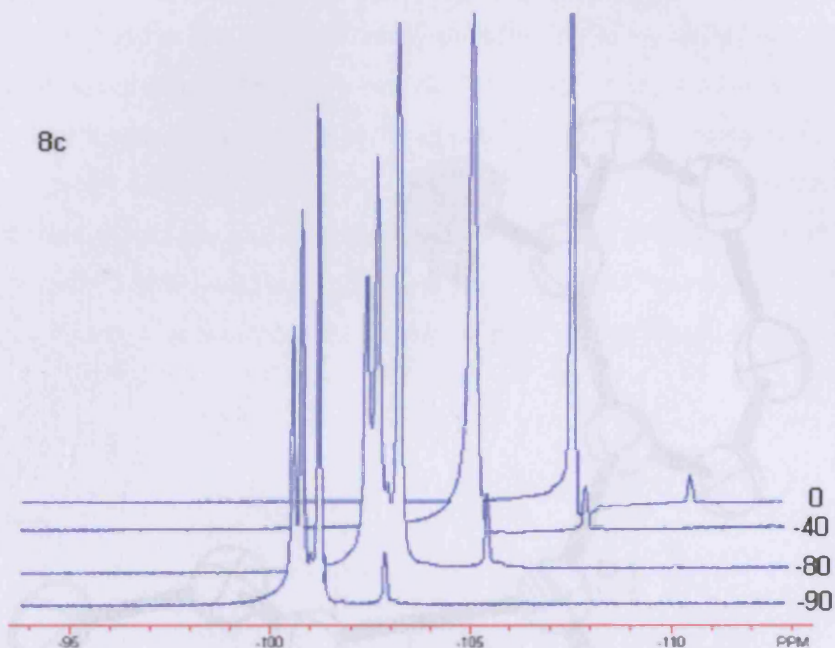


Figure 2.15, Variable temperature ¹⁹F NMR spectra for [CpFeAs(C₆H₄F)(C₆H₄)As(C₆H₄F)(C₆H₄)As(C₆H₅)(C₆H₄)] [B(C₆H₅)] taken at -90°C, -80°C, -40°C and 0°C.

Crystal Structures

Crystal Structure of $P(C_6H_4F)_3$

White crystalline blocks were obtained from a solution of $P(C_6H_4F)_3$ from acetonitrile at room temperature. The crystals were crystallographically analysed for the first time to give the following crystal structure (Figure 2.16).

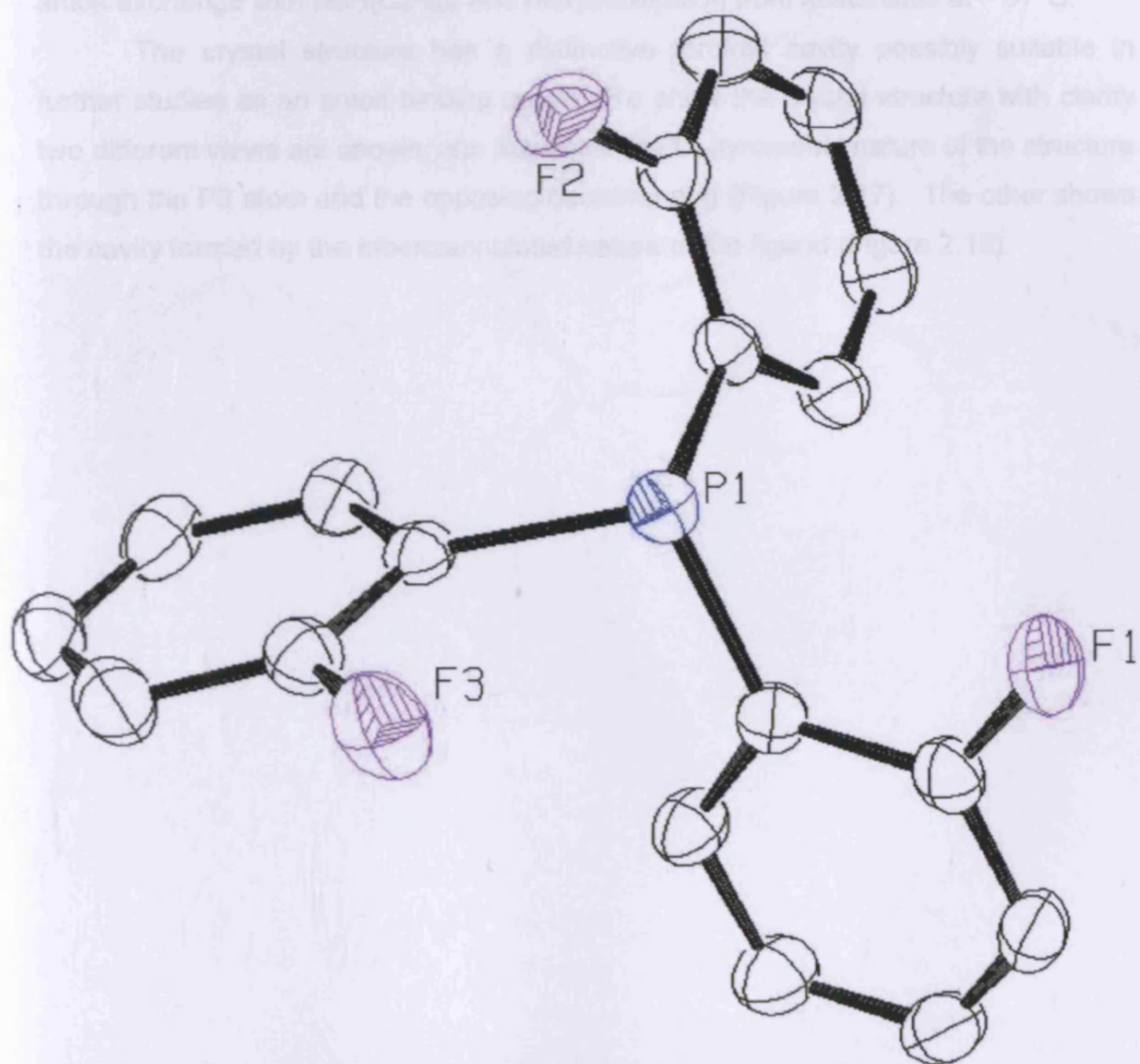


Figure 2.16

The crystals were monoclinic with a space group of $P2(1)/n$, the final R indices were $R1 = 0.0432$ and $wR2 = 0.1006$. The novel crystal structure has P-C bond lengths of $1.837(2)\text{\AA}$ (average) and C-F bond lengths of $1.362(2)\text{\AA}$ (average) both within the Van der Waals radii of the constituent atoms and similar to other known examples. The angles around the phosphines are 302.28° indicating a pyramidal geometry as expected.

Crystal Structure of $[\text{CpFeP}(\text{C}_6\text{H}_4\text{F})(\text{C}_6\text{H}_4)\text{P}(\text{C}_6\text{H}_4\text{F})(\text{C}_6\text{H}_4)\text{P}(\text{C}_6\text{H}_5)(\text{C}_6\text{H}_4)][\text{B}(\text{C}_6\text{H}_5)_4]$ 1c

Fine needle like yellow crystals suitable for X-ray diffraction were obtained by anion exchange with $\text{NaB}(\text{C}_6\text{H}_5)_4$ and recrystallisation from acetonitrile at -37°C .

The crystal structure has a distinctive toroidal cavity possibly suitable in further studies as an anion binding space. To show the crystal structure with clarity two different views are shown, one illustrates the C_v symmetric nature of the structure through the P3 atom and the opposing benzene ring (Figure 2.17). The other shows the cavity formed by the tribenzannulated nature of the ligand (Figure 2.18).

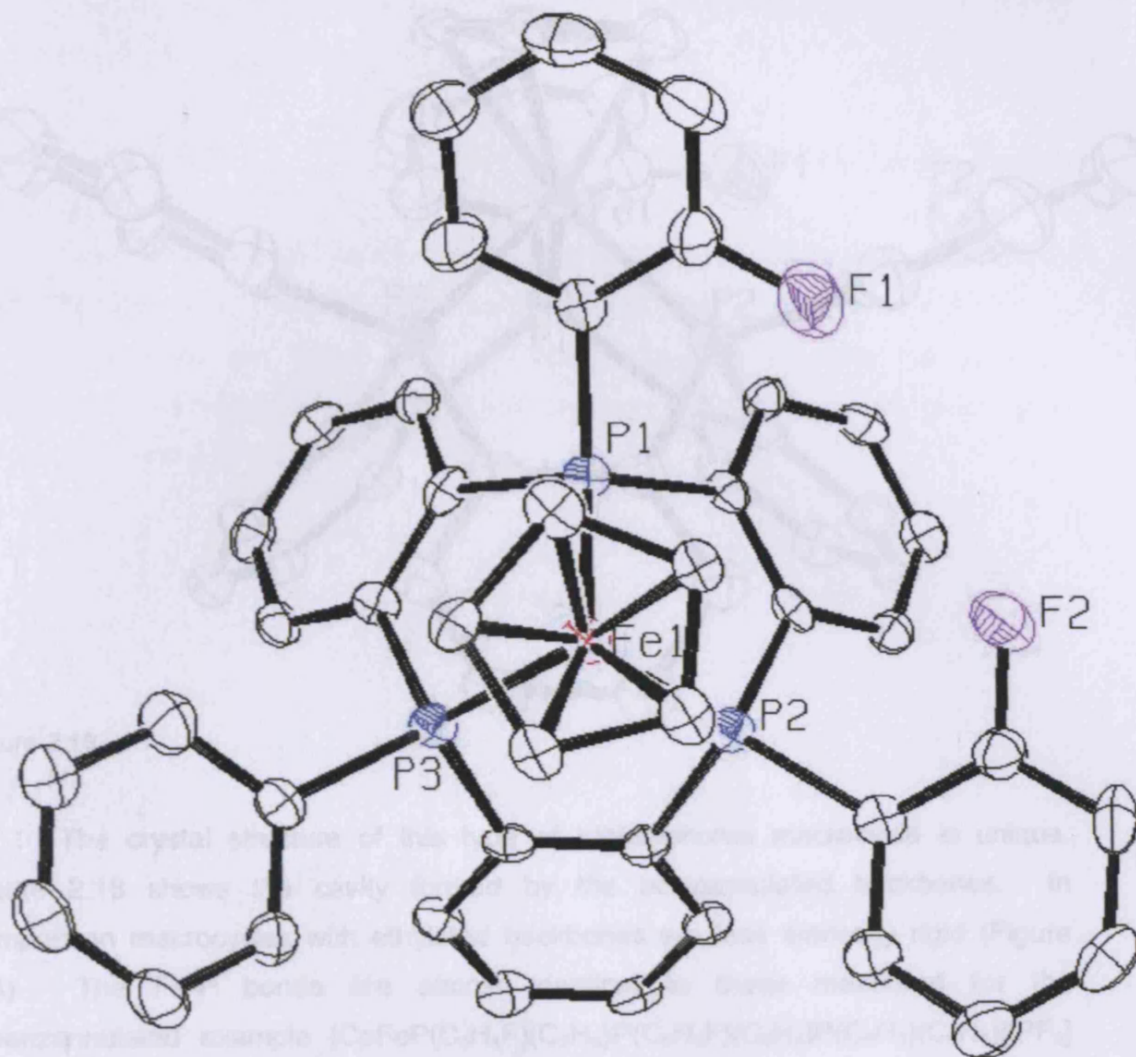


Figure 2.17

2.146(3) Å. The average C-P bond length is 1.55(7) Å which is significantly shorter than the C-F bond length of 1.35(3) Å seen in $\text{P}(\text{O}-\text{C}_6\text{H}_4\text{F}_2)_3$ crystal structure (although the values are not directly comparable as the macrocycle is bound to a metal ion and the free ligand is not). The $R1$ value for this crystal structure (0.0784) indicates a degree of unreliability possibly resulting from disorder within the crystal structure. This can partially be explained by the 2-fluorid disorder which has been partially modelled within the C_6 ring (i.e. it relates the predicted positions of the individual atoms between most uncertain) and the rotation of the orthodifluorophenyl rings about the C-P bond. The crystal structure data shows three orthodifluorophenyl rings attached at the meta-positions about the iron, this is due to the inability of x-ray crystallography to define a particular orientation of a molecule when the structure is solved.

The distance between the centers of the C_6 ring and the Fe is 1.535 Å. The distance between the Fe and the center of the P₃ ring is 1.313 Å. The bond angles

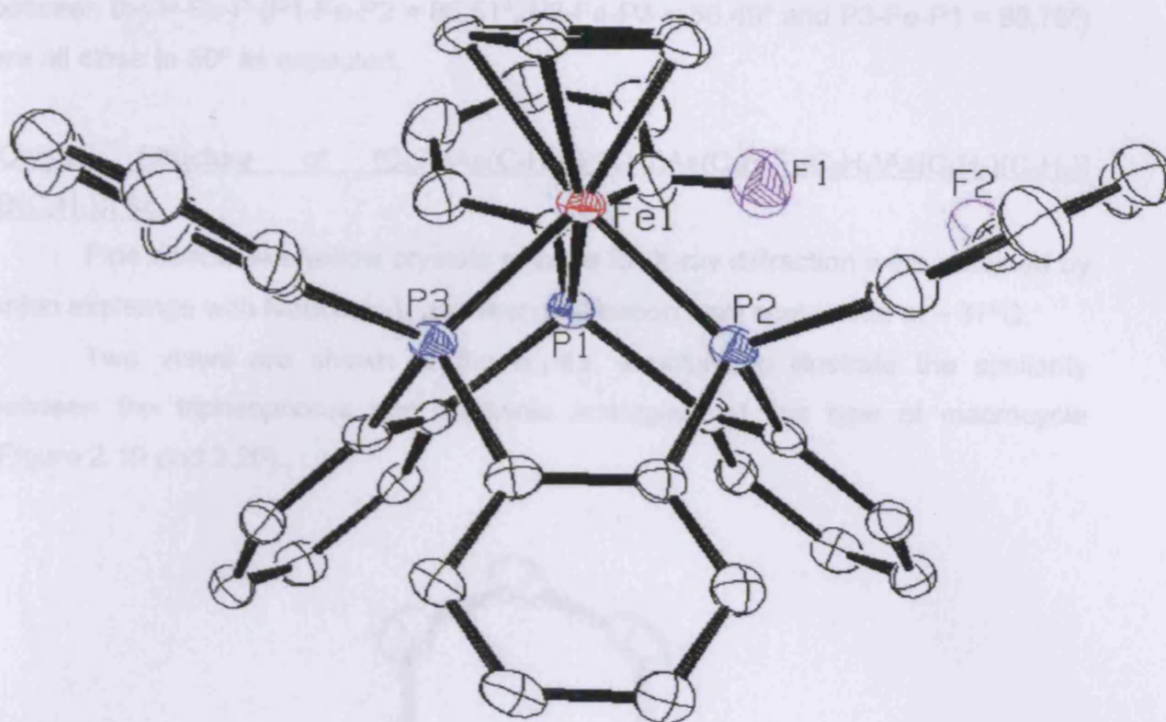


Figure 2.18

The crystal structure of this type of triphosphorus macrocycle is unique. Figure 2.18 shows the cavity formed by the benzannulated backbones. In comparison macrocycles with ethylated backbones are less sterically rigid (Figure 2.4). The Fe-P bonds are almost identical to those measured for the dibenzannulated example $[\text{CpFeP}(\text{C}_6\text{H}_4\text{F})(\text{C}_2\text{H}_4)\text{P}(\text{C}_6\text{H}_4\text{F})(\text{C}_6\text{H}_4)\text{P}(\text{C}_6\text{H}_5)(\text{C}_6\text{H}_4)][\text{PF}_6]$ (2.151 Å) at 2.149(3) Å. The average C-F bond length is 1.310(7) Å which is significantly shorter than the C-F bond length of 1.362(2) Å seen in $\text{P}(\text{o-C}_6\text{H}_4\text{F})_3$ crystal structure (although the values are not directly comparable as the macrocycle is bound to a metal ion and the free ligand is not). The R1 values for this crystal structure (0.0784) indicate a degree of uncertainty possibly resulting from disorder within the crystal structure. This can partially be explained by the inherent disorder (which has been partially modelled) within the Cp ring (as it rotates the predicted positions of the individual atoms become more uncertain) and the rotation of the *ortho*fluorophenyl rings about the C-P bond. The crystal structure data shows three *ortho*fluorophenyl rings attached to the three phosphorus atoms, this is due to the inability of x-ray crystallography to isolate a particular orientation of a molecule when the structure is solved.

The distance between the centroid of the Cp ring and the Fe is 1.535 Å. The distance between the Fe and the centroid of the P_3 ring is 1.313 Å. The bond angles

between the P-Fe-P (P1-Fe-P2 = 86.51°, P2-Fe-P3 = 86.49° and P3-Fe-P1 = 86.75°) are all close to 90° as expected.

Crystal Structure of [CpFeAs(C₆H₄F)(C₆H₄)As(C₆H₄F)(C₆H₄)As(C₆H₅)(C₆H₄)] [B(C₆H₅)₄] 8c

Fine needle like yellow crystals suitable for X-ray diffraction were obtained by anion exchange with NaB(C₆H₅)₄ and recrystallisation from acetonitrile at -37°C.

Two views are shown of the crystal structure to illustrate the similarity between the triphosphorus and triarsenic analogues of this type of macrocycle (Figure 2.19 and 2.20).

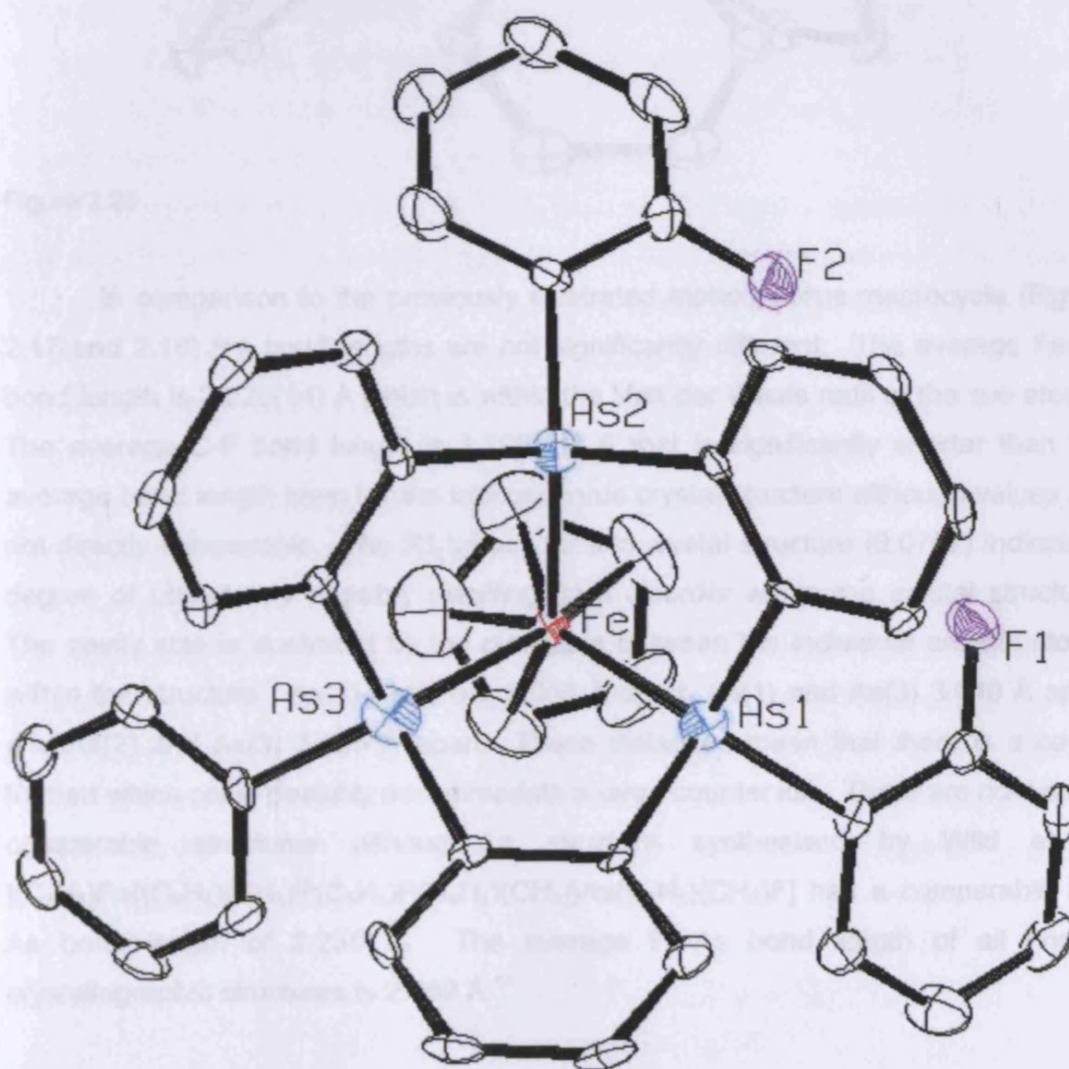


Figure 2.19

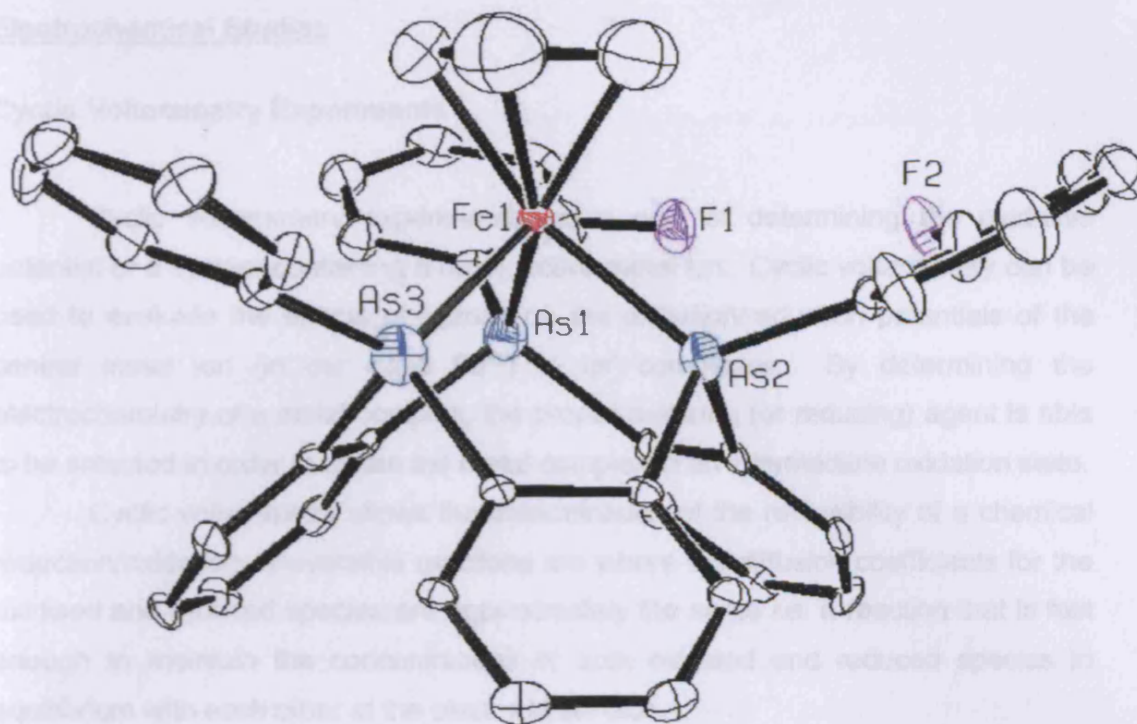


Figure 2.20

In comparison to the previously illustrated triphosphorus macrocycle (Figure 2.17 and 2.18) the bond lengths are not significantly different. The average Fe-As bond length is 2.228(14) Å which is within the Van der Waals radii of the two atoms. The average C-F bond length is 1.295(11) Å that is significantly shorter than the average bond length seen for the triphosphorus crystal structure although values are not directly comparable. The R1 values for this crystal structure (0.0707) indicate a degree of uncertainty possibly resulting from disorder within the crystal structure. The cavity size is illustrated by the distances between the individual arsenic atoms within the structure. As(1)-As(2) are 3.063 Å apart, As(1) and As(3) 3.049 Å apart and As(2) and As(3) 3.065 Å apart. These distances mean that there is a cavity formed which could possibly accommodate a large counter ion. There are no directly comparable structures although a structure synthesised by Wild et al $[(C_5H_5)Fe\{(C_6H_5)(CH_3)P(C_6H_4)P(C_6H_5)(CH_3)\}As(C_6H_5)(CH_3)F]$ has a comparable Fe-As bond length of 2.235 Å. The average Fe-As bond length of all known crystallographic structures is 2.369 Å.¹⁵

	Oxidation potential, M(0)-M(II), Fe-Fe ²⁺
Reference	
$[1] [As]_3P_3O_3$	+0.21V
$[1] [As]_3P_3O_3$	+0.20V
$[1] [As]_3P_3O_3$	+0.18V

Electrochemical Studies

Cyclic Voltammetry Experiments

Cyclic voltammetry experiments are a way of determining the oxidative potential of a system containing a redox active metal ion. Cyclic voltammetry can be used to evaluate the effects of ligands on the oxidation/reduction potentials of the central metal ion (in our case Fe^{2+}) in its' complexes. By determining the electrochemistry of a metal complex, the proper oxidising (or reducing) agent is able to be selected in order to obtain the metal complex in an intermediate oxidation state.

Cyclic voltammetry allows the determination of the reversibility of a chemical reduction/oxidation. Reversible reactions are where the diffusion coefficients for the oxidised and reduced species are approximately the same *i.e.* a reaction that is fast enough to maintain the concentrations of both oxidised and reduced species in equilibrium with each other at the electrode surface.

Many systems do in fact look fully reversible when the voltage sweep is done slowly but on increasing the scan rate, the peak separation increases. This indicates that the nature of the peak separation is dependant on the stress applied to the system. These reactions are classed as quasi-reversible reactions. Where the peaks are separated so that there are no overlap of peaks the reactions are classed as irreversible.

Cyclic voltammetry has been used to compare and contrast the oxidation potentials of the macrocycles synthesised to compare their lability. The oxidation potential of the macrocyclic complexes measures their ease of oxidation, metal oxidation destabilises the complexes away from the more stable d^6 electron configuration of Fe^{2+} to the less stable d^5 configuration for Fe^{3+} which would lead to the increased lability of the attached macrocycle. In turn Kyba has investigated the cyclic voltammetry of his complexes.¹⁶ The complexes studied involve the oxidation of the metal from a +1 to a +2 oxidation state with reference to ferrocene. Examples are shown below (Table 2.2).

Compound	Oxidation potential, M(I)-M(II), Fc-Fc ⁺ Reference
11[ane]P ₃ Cr	+0.21V
11[ane]P ₂ SCr	+0.05V
11[ane]P ₂ SMo	+0.18V

11[ane]As ₂ S ₂ Mo	-0.08V
--	--------

Table 2.2 Oxidation potentials for some phosphorus and arsenic containing macrocycles synthesised by Kyba.

The data can be interpreted in terms of the π -accepting ability of the ligand. This is due to the dependence of the energy levels of the t_{2g} orbitals (d_{xy} , d_{xz} , d_{yz}) on the ligands π -acidity. The energies of the t_{2g} orbitals will increase as the π -acidity of the ligands decreases which leads to an increasing ease of oxidation. In conclusion the results from Kyba's experimentation lead us to believe that the ease of oxidation of macrocyclic complexes is N>P>As>Sb based on the results obtained for the tricarbonyl complexes studied.

Electrochemical studies have also investigated the reduction potentials for Co(III) complexes.^{17,18} It was found that increasing the ligand size made ligands easier to reduce, $\text{PMe}_2\text{Ph} < \text{PBu}_3 < \text{PMePh}_2 < \text{PPh}_3$. Further studies on the oxidation potentials of $\text{M}(\text{CO})_2[\text{Ph}_2\text{P}(\text{CH}_2)_n\text{PPh}_2]_2$ (where M = Cr, Mo, W) show that complexes with smaller chains ($n=1$) are more easily oxidised than complexes with larger chains ($n=2$).¹⁷ Similar triphosphorus macrocyclic complexes which have been studied using cyclic voltammetry include the following examples in Table 2.3.

Macrocyclic	Electrode Potential (V) Scan rate 50mVs ⁻¹
$[(\text{C}_5\text{Me}_5)\text{FePET}(\text{C}_6\text{H}_4)\text{PET}(\text{C}_6\text{H}_4)\text{PET}(\text{C}_6\text{H}_4)][\text{PF}_6]$	0.044(irreversible)
$[(\text{C}_5\text{Me}_5)\text{FePPh}(\text{C}_3\text{H}_6)\text{PPh}(\text{C}_3\text{H}_6)\text{PPh}(\text{C}_3\text{H}_6)][\text{PF}_6]$	0.307(irreversible)
$[(\text{C}_5\text{H}_5)\text{FeAs}(\text{C}_6\text{H}_4\text{F})(\text{C}_6\text{H}_4)\text{As}(\text{C}_6\text{H}_4\text{F})(\text{C}_6\text{H}_4)\text{As}(\text{C}_6\text{H}_5)(\text{C}_6\text{H}_4)][\text{B}(\text{C}_6\text{H}_5)_4]$	0.517 (quasi reversible)
$[(\text{C}_5\text{H}_5)\text{FeP}(\text{C}_6\text{H}_4\text{F})(\text{C}_6\text{H}_4)\text{P}(\text{C}_6\text{H}_4\text{F})(\text{C}_6\text{H}_4)\text{P}(\text{C}_6\text{H}_5)(\text{C}_6\text{H}_4)][\text{B}(\text{C}_6\text{H}_5)_4]$	0.427 (irreversible), 0.699(quasi reversible)

Table 2.3 Examples of oxidation potentials for phosphorus and arsenic containing macrocycles synthesised by the Edwards group.

The electrode potential of the increasingly stable macrocycles indicates oxidation becoming less favourable due to the decreased lability of the macrocyclic fragment. The 12[ane] macrocycle in this case proves to be more stable to oxidation than the 9[ane]. The increasing electrode potentials indicate that the novel macrocycles (dibenzannulated and tribenzannulated) are more stable to oxidation

due to the fluorinated aryl groups. These conclusions are based on the limited amount of data available.

Experiments for both the tribenzannulated triphosphorus macrocycle and the tribenzannulated triarsenic macrocycle were carried out using a silver/silver chloride electrode, all readings were referenced to ferrocene. Cyclic voltammetry was performed on a Windsor PGstat 12 potentiostat in CH_2Cl_2 with Bu_4NPF_6 (0.1M) as a supporting electrolyte versus an Ag/Ag^+ reference electrode a Ferrocene/Ferrocene⁺ internal reference and a carbon working electrode.

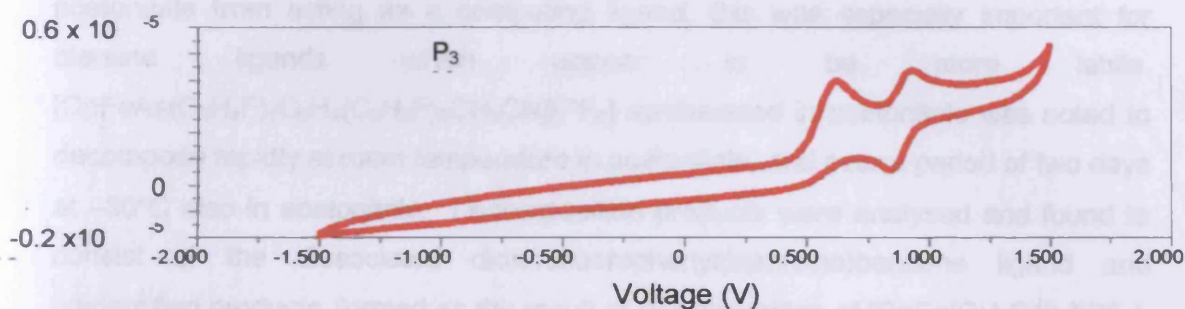


Figure 2.21 The cyclic voltammetry data for the $[\text{CpFeP}(\text{C}_6\text{H}_4)(\text{C}_6\text{H}_4\text{F})\text{P}(\text{C}_6\text{H}_4)(\text{C}_6\text{H}_4\text{F})\text{P}(\text{C}_6\text{H}_4)(\text{C}_6\text{H}_5)][\text{B}(\text{C}_6\text{H}_5)_4]$, **1c**.

The cyclic voltammetry for the triphosphorus macrocycle illustrates an irreversible oxidation taking place at 0.427V and a quasi reversible oxidation occurring at 0.699V. The irreversible oxidation taking place at 0.427V is possibly due to the metal oxidation and the quasi reversible oxidation at 0.699V is possibly as a result of ligand oxidation. The quasi reversible oxidation for the triarsenic macrocycle takes place at 0.517V indicating that it is harder to oxidise the metal complex than its' triphosphorus analogue by comparison to the quasi reversible oxidation at 0.699V. This was expected due to the better σ -donor ability of the arsenic ligand which means that the donor is more easily oxidised.

Conclusions

The results obtained illustrate the synthesis of the novel tripnictide tribenzannulated and dibenzannulated macrocycles via dehydrofluorinative cyclisation.

Both CpFe^+ and Cp^*Fe^+ can be used as template ligands. When comparing CpFe^+ and Cp^*Fe^+ as reaction templates it is important to look at their steric and electronic

contributions to both the cyclisation and the bonding within the macrocycle. It can be seen from the reactions and the yields obtained that the Cp*Fe⁺ template forms complexes in slightly lower yields, although this could be due to the increased timescale of these reactions, which take longer than the corresponding Cp alternatives. In some cases the increased steric bulk on the Cp*Fe⁺ aids cyclisation e.g. between triortho-fluorophenyl phosphine and bisphosphinobenzene, which does not occur as rapidly on a Cp template.

The solvent system for the precursor and macrocyclic complexes is important to consider. The replacement of acetonitrile as a solvent with THF prevents the acetonitrile from acting as a competing ligand, this was especially important for diarsine ligands which appear to be more labile. [CpFeAs(C₆H₄F)₂C₆H₄(C₆H₄F)₂CH₃CN][PF₆] synthesised in acetonitrile was noted to decompose rapidly at room temperature in acetonitrile, and over a period of two days at -30°C also in acetonitrile. Decomposition products were analysed and found to consist of the dissociated diortho-fluorophenyl(bisarsino)benzene ligand and unidentified products, formed as the result of decomposition of [CpFe(CH₃CN)₃][PF₆]. This indicates the lability of the system and the importance of the use of THF as an alternative solvent to acetonitrile. Precursor complexes were prepared using a dicarbonyl template and THF as a solvent which resulted in a much higher yield. This is due to the removal of competition from the acetonitrile solvent which is especially useful for weaker σ-donors. The use of THF to synthesise the diphosphine complex resulted in an increase in yield for the diortho-fluorophenyl(bisphosphino)benzene from 30% to 94%.

The diortho-fluorophenyl(bisphosphino)ethane ligand is much more labile than the benzyl equivalent which results in lower yields and the increased risk of decomposition, particularly during the co-ordination of phenyl phosphine.

We have made a series of novel tripnictide macrocycles which will help to expand the scientific knowledge about phosphorus and arsenic chemistry. The complexes which we have synthesised have been characterised by NMR, infra red spectroscopy, mass spectrometry and crystallography for both the tribenzannulated triphosphorus and triarsenic macrocycles. Novel crystal structures were obtained which show the unique conformation of these original macrocycles with a 'cup shaped' cavity formed by the benzyl backbones. The benzyl nature of the backbones aids retaining a facially capping orientation on demetallation due to the steric bulk and stability (in comparison to ethyl backbones) of the benzyl backbones.

As the ligands become better π-acids there is an easier release of electrons

to the metal centre, more electron density on the metal centre enables the metal to back donate more to the ligand σ^* orbitals. The ligands which have been used vary both in their stability and π -acidity. Phosphorus ligands are better π -acids than arsenic ligands. In comparison to phosphorus, arsenic ligands are weaker ligands due to their size and increased s-orbital bonding character.

During syntheses excess phenyl phosphine/arsine is used for convenience and to increase the rate of reaction.

In the future we hope to be able to obtain crystal structures for all of the macrocyclic complexes synthesised along with some of the precursor complexes to monitor cyclisation requirements. We also hope to be able to synthesise alternative ligands based on the same methodology to prepare further novel macrocycles. Demetallation should be attempted in the future by adjusting the nature of the macrocyclic complex to facilitate ligand dissociation from the template.

Experimental

Ligand Preparation

All experiments were carried out using Schlenk techniques under nitrogen. Solvents were dried according to methods described in solvent preparation appendix 1, 1,2-bis(bis-2-fluorophenylphosphino)benzene, 1,2-bis(bis-2-fluorophenylphosphino) ethane, 1,2-bis(bis-2-fluorophenylarsino)benzene and $\{\text{Cp}^*\text{Fe}[\text{H}_2\text{AsC}_6\text{H}_4\text{AsH}_2]\text{CH}_3\text{CN}\}\text{BF}_4$ were prepared using literature methods.¹⁹ This reference also illustrates the preparation of the $[\text{CpFe}\{(o\text{-C}_6\text{H}_4\text{F})_2\text{PC}_2\text{H}_4\text{P}(o\text{-C}_6\text{H}_4\text{F})_2\}\text{CH}_3\text{CN}][\text{PF}_6]$ and $[\text{CpFe}\{(o\text{-C}_6\text{H}_4\text{F})_2\text{PC}_6\text{H}_4\text{P}(o\text{-C}_6\text{H}_4\text{F})_2\}\text{CH}_3\text{CN}][\text{PF}_6]$ although we have used a modified synthetic procedure. Other starting materials that had previously been prepared which are utilised in the experimental procedure include trivinyl stibine, trivinyl arsine,^{20,21,22} $\{\text{CpFe}[\text{H}_2\text{PC}_6\text{H}_4\text{PH}_2]\text{CH}_3\text{CN}\}\text{PF}_6$,¹⁰ $\{\text{Cp}^*\text{Fe}[\text{H}_2\text{PC}_6\text{H}_4\text{PH}_2]\text{CH}_3\text{CN}\}\text{PF}_6$, $\{\text{CpFe}[\text{H}_2\text{PC}_2\text{H}_4\text{PH}_2]\text{CH}_3\text{CN}\}\text{PF}_6$ ¹⁰ and $\{\text{Cp}^*\text{Fe}[\text{H}_2\text{PC}_2\text{H}_4\text{PH}_2]\text{CH}_3\text{CN}\}\text{PF}_6$.¹⁰

Macrocyclic Precursor Preparation

1a Preparation of $[\text{CpFe}\{(o\text{-C}_6\text{H}_4\text{F})_2\text{PC}_6\text{H}_4\text{P}(o\text{-C}_6\text{H}_4\text{F})_2\}\text{CH}_3\text{CN}][\text{PF}_6]$

To a solution of $[\text{CpFe}(\text{CO})_2(\text{CH}_3\text{CN})][\text{PF}_6]$ (0.36g, 0.001mol) in THF (15ml) was added a solution of 1,2-bis(bis-2-fluorophenylphosphino)benzene (0.47g, 0.001mol) in THF (30ml) at room temperature. The solution was photolysed with a 100W table top lamp for 24 hours resulting in a colour change from yellow to red. The reaction mixture was filtered through celite and the solvent removed *in vacuo*. Trituration with ether gave a red powder (M_r 825.38, 0.78g, 94%).

Measured	Data
¹ H NMR (CDCl ₃)	2.29 (s, 3H, CH ₃ CN), 3.96 (s, 5H, Cp), 6.9-7.7 (m, 20H, Ar-H).
¹³ C{ ¹ H} NMR(CDCl ₃)	2.8 (CH ₃ CN), 81.4 (Cp), 115.67 (d, ² J _{C-F} 23.48Hz), 123.17-133.89 (m), 165.02 (dd, ¹ J _{C-F} 242.89Hz)
³¹ P NMR (CDCl ₃)	92.5 (s, br), -143.73 (septet, ¹ J _{P-F} 714.42)
¹⁹ F NMR (CDCl ₃)	-98.04(s), -73.46 (d, ¹ J _{P-F} 714.42, PF ₆).
MS (APCI)	680 (M ⁺).

ν/cm^{-1} (nujol)	3073(s, br), 2266(s, br, CH ₃ CN), 1636 (w), 1599(w), 1568(w), 1470(w), 1441(s, sh), 1290(s, sh), 1260(m), 1212(w), 1123(w), 1074(m), 840(w, sh), 762(w).
------------------------------	--

2a Preparation of [Cp*Fe((*o*-C₆H₄F)₂PC₆H₄P(*o*-C₆H₄F)₂)CH₃CN][BF₄]

To a solution of [Cp*Fe(CO)₂(CH₃CN)]BF₄ (2.54g, 0.003mol) in THF (10ml) was added a solution of 1,2-bis(bis-2-fluorophenylphosphino)benzene (1.56g, 0.003mol) in THF (15ml) at room temperature. The solution was photolyzed with a 100W table top lamp for 24 hours resulting in a colour change from yellow to red. The reaction mixture was filtered through celite, the solvent removed *in vacuo* and the solid triturated with ether to give a red powder (M_R 895.52, 2.53g, 94% yield).

Measured	Data
¹ H-NMR (CDCl ₃)	1.63 (s, 15H, Cp*), 2.19 (s, CH ₃ CN), 6.69-7.86 (m, 16H, Ar-H).
¹³ C{ ¹ H} NMR (CDCl ₃)	3.92 (s, CH ₃ CN), 9.54 (s, Cp*), 87.31 (s, Cp*), 115.67 (d, ² J _{C-F} 23.48Hz), 118.10 (s, CH ₃ CN), 123.17-133.89 (m), 165.02 (dd, ¹ J _{C-F} 242.89Hz)
³¹ P-NMR (CDCl ₃)	90.13 (s, br)
¹⁹ F-NMR (CDCl ₃)	-99.61(s)
MS (APCI)	750.6 Da/e (M ⁺).

3a Preparation of {CpFe[(*o*-C₆H₄F)₂PC₂H₄P(*o*-C₆H₄F)₂]CH₃CN}PF₆

To a solution of [CpFe(*p*-xylene)]PF₆ (0.37g, 0.001mol) in THF (15ml) was added a solution of 1,2-bis(bis-2-fluorophenylphosphino)ethane (0.52g, 0.001mol) at room temperature. The solution was photolyzed with a 100W table top lamp for 24 hours resulting in a colour change from yellow to red. The reaction mixture was filtered through celite and the solvent removed *in vacuo*. Trituration with ether gave a red powder (M_R 777.34, 0.73g, 94% yield).

Measured	Data
¹ H NMR (CDCl ₃)	2.30 (s, 3H, CH ₃ CN), 2.92 (m, 4H, CH ₂), 3.99 (s, 5H, Cp), 7.0-7.7 (m, 16H, Ar-H).
¹³ C{ ¹ H} NMR	5.5 (s, CH ₃ CN), 29.0 (m, CH ₂), 87.4 (s, Cp), 115.53 (d, ³ J _{C-P})

(CDCl ₃)	23.4Hz), 118.4 (s, CH ₃ CN), 120.0 (s), 123.4 (s), 136-127.5 (m), 164.65 (dd, ¹ J _{C-F} 242.89Hz, ² J _{C-P} 12.00Hz, CF),.
³¹ P NMR (CDCl ₃)	85.4 (s), -143.73 (sept, ¹ J _{P-F} 714.42)
¹⁹ F NMR (CDCl ₃)	-97.63(s), -73.46 (d, PF ₆ , ¹ J _{P-F} 714.42)
MS (APCI)	632 (M ⁺).
v/cm ⁻¹ (KBr)	3076(s,br), 2935(s), 2262(m, CN), 1598(w), 1568(w), 1468(w), 1437(s, sh), 1260(s, sh), 1214(w, sh), 1123(w), 1076(w).

7a Preparation of [Cp*Fe{(o-C₆H₄F)₂PC₂H₄P(o-C₆H₄F)₂}CH₃CN][BF₄]

To a solution of [Cp*Fe(CO)₂(CH₃CN)]BF₄ (0.85g, 0.001mol) in THF (20ml) was added a solution of 1,2-bis(bis-2-fluorophenylphosphino)benzene (0.47g, 0.001mol) in THF (10ml). The solution was photolyzed with a 100W table top lamp for 24 hours resulting in a colour change from yellow to red. The reaction mixture was filtered through celite, the solvent removed *in vacuo* and the solid triturated with ether to give a red powder (M_R 847.48, 0.80g, 94% yield).

Measured	Data
¹ H NMR (CDCl ₃)	1.70 (s, 15H, Cp*), 2.22 (s, 3H, CH ₃ CN), 6.72-7.32 (m, 16H, Ar-H).
¹³ C{ ¹ H} NMR (CDCl ₃)	4.20 (s, CH ₃ CN), 9.81 (s, Cp*), 86.42 (s, Cp*), 115.32 (² J _{C-F} 23.92Hz), 119.03 (s, CH ₃ CN), 121.38-136.83 (m), 165.33 (dd, ¹ J _{C-F} 238.92).
³¹ P NMR (CDCl ₃)	83.2(s)
¹⁹ F NMR (CDCl ₃)	-98.70(s)
MS (APCI)	703 Da/e (M ⁺)

8a Preparation of [CpFe{(o-C₆H₄F)₂AsC₆H₄As(o-C₆H₄F)₂}CH₃CN][PF₆]

To a solution of [CpFe(*p*-xylene)][PF₆] (0.37g, 0.001mol) in acetonitrile (15ml) was added a solution of 1,2-bis(bis-2-fluorophenylarsino)benzene (0.001mol) in acetonitrile (15ml). This was photolyzed with a 100W table top lamp for 24hours resulting in a colour change from yellow to dark blue. The reaction mixture was filtered through celite, the solvent removed *in vacuo* and the solid triturated with ether to give a blue powder (M_R 913.22, 0.87g, 95% yield).

Measured	Data
^1H NMR (CD_3CN)	2.29 (s, 3H, CH_3CN), 3.95 (s, 5H, Cp), 6.69-7.49 (m, 20H, Ar-H).
$^{13}\text{C}\{^1\text{H}\}$ NMR (CD_3CN)	2.6 (CH_3CN), 76.4 (Cp), 115.52 (d, $^2J_{\text{C-F}}$ 24.11Hz), 121.60 (s), 125.49-136.41 (m), 164.99 (d, $^1J_{\text{C-F}}$ 241.93Hz).
^{19}F NMR (CD_3CN)	-99.77 (s), -73.46 (d, $^1J_{\text{P-F}}$ 714.42)
MS (APCI)	788 Da/e (M^+).
ν/cm^{-1} (KBr)	3076, 2262 (CH_3CN), 1595, 1573, 1470, 1447, 1260, 1212, 1096, 840, 762.

12a Preparation of $\{\text{Cp}^*\text{Fe}[(o\text{-C}_6\text{H}_4\text{F})_2\text{AsC}_6\text{H}_4\text{As}(o\text{-C}_6\text{H}_4\text{F})_2]\text{CH}_3\text{CN}\}\text{BF}_4$

To a solution of $[\text{CpFe}(p\text{-xylene})][\text{BF}_4]$ (0.37g, 0.001mol) in acetonitrile (20ml) was added 1,2-bis(bis-2-fluorophenylarsino)benzene (0.61g, 0.001mol) in acetonitrile (10ml). This was photolyzed with a 100W table top lamp for 24 hours resulting in a colour change from yellow to dark blue. The reaction mixture was filtered through celite, the solvent removed *in vacuo* and the solid triturated with ether to give a blue powder (M_r 983.36, 0.93g, 95% yield).

Measured	Data
^1H NMR (CDCl_3)	2.30 (s, 3H, CH_3CN), 3.92 (s, 5H, Cp), 7.26-7.65 (m, 20H, Ar-H).
$^{13}\text{C}\{^1\text{H}\}$ NMR (CDCl_3)	3.97 (CH_3CN), 82.03(Cp), 115.45 (d, $^2J_{\text{C-F}}$ 24.18Hz), 120.87 (s), 124.36-134.42 (m), 165.03 (d, $^1J_{\text{C-F}}$ 242.14Hz).
^{19}F NMR (CDCl_3)	-100.03 (s).
MS (APCI)	838.4 (M^+).
ν/cm^{-1} (nujol)	2927.3(s), 2359.4(w), 2329.1(w), 2075.7(w), 2021.8(w), 1642.3(m), 1462.3(s), 1376.5(m), 1298.3(s), 1257.5(w), 1156.7(w), 1106.4(m), 1026.8(m), 831.5 (w), 721.6(w).

13a Preparation of $\{\text{CpFe}[\text{H}_2\text{AsC}_6\text{H}_4\text{AsH}_2]\text{CH}_3\text{CN}\}\text{PF}_6$

To a solution of $[\text{CpFe}(p\text{-xylene})]\text{PF}_6$ (0.37g, 0.001mol) in acetonitrile (15ml) was added a solution of 1,2-bis(bis-2-fluorophenylarsino)benzene (0.61g, 0.001mol) in acetonitrile (15ml). The solution was photolyzed with a 200W UV lamp for 18

hours resulting in a colour change from a yellow to dark blue. This was filtered through celite and the solvent removed *in vacuo*. Trituration with ether gave a blue powder (M_R 536.99, 0.17g, 32% yield).

Measured	Data
^1H NMR (CDCl_3)	2.21 (CH_3CN), 7.03-7.47 (m, 4H, Ar-H).
$^{13}\text{C}\{^1\text{H}\}$ NMR (CDCl_3)	4.10 (CH_3CN), 126.47 (s), 130.20-132.78 (m).
MS (APCI)	392.0 Da/e (M^+).

Preparation of Macrocyclic Precursors and Complexes

Precursor complexes containing both the mono and bispnictides are numbered and given the descriptor b, macrocyclic complexes are given the descriptor c.

1b Preparation of $[\text{CpFe}(\text{o-C}_6\text{H}_4\text{F})_2\text{PC}_6\text{H}_4\text{P}(\text{o-C}_6\text{H}_4\text{F})_2\text{PH}_2\text{C}_6\text{H}_5][\text{PF}_6]$

$[\text{CpFe}(\text{o-C}_6\text{H}_4\text{F})_2\text{P}(\text{C}_6\text{H}_4)\text{P}(\text{o-C}_6\text{H}_4\text{F})\text{CH}_3\text{CN}][\text{PF}_6]$ (0.75g, 0.96mmol) was dissolved in 1,2-dichloroethane (40ml). Phenyl phosphine (M_R 110.10, δ 1.001, 0.5ml) was added and the reaction mixture heated to 60°C for 6 hours until the colour changed from red to orange. The solvent was removed *in vacuo* and the solid residue triturated with ether to give a yellow powder (M_R 894.42, 0.80g, 93% yield).

Measured	Data
^1H NMR (CD_2Cl_2)	3.81 (s, 5H, Cp), 4.38 (d, $^1J_{\text{P-H}}$ 331Hz, PH_2Ph), 7.6-6.8 (m, 25H, aromatic protons).
$^{13}\text{C}\{^1\text{H}\}$ NMR (CDCl_3)	82.9 (Cp), 117.6 (d, $^1J_{\text{P-C}}$ 23Hz), 135-125 (m), 163.29 (dd, $^1J_{\text{C-F}}$ 252.69Hz).
$^{31}\text{P}\{^1\text{H}\}$ NMR (CDCl_3)	-143.73 (septet, $^1J_{\text{P-F}}$ 714.42), 12.09 (s), 66.47 (m), 84.6 (d, $^2J_{\text{P-P}}$ 51Hz).
^{19}F NMR (CDCl_3)	-98.02(s), -73.46(d, $^1J_{\text{P-F}}$ 714.42)
MS (APCI)	749 Da/e (M^+).
ν/cm^{-1} (KBr)	3067(s, Cp), 2341(w), 1598(w), 1567(w), 1469(w), 1439(s), 1258(s), 1210(w), 1123(w), 1071(w), 949(w), 849(w), 771(w).

1c Preparation of $[\text{CpFe}(\text{P}(\text{C}_6\text{H}_4\text{F})(\text{C}_6\text{H}_4)\text{P}(\text{C}_6\text{H}_4\text{F})(\text{C}_6\text{H}_4)\text{P}(\text{C}_6\text{H}_5)(\text{C}_6\text{H}_4)]\text{PF}_6$

Potassium *tert*butoxide (2 mole equivalents, 0.09g, 0.78mmol) was added to a solution of $[\text{CpFe}(\text{o-C}_6\text{H}_4\text{F})_2\text{PC}_6\text{H}_4\text{P}(\text{o-C}_6\text{H}_4\text{F})_2\text{PH}_2\text{C}_6\text{H}_5]\text{PF}_6$ (0.33g, 0.39mmol) in THF (40ml). The reaction was left to stir overnight and filtered. The solvent was removed *in vacuo* to give a yellow solid (M_r 778.32, 78% yield).

Measured	Data
^1H NMR (CDCl_3)	3.81 (5H, Cp), 7.29-7.64 (m, 25H, aromatic protons).
$^{13}\text{C}\{^1\text{H}\}$ NMR (CDCl_3)	82.13 (s, 5C, Cp), 115.34 (d, $^2J_{\text{C-F}}$ 23.08Hz), 134.74-129.89 (m), 163.29 (dd, $^1J_{\text{C-F}}$ 252.69).
$^{31}\text{P}\{^1\text{H}\}$ NMR (CDCl_3) Room temperature and -90°C	-143.73 (septet, $^1J_{\text{P-F}}$ 714.42), 119.56 (triplet of triplets, $^2J_{\text{P-P}}$ 116.12, $^6J_{\text{P-F}}$ 32.75), 127.52 (doublet of triplets, $^2J_{\text{P-P}}$ 110.17).
^{19}F NMR (CDCl_3)	-98.41 (s), -73.46 (d, PF_6 , $^1J_{\text{P-F}}$ 714.42). Under VT conditions (183K) -99.21 (dd, $^3J_{\text{F-P}}$ 100.56Hz, $^6J_{\text{F-P}}$ 38.15Hz).
MS (APCI)	709.1 Da/e (M^+).
ν/cm^{-1} (nujol)	3413.47(s), 2923.39 (s), 2853.47(w), 1460.71(s), 1376.90(w), 1260.58(m), 1077.87(w), 1020.93(w), 835.80(m).
CV	0.427V (irreversible), 0.699 (quasi reversible).

X-ray quality crystals were obtained by anion exchange with $\text{NaB}(\text{C}_6\text{H}_5)_4$ and recrystallisation in acetonitrile at -37°C to form fine yellow, needle-like crystals.

2b Preparation of $\{\text{Cp}^*\text{Fe}[(\text{o-C}_6\text{H}_4\text{F})_2\text{PC}_6\text{H}_4\text{P}(\text{o-C}_6\text{H}_4\text{F})_2\text{PH}_2\text{C}_6\text{H}_5]\text{BF}_4$

Phenylphosphine (0.4ml, 3.6mmol) was added to a solution of $[\text{Cp}^*\text{Fe}(\text{o-C}_6\text{H}_4\text{F})_2\text{PC}_6\text{H}_4\text{P}(\text{o-C}_6\text{H}_4\text{F})_2\text{PH}_2\text{C}_6\text{H}_5]\text{PF}_6$ (0.80g, 0.96mmol) in THF (30ml). The reaction mixture was heated to 60°C for 24 hours until the colour changed from red to orange. The solvent was removed *in vacuo* and the residue triturated with ether to give a yellow powder (M_r 906.39, 0.80g, 92% yield).

Measured	Data
^1H NMR (CDCl_3)	1.63 (s, 15H, Cp^*), 6.91-7.50 (m, 25H, Ar-H)
$^{13}\text{C}\{^1\text{H}\}$ NMR	9.70 (s, Cp^*), 87.70 (s, Cp^*), 135.05-124.88 (m), 165.85 (d,

(CDCl ₃)	¹ J _{C-F} 325.70Hz).
³¹ P{ ¹ H} NMR (CDCl ₃)	10.09 (s, co-ordinated PPhH ₂), 18.68 (s, co-ordinated diphosphine).
¹⁹ F NMR (CDCl ₃)	-98.15 (s)
MS (APCI)	750.6 Da/e (M ⁺).

2c Preparation of [Cp*Fe(P(C₆H₄F)(C₆H₄)P(C₆H₄F)(C₆H₄)P(C₆H₅)(C₆H₄)] [BF₄]

[Cp*Fe{(o-C₆H₄F)₂PC₆H₄P(o-C₆H₄F)₂]PH₂C₆H₅]BF₄ (0.35g, 0.39mmol) was dissolved in THF (30ml), potassium *tert*butoxide (catalytic quantity) was added to the solution. The reaction was heated to 60°C for 16 hours. After filtration, the solvent was removed *in vacuo* to give a yellow solid (M_R 866.38, 0.23g, 78% yield).

Measured	Data
¹ H-NMR (CDCl ₃)	1.67 (s, Cp*), 6.90-7.34 (m, Ar-H)
¹³ C{ ¹ H} NMR (CDCl ₃)	134.90-123.94 (m), 165.80 (d, ¹ J _{C-F} 324.33Hz).
³¹ P-NMR (CDCl ₃)	112.02-111.68 (m), 117.32 (tt, ² J _{P-P} 102.38Hz, ⁶ J _{P-F} 35.26Hz).
¹⁹ F-NMR (CDCl ₃)	-100.91 (s).
MS (APCI)	779.6 Da/e (M ⁺).

3b Preparation of [CpFe{(o-C₆H₄F)₂PC₂H₄P(o-C₆H₄F)₂]PH₂(C₆H₅)] [PF₆]

[CpFe{(o-C₆H₄F)₂PC₂H₄P(o-C₆H₄F)₂]CH₃CN]PF₆ (0.75g, 0.96mmol) was dissolved in 1,2-dichloroethane (40ml). Phenyl phosphine (0.5ml, 5mmol) was added and the reaction mixture heated to 60°C for 6 hours. The solution changed in colour from red to orange. The solvent was removed *in vacuo* and the oily solid triturated with ether to yield a yellow powder (M_R 846.38, 0.58g, 72% yield).

Measured	Data
¹ H NMR (CDCl ₃)	2.84 (m, 2H, CH ₂), 3.96 (s, 5H, Cp), 4.84 (d, ¹ J _{P-H} 347.4Hz, 2H, PH ₂ Ph), 6.57 (m, 1H, aromatic protons), 7.7-7.0 (m, 20H, aromatic protons).
¹³ C{ ¹ H} NMR (CDCl ₃)	25.2 (CH ₂), 80.7 (s, 5H, Cp), 115.9 (d, ² J _{C-F} 23.01Hz), 124.4 (s), 127.4-133.12 (m), 162.25 (dd, ¹ J _{C-F} 242.92Hz, ² J _{C-P}

	10.92Hz).
³¹ P NMR (CDCl ₃)	8.70 (s, co-ordinated bisphosphine), 80.9 (s, br). -143.73 (septet, ¹ J _{P-F} 714.42, PF ₆).
¹⁹ F NMR (CDCl ₃)	-97.63(s), -73.46 (d, ¹ J _{P-F} 714.42).
MS (APCI)	701 Da/e (M ⁺).
v/cm ⁻¹ (KBr)	3066 (Cp), 2955, 2327 (PH), 1597, 1566, 1471, 1438, 1258, 1213, 1123, 1076, 937.

3c Preparation of [CpFe(P(C₆H₄F)(C₂H₄)P(C₆H₄F)(C₆H₄)P(C₆H₅)(C₆H₄))]PF₆

[CpFe{(o-C₆H₄F)2P(C₂H₄)P(o-C₆H₄F)₂}PH₂(C₆H₅)]PF₆ (0.50g, 0.59mmol) was suspended in THF (50ml), potassium *tert*butoxide (0.19g, 1.68mmol) was added, both solids dissolve to form a dark red solution which becomes orange as the reaction completes. The solvent was removed *in vacuo* and the solid triturated in ether to yield a yellow powder (M_R 806.38, 0.30g, 62% yield).

Measured	Data
¹ H-NMR (CDCl ₃)	2.88 (m, CH ₂ , 4H), 3.72 (s, 5H, Cp), 4.78 (d, ¹ J _{P-H} 347.4Hz), 7.85-7.05 (m, 21H, Ar-H).
¹³ C{ ¹ H} NMR (CDCl ₃)	26.11 (s, CH ₂), 81.2 (s, Cp), 115.91 (d, ² J _{C-F} 23.01Hz), 124.4 (s), 127.4-133.00 (m), 165.25 (dd, ¹ J _{C-F} 242.92Hz).
³¹ P-NMR (CDCl ₃)	127.7 (t, ³ J _{P-P} 31Hz), 122.84-124.05(m), -143.73 (septet, ¹ J _{P-F} 714.42).
¹⁹ F-NMR (CDCl ₃)	-103.0 (br), -73.46 (d, ¹ J _{P-F} 714.42).
MS (APCI)	661 Da/e (M ⁺).
v/cm ⁻¹ (KBr)	3051, 1600, 1570, 1473, 1434, 1260, 1210, 1109, 1078, 828, 758, 682.

Preparation of [Cp*Fe{(o-C₆H₄F)₂PC₂H₄P(o-C₆H₄F)₂}PH₂(C₆H₅)]BF₄

{Cp*Fe[(o-C₆H₄F)₂PC₂H₄P(o-C₆H₄F)₂]}CH₃CN}BF₄ (0.95g, 1.20mmol) was dissolved in 1,2-dichloroethane (40ml). Phenyl phosphine (0.5ml, 5mmol) was added and the reaction mixture heated to 60°C for 18 hours. The solution changed in colour from red to orange. The solvent was removed *in vacuo* and the oily solid triturated with ether to yield a yellow powder (M_R 858.34, 0.92g, 89% yield).

Measured	Data
¹ H-NMR (CDCl ₃)	1.72(s, Cp*), 2.72(m, 2H, CH ₂), 4.73 (d, ¹ J _{P-H} 328.7Hz, 2H), 6.98-7.13 (m, Ar-H).
¹³ C{ ¹ H} NMR (CDCl ₃)	10.01 (Cp*), 26.11 (CH ₂), 90.13 (Cp*), 115.32-127.31 (m), 161.78-162.03 (m).
³¹ P-NMR (CDCl ₃)	9.01 (s, br), 81.00 (s, br).
¹⁹ F-NMR (CDCl ₃)	-100.01 (s)
MS (APCI)	771.5 Da/e (M ⁺).

Attempted Preparation of [Cp*Fe(P(C₆H₄F)(C₂H₄)P(C₆H₄F)(C₆H₄)P(C₆H₅)(C₆H₄))[BF₄]

[Cp*Fe((*o*-C₆H₄F)₂PC₂H₄P(*o*-C₆H₄F)₂)PH₂(C₆H₅))[BF₄] (0.46g, 0.54mmol) was suspended in THF (50ml), potassium *tert*butoxide (0.19g, 1.68mmol) was added, both solids dissolve to form a red/orange solution which after refluxing for 65 hours became dark orange as the reaction completed. The solvent was removed *in vacuo* and the solid triturated in ether. ³¹P NMR spectra showed peaks consistent with the starting materials.

Attempted Preparation of [CpFe((*o*-C₆H₄F)₂(PC₂H₄)P(*o*-C₆H₄F)₂)AsH₂C₆H₅][PF₆]

[CpFe((*o*-C₆H₄F)₂PC₂H₄P(*o*-C₆H₄F)₂)CH₃CN][PF₆] (0.75g, 0.96mmol) was dissolved in 1,2-dichloroethane (35ml). Phenyl arsine (0.8ml, 5mmol) was added and the reaction mixture heated to 60°C for 8 hours. The solution did not change colour. The mixture was refluxed for a further 12 hours and a change from red to dark orange/brown was observed. The solvent was removed *in vacuo*, ³¹P NMR studies showed no reaction had taken place.

4b Preparation of [CpFe(H₂PC₆H₄PH₂)P(C₆H₄F)₃][PF₆]

[CpFe((H₂PC₆H₄PH₂)CH₃CN][PF₆] (0.43g, 0.96mmol) was dissolved in acetonitrile (30ml). Tri*ortho*fluorophenyl phosphine (0.32g, 1mmol) was added and the reaction mixture heated to 60°C for 18 hours. A change in colour from red to yellow was observed. The solvent was removed *in vacuo* and the solid triturated with ether to give a yellow powder (M_R 724.24, 0.57g, 82% yield).

Measured	Data
^1H NMR (CDCl_3)	3.61 (s, 5H, Cp), 6.94-7.39 (m, 16H)
$^{13}\text{C}\{^1\text{H}\}$ NMR (CDCl_3)	131.71-134.39 (m), 164.99 (dd, $^1J_{\text{C-F}}$ 285.33Hz)
$^{31}\text{P}\{^1\text{H}\}$ NMR (CDCl_3)	15.99 (co-ordinated $\text{H}_2\text{PC}_6\text{H}_4\text{PH}_2$), 22.03 [co-ordinated $\text{P}(\text{C}_6\text{H}_4\text{F})_3$] -143.61 (sept, PF_6 , $^1J_{\text{P-F}}$ 714.42)
^{19}F NMR (CDCl_3)	-97.89 (s), -73.52 (d, $^1J_{\text{P-F}}$ 714.42)

4c Preparation of $[\text{CpFePH}(\text{C}_6\text{H}_4)\text{PH}(\text{C}_6\text{H}_4)\text{P}(\text{C}_6\text{H}_4)(\text{C}_6\text{H}_4\text{F})][\text{PF}_6]$

Triethyl amine (0.5ml, 5mmol) was added to a solution of $[\text{CpFe}\{(\text{H}_2\text{PC}_6\text{H}_4\text{PH}_2)\text{P}(\text{C}_6\text{H}_4\text{F})_3\}]\text{PF}_6$ (0.57g, 0.78mmol) in THF (30ml). The reaction mixture was heated to 60°C for 8 hours, no significant colour change was observed. The solvent was removed *in vacuo* to give a yellow powder (M_R 684.23, 0.20g, 74% yield).

Measured	Data
^1H NMR (CDCl_3)	3.73 (s, 5H, Cp), 6.95-7.71 (m, 16H).
$^{13}\text{C}\{^1\text{H}\}$ NMR (CDCl_3)	131.71 (s), 131.81-134.39 (m), 165.03 (dd, $^1J_{\text{C-F}}$ 286.03Hz).
^{31}P NMR (CDCl_3)	-143.61 (sept, PF_6 , $^1J_{\text{P-F}}$ 714.42), 89.10 (t, $^3J_{\text{P-P}}$ 35.73Hz), 90.66 (d, $^3J_{\text{P-P}}$ 35.72Hz), 118.40-122.80 (m).
^{19}F NMR (CDCl_3)	-101.76 (s), -73.52 (d, $^1J_{\text{P-F}}$ 714.42).
MS (APCI)	539.0 Da/e (M^+).
ν/cm^{-1} (nujol)	2955.9(s), 2932.4(s), 2853.6(w), 2727.13 (m), 2677.3(w), 1461.9(s), 1377.2(w), 1309.9(w), 1260.6(s), 1082.7(w), 1024.4(w), 873.4(w), 799.5(w), 722.1(w), 402.0(w).

5b Preparation of $[\text{Cp}^*\text{Fe}(\text{H}_2\text{PC}_6\text{H}_4\text{PH}_2)\text{P}(\text{C}_6\text{H}_4\text{F})_3][\text{BF}_4]$

$[\text{Cp}^*\text{Fe}\{(\text{H}_2\text{PC}_6\text{H}_4\text{PH}_2)\text{CH}_3\text{CN}\}]\text{BF}_4$ (0.45g, 0.98mmol) was dissolved in acetonitrile (30ml). Triortho fluorophenyl phosphine (1.6g, 5mmol) was added and the reaction mixture heated to 60°C for 10 hours and a change from red to yellow was observed. The solvent was removed *in vacuo* to give a yellow powder (M_R 736.21, 0.59g, 82% yield).

Measured	Data
¹ H NMR (CDCl ₃)	1.72 (s, 15H, Cp*), 6.71-7.40 (m)
¹³ C{ ¹ H} NMR (CDCl ₃)	9.91 (s, Cp*), 87.24 (s, Cp*), 115.24 (d, ² J _{P-F} 24.01Hz), 121.52-133.78 (m), 163.99 (dd, ¹ J _{C-F} 234.26Hz, ² J _{C-F} 6.36Hz)
³¹ P{ ¹ H} NMR (CDCl ₃)	15.09 (s, co-ordinated H ₂ PC ₆ H ₄ PH ₂), 18.00 (d, ³ J _{P-F} 41.69Hz), 63.24 (m).
¹⁹ F NMR (CDCl ₃)	-100.82 (s)
MS (APCI)	649.4 Da/e (M ⁺).

5c Preparation of [Cp*FePH(C₆H₄)PH(C₆H₄)P(C₆H₄)(C₆H₄F)] [BF₄]

Triethyl amine (0.5ml, 5mmol) was added to a solution of [Cp*Fe{(H₂PC₆H₄PH₂)P(C₆H₄F)₃}BF₄] (0.59g, 0.80mmol) in THF (30ml) and the reaction mixture heated to 60°C for 8 hours, no significant colour change was observed. The solvent was removed *in vacuo* to give a yellow powder (M_R 696.20, 0.50g, 90% yield).

Measured	Data
¹ H NMR (CDCl ₃)	1.70 (s, 5H, Cp*), 6.79-7.35 (m, 16H, aromatic)
¹³ C{ ¹ H} NMR (CDCl ₃)	115.54 (d, ² J _{C-F} 23.07Hz), 121.52-133.78 (m), 164.71 (dd, ¹ J _{C-F} 234.26Hz).
³¹ P{ ¹ H} NMR (CDCl ₃)	61.46 (partially cyclised macrocycle), 115.07 (s), 105.23-111.32 (m)
¹⁹ F NMR (CDCl ₃)	-103.42 (s)
MS (APCI)	609.4 Da/e (M ⁺).
v/cm ⁻¹ (KBr)	2918.2, 2310.4 (P-H), 2270.3, 1928.0, 1654.3, 1596.4, 1567.7, 1467.9, 1442.8, 1261.3, 1215.3, 1072.1, 841.8, 807.6, 758.9

6b Preparation of [CpFe(H₂PC₂H₄PH₂)P(C₆H₄F)₃] [PF₆]

Triortho-fluorophenyl phosphine (0.32g, 1mmol) was added to a solution of [CpFe{(H₂PC₂H₄PH₂)CH₃CN}] [PF₆] (0.40g, 1.00mmol) in acetonitrile (35ml). The reaction mixture was heated to 60°C for 10 hours, a colour change from red to yellow was observed. The solvent was removed *in vacuo* and triturated with ether to give a yellow powder (M_R 676.20, 0.31g, 46% yield).

Measured	Data
¹ H-NMR (CDCl ₃)	3.47 (d, ¹ J _{P-H} 6.82Hz, PH ₂), 3.73 (s, 5H, Cp), 6.95-7.71 (m, 12H, aromatic).
¹³ C{ ¹ H} NMR (CDCl ₃)	124.80 (s), 131.69 (s), 131.81 (s), 134.42 (s), 165.18 (dd, ¹ J _{C-F} 279.60Hz, ² J _{C-P} 9.82Hz).
³¹ P-NMR (CDCl ₃)	-143.61 (sept, PF ₆ , ¹ J _{P-F} 714.42), 15.95 (s, co-ordinated H ₂ PC ₆ H ₄ PH ₂), 22.80 [co-ordinated P(C ₆ H ₄ F) ₃].
¹⁹ F-NMR (CDCl ₃)	-98.03 (s), -73.52 (d, ¹ J _{P-F} 714.42).

6c Preparation of [CpFePH(C₂H₄)PH(C₆H₄)P(C₆H₄)(C₆H₄F)][PF₆]

Triethylamine (0.5ml, 5mmol) was added to a solution of [CpFe{(H₂PC₂H₄PH₂)P(C₆H₄F)₃][PF₆] (0.31g, 0.46mmol) in THF (30ml) and the reaction mixture heated to 60°C for 8 hours. The solvent was removed *in vacuo*, washed with ether and dried to give a yellow powder (M_R 636.19, 0.19g, 65% yield).

Measured	Data
¹ H NMR (CDCl ₃)	6.95-7.71 (m, 12H, aromatic), 3.73 (s, 5H, Cp)
¹³ C{ ¹ H} NMR (CDCl ₃)	115.55 (d, ² J _{C-F} 23.08Hz), 121.78 (m), 124.80 (s), 131.75 (d, ³ J _{C-F} 9.23Hz), 134.42 (s), 164.88 (dd, ¹ J _{C-F} 283.88Hz, ² J _{C-P} 9.75Hz).
³¹ P NMR (CDCl ₃)	111.52 (s), 105.89-105.23 (m), 64.38 (s, partially cyclised macrocycle)
¹⁹ F NMR (CDCl ₃)	-101.76 (s)
MS (APCI)	491.2 Da/e (M ⁺).
v/cm ⁻¹ (nujol)	2955.94(s, br), 2932.41(w, sh), 2853.55(w), 2727.13 (w, PH), 2677.27(w), 1461.90(s, sh), 1377.16(w), 1309.84(m, br), 1260.56(s, sh), 1082.74(w), 1024.40(w), 873.35(w, br), 799.47(w), 722.09(w), 401.99(w, sh).

7b Preparation of [Cp*Fe(H₂PC₂H₄PH₂)P(C₆H₄F)₃][BF₄]

Triorthofluorophenyl phosphine (1.5g, 5mmol) was added to a solution of [Cp*Fe{(H₂PC₂H₄PH₂)CH₃CN][BF₄] (0.12g, 0.30mmol) in acetonitrile (30ml). The reaction mixture was heated to 60°C for 10 hours, a colour change from red to yellow

was observed. The solvent was removed *in vacuo* to give a yellow powder (M_R 688.17, 0.10g, 48% yield).

Measured	Data
^1H NMR (CDCl_3)	1.72 (s, 15H, Cp*), 6.29-7.27 (m, 12H)
$^{13}\text{C}\{^1\text{H}\}$ NMR (CDCl_3)	9.81 (s, Cp*), 20.31 (CH_2), 86.66 (s, Cp*), 120.88 (d, $^2J_{\text{C-F}}$ 23.08Hz), 121.03 (s), 126.13 (s), 130.67 (s), 137.71 (s), 137.81 (s), 139.59 (s), 166.13 (dd, $^1J_{\text{C-F}}$ 253.33Hz, $^2J_{\text{C-P}}$ 8.12Hz).
$^{31}\text{P}\{^1\text{H}\}$ NMR (CDCl_3)	18.98 [m, co-ordinated $\text{P}(\text{C}_6\text{H}_4\text{F})_3$], 12.32 (s, co-ordinated $\text{H}_2\text{PC}_2\text{H}_4\text{PH}_2$).
^{19}F NMR (CDCl_3)	-99.98 (s).
MS (APCI)	601.4 Da/e (M^+).

7c Preparation of $[\text{Cp}^*\text{FePHC}_2\text{H}_4\text{PH}(\text{C}_6\text{H}_4)\text{P}(\text{C}_6\text{H}_4)(\text{C}_6\text{H}_4\text{F})][\text{BF}_4]$

Triethylamine (0.5ml, 5mmol) was added to a solution of $[\text{Cp}^*\text{Fe}(\text{H}_2\text{PC}_2\text{H}_4\text{PH}_2)\text{P}(\text{C}_6\text{H}_4\text{F})_3]\text{BF}_4$ (0.10g, 0.15mmol) in THF (30ml). The reaction mixture was heated to 40°C for 6 hours. The solvent was removed *in vacuo* to give a yellow powder (M_R 648.16, 0.03g, 32% yield).

Measured	Data
^1H -NMR (CDCl_3)	1.86 (Cp*), 6.31-7.09 (m, Ar-H)
$^{13}\text{C}\{^1\text{H}\}$ NMR (CDCl_3)	10.00 (s, Cp*), 20.01 (CH_2), 90.30 (Cp*), 121.31-131.82 (m), 166.23 (dd, $^1J_{\text{C-F}}$ 248.41Hz, $^2J_{\text{C-P}}$ 9.21Hz).
^{31}P -NMR (CDCl_3)	112.3-117.4 (m)
^{19}F -NMR (CDCl_3)	-102.38 (s).
MS (APCI)	561.4 Da/e (M^+).
ν/cm^{-1} (nujol)	3412.1, 2962.0, 2851.2, 2362.9 (P-H), 2019.9, 1920.5, 1797.6, 1597.0, 1568.0, 1468.4, 1443.6, 1261.3, 1215.9, 1084.3, 1020.9, 871.8, 814.6, 770.3

8b Preparation of $[\text{CpFe}(\text{o-C}_6\text{H}_4\text{F})_2\text{AsC}_6\text{H}_4\text{As}(\text{o-C}_6\text{H}_4\text{F})_2]\text{AsH}_2\text{C}_6\text{H}_5][\text{PF}_6]$

Phenyl arsine (0.8ml, 0.96mmol) was added to a solution of $[\text{CpFe}(\text{o-C}_6\text{H}_4\text{F})_2\text{AsC}_6\text{H}_4\text{As}(\text{o-C}_6\text{H}_4\text{F})\text{CH}_3\text{CN}][\text{PF}_6]$ (0.88g, 0.96mmol) in 1,2-dichloroethane

(30ml) and the reaction mixture heated to 60°C for 6 hours until the colour changed from red to orange. The solvent was removed *in vacuo* and the residue triturated with ether to give an orange powder (M_R 1026.21, 0.86g, 87% yield).

Measured	Data
$^1\text{H-NMR}$ (CDCl_3)	4.01 (s, 5H, Cp), 7.6-6.8 (m, 30H, aromatic protons).
$^{13}\text{C}\{^1\text{H}\}$ NMR (CDCl_3)	128.91-135.10 (m), 164.91 (d, $^1J_{\text{C-F}}$ 239.83Hz).
$^{19}\text{F-NMR}$ (CDCl_3)	-101.49 (s)
MS (APCI)	881 Da/e (M^+).
ν/cm^{-1} (KBr)	3066(s, br), 2330(w, br), 1594(w,sh), 1468(s, sh), 1438(m, sh), 1260(s, sh), 1210(w), 1096(w), 839(w), 770(w).

8c Preparation of $[\text{CpFe}(\text{As}(\text{C}_6\text{H}_4\text{F})(\text{C}_6\text{H}_4)\text{As}(\text{C}_6\text{H}_4\text{F})(\text{C}_6\text{H}_4)\text{As}(\text{C}_6\text{H}_5)(\text{C}_6\text{H}_4))][\text{PF}_6]$

$[\text{CpFe}\{(\text{o-C}_6\text{H}_4\text{F})_2\text{AsC}_6\text{H}_4\text{As}(\text{o-C}_6\text{H}_4\text{F})_2\}\text{PH}_2\text{C}_6\text{H}_5][\text{PF}_6]$ (0.22g, 0.22mmol) was dissolved in THF (40ml), potassium *tert*butoxide (0.50g) was added to the solution. The reaction was left to stir overnight and filtered. The solvent was removed *in vacuo* to give a yellow solid (M_R 986.20, 0.16g, 73% yield).

Measured	Data
$^1\text{H-NMR}$ (CDCl_3)	7.80-6.90 (m, 25H, aromatic protons), 3.98 (s, 5H, Cp).
$^{13}\text{C}\{^1\text{H}\}$ NMR (CDCl_3)	78.07 (Cp), 132.35-130.10 (m, aromatic carbons), 164.92 (d, $^1J_{\text{C-F}}$ 239.99Hz).
$^{31}\text{P-NMR}$ (CDCl_3)	-143.73 (sept, PF_6 , $^1J_{\text{P-F}}$ 714.42).
$^{19}\text{F-NMR}$ (CDCl_3)	-101.4906 (minor peak), -100.09 (major peak), -73.52 (d, PF_6 , $^1J_{\text{P-F}}$ 714.42).
MS (APCI)	411 Da/e ($\text{M}^+ - \text{F}$), 821.6 ($\text{M}^+ - \text{F}$).
ν/cm^{-1} (nujol)	3412.86(m), 2923.55(s), 2853.62(s), 1463.31(s), 1376.97(m), 1259.92(m), 1100.72(m), 1022.38(m), 837.91(m), 801.70(m), 752.40(w), 722.95 (w), 557.40 (w), 538.18 (w).
CV	0.517V (quasi reversible).

X-ray quality crystals were obtained by anion exchange with $\text{NaB}(\text{C}_6\text{H}_5)_4$ and recrystallisation in acetonitrile at -37°C to form fine yellow, needle-like crystals.

9b Preparation of $[\text{CpFe}\{(o\text{-C}_6\text{H}_4\text{F})_2\text{PC}_6\text{H}_4\text{P}(o\text{-C}_6\text{H}_4\text{F})_2\}\text{AsH}_2\text{C}_6\text{H}_5][\text{PF}_6]$

Phenylarsine (0.9ml, 0.004mol) was added to a solution of $[\text{CpFe}(o\text{-C}_6\text{H}_4\text{F})_2\text{PC}_6\text{H}_4\text{P}(o\text{-C}_6\text{H}_4\text{F})_2\text{CH}_3\text{CN}][\text{PF}_6]$ (0.79g, 0.96mmol) in 1,2-dichloroethane (40ml). The reaction mixture was heated to 60°C for 6 hours until the colour changed from red to orange. The solvent was removed *in vacuo* and the residue triturated with ether to give a yellow powder (M_r 938.39, 0.78g, 87% yield).

Measured	Data
$^1\text{H-NMR}$ (CD_3CN)	3.82 (s, 5H, Cp), 6.98-7.58 (m, 25H)
$^{13}\text{C}\{^1\text{H}\}$ NMR (CD_3CN)	82.23 (s, 5C, Cp), 133.78-126.84 (m, 36C), 163.31 (dd, $^1J_{\text{C-F}}$ 252.59).
$^{31}\text{P-NMR}$ (CD_3CN)	-143.73 (septet, $^1J_{\text{P-F}}$ 714.42), 80.23 (s).
$^{19}\text{F-NMR}$ (CD_3CN)	-98.38 (s), -73.46 (d, $^1J_{\text{P-F}}$ 714.42)
MS (APCI)	793.4 Da/e (M^+).

9c Preparation of $[\text{CpFeP}(\text{C}_6\text{H}_4\text{F})(\text{C}_6\text{H}_4)\text{P}(\text{C}_6\text{H}_4\text{F})(\text{C}_6\text{H}_4)\text{As}(\text{C}_6\text{H}_5)(\text{C}_6\text{H}_4)][\text{PF}_6]$

Potassium *tert*butoxide (2 mole equivalents, 0.09g, 0.78mol) was added to a solution of $[\text{CpFe}\{(o\text{-C}_6\text{H}_4\text{F})_2\text{PC}_6\text{H}_4\text{P}(o\text{-C}_6\text{H}_4\text{F})_2\}\text{AsH}_2\text{C}_6\text{H}_5][\text{PF}_6]$ (0.33g, 0.39mmol) in THF (40ml). The reaction was left to stir overnight and filtered. The solvent was removed *in vacuo* to give a yellow solid (M_r 898.37, 0.27g, 78% yield).

Measured	Data
$^1\text{H-NMR}$ (CDCl_3)	3.80 (s, 5H, Cp), 7.18-7.74 (m, 25H, Ar-H)
$^{13}\text{C}\{^1\text{H}\}$ NMR (CDCl_3)	83.03 (s, 5C, Cp), 126.93 (d, $^2J_{\text{C-F}}$ 15.00Hz), 128.59-130.24 (m), 133.78 (s), 162.25 (dd, $^1J_{\text{C-F}}$ 241.83Hz)
$^{31}\text{P-NMR}$ (CDCl_3)	-143.39 (septet, $^1J_{\text{P-F}}$ 720.58), 134.99 (s), 135.60 (s).
$^{19}\text{F-NMR}$ (CDCl_3)	-102.42 (s), -73.46 (d, $^1J_{\text{P-F}}$ 714.42)
MS (APCI)	753.4 Da/e (M^+).

10b Preparation of $\{\text{Cp}^*\text{Fe}\{(o\text{-C}_6\text{H}_4\text{F})_2\text{PC}_6\text{H}_4\text{P}(o\text{-C}_6\text{H}_4\text{F})_2\}\text{AsH}_2\text{C}_6\text{H}_5\}\text{BF}_4$

$[\text{Cp}^*\text{Fe}(o\text{-C}_6\text{H}_4\text{F})_2\text{PC}_6\text{H}_4\text{P}(o\text{-C}_6\text{H}_4\text{F})_2\text{CH}_3\text{CN}]\text{BF}_4$ (0.40g, 0.48mmol) was dissolved in 1,2-dichloroethane (40ml). Phenyl arsine (0.9ml, 0.004mol) was added and the reaction mixture heated to 60°C for 16 hours until the colour changed from

red to orange. The solvent was removed *in vacuo* and the residue triturated with ether to give a yellow powder (M_R 950.34, 0.40g, 88% yield).

Measured	Data
$^1\text{H-NMR}$ (CDCl_3)	1.69 (s, Cp*), 6.99-7.28 (m).
$^{13}\text{C}\{^1\text{H}\}$ NMR (CDCl_3)	9.99 (s, Cp*), 87.03 (s, Cp*), 127.82-134.00(m), 164.01 (dd, $^1J_{\text{C-F}}248.01\text{Hz}$).
$^{31}\text{P-NMR}$ (CDCl_3)	79.48 (br, s)
$^{19}\text{F-NMR}$ (CDCl_3)	-100.02 (s)

10c Preparation of $[\text{Cp}^*\text{Fe}(\text{P}(\text{C}_6\text{H}_4\text{F})(\text{C}_6\text{H}_4)\text{P}(\text{C}_6\text{H}_4\text{F})(\text{C}_6\text{H}_4)\text{As}(\text{C}_6\text{H}_5)(\text{C}_6\text{H}_4))][\text{BF}_4]$

$[\text{Cp}^*\text{Fe}\{\text{(o-C}_6\text{H}_4\text{F)}_2\text{PC}_6\text{H}_4\text{P}(\text{o-C}_6\text{H}_4\text{F})_2\}\text{AsH}_2\text{C}_6\text{H}_5]\text{BF}_4$ (0.20g, 0.21mmol) was dissolved in THF (40ml), potassium *tert*butoxide (0.50g) was added to the solution. The reaction was left to stir overnight and filtered. The solvent was removed *in vacuo* to give a yellow solid (M_R 910.33, 0.15g, 78% yield).

Measured	Data
$^1\text{H-NMR}$ (CDCl_3)	1.69 (s, Cp*), 6.98-7.30 (m)
$^{13}\text{C}\{^1\text{H}\}$ NMR (CDCl_3)	10.00 (Cp*), 87.04 (s, Cp*), 127.62-134.12 (m), 164.10 (dd, $^1J_{\text{C-F}}249.00\text{Hz}$).
$^{31}\text{P-NMR}$ (CDCl_3)	130.38-132.09 (m)
$^{19}\text{F-NMR}$ (CDCl_3)	-102.68 (s)
MS (APCI)	823.53 Da/e (M^+).

11b Preparation of $[\text{CpFe}\{\text{(o-C}_6\text{H}_4\text{F)}_2\text{AsC}_6\text{H}_4\text{As}(\text{o-C}_6\text{H}_4\text{F})_2\}\text{PH}_2\text{C}_6\text{H}_5][\text{PF}_6]$

$[\text{CpFe}(\text{o-C}_6\text{H}_4\text{F})_2\text{AsC}_6\text{H}_4\text{As}(\text{o-C}_6\text{H}_4\text{F})(\text{CH}_3\text{CN})][\text{PF}_6]$ (0.88g, 0.96mol) was dissolved in 1,2-dichlorobenzene (30ml). Phenyl phosphine (M_R 110.10, δ 1.001, 0.5ml, 5.0mmol) was added and the reaction mixture heated to 60°C for 16 hours until the colour changed from dark blue to orange. The solvent was removed *in vacuo* and the residue triturated with ether to give a yellow powder (M_R 982.26, 0.86g, 91% yield).

Measured	Data
$^1\text{H NMR}$ (CDCl_3)	3.98 (s, 5H, Cp), 4.63 (d, $^1J_{\text{P-H}} 338.1\text{Hz}$, PH_2Ph), 7.49-6.69

	(m, 30H, aromatic protons).
$^{13}\text{C}\{^1\text{H}\}$ NMR (CDCl ₃)	115.61 (d, $^2J_{\text{C-F}}$ 23.24Hz), 124.03-136.02 (m), 164.32 (d, $^1J_{\text{C-F}}$ 243.22Hz).
^{31}P NMR (CDCl ₃)	-143.73 (sept, PF ₆ , $^1J_{\text{P-F}}$ 714.42), 11.83 (co-ordinated PH ₂ Ph).
^{19}F NMR (CDCl ₃)	-101.38 (s)
MS (APCI)	837 (M ⁺).
ν/cm^{-1} (KBr)	3066(s), 2330(w), 1594(w), 1468(m), 1438(w), 1260(w), 1210(w), 1096(w), 839(w), 770(m).

11c Preparation of [CpFe(As(C₆H₄F)(C₆H₄)As(C₆H₄F)(C₆H₄)P(C₆H₅)(C₆H₄)]PF₆

[CpFe{(o-C₆H₄F)₂AsC₆H₄As(o-C₆H₄F)₂}PH₂C₆H₅][PF₆] (0.22g, 0.22mmol) was dissolved in THF (40ml), potassium *tert*butoxide (catalytic quantities) was added to the solution. The reaction was left to stir overnight and filtered. The solvent was removed *in vacuo* to give a yellow solid (M_R942.25, 0.15g, 73% yield).

Measured	Data
^1H NMR (CDCl ₃)	3.98 (s, Cp, 5H), 6.90-7.74 (m, aromatic protons, 25H).
$^{13}\text{C}\{^1\text{H}\}$ NMR (CDCl ₃)	82.0 (s, Cp), 128.90-135.12 (m).
^{31}P NMR (CDCl ₃)	134.55 (s broad, macrocycle), -143.73 (sept, PF ₆ , $^1J_{\text{P-F}}$ 714.42)
^{19}F NMR (CDCl ₃)	-100.09 (s, macrocycle), -73.52 (d, PF ₆ , $^1J_{\text{P-F}}$ 714.42).
MS (APCI)	796.8 Da/e (M ⁺).
ν/cm^{-1} (nujol)	2923.76(s), 1958.59(w), 1600.12(m), 1461.61(s), 1377.07(w), 1260.53(s), 1077.59(m), 1019.29(w), 838.64(w), 801.83(w), 722.52(m), 579.65(w), 574.37(w), 557.39(w).

12b Preparation of [Cp*Fe{(o-C₆H₄F)₂AsC₆H₄As(o-C₆H₄F)₂}PH₂C₆H₅][BF₄]

[Cp*Fe(o-C₆H₄F)₂AsC₆H₄As(o-C₆H₄F)₂](CH₃CN)][BF₄] (0.50g, 0.54mol) was dissolved in THF (30ml). Phenyl phosphine (M_R110.10, δ 1.001, 0.5ml, 5.0mmol) was added and the reaction mixture heated to 60°C for 16 hours until the colour changed from dark purple to orange. The solvent was removed *in vacuo* and the residue washed with ether to give an orange powder (M_R 994.29, 0.50g, 93% yield).

Measured	Data
^1H NMR (CDCl_3)	6.86-7.73 (m, 25H),
$^{13}\text{C}\{^1\text{H}\}$ NMR (CDCl_3)	115.38 (d, $^2J_{\text{C-F}}$ 24.24Hz), 124.32-137.67 (m), 164.71 (d, $^1J_{\text{C-F}}$ 246.35Hz).
^{31}P NMR (CDCl_3)	16.75 (t, $^1J_{\text{P-H}}$ 342.0Hz)
^{19}F NMR (CDCl_3)	-99.78 (s)

12c Preparation of $[\text{Cp}^*\text{Fe}(\text{As}(\text{C}_6\text{H}_4\text{F})(\text{C}_6\text{H}_4)\text{As}(\text{C}_6\text{H}_4\text{F})(\text{C}_6\text{H}_4)\text{P}(\text{C}_6\text{H}_5)(\text{C}_6\text{H}_4)]\text{[BF}_4\text{]}$

Potassium *tert*butoxide (catalytic quantities) was added to a solution of $[\text{Cp}^*\text{Fe}\{\text{(o-C}_6\text{H}_4\text{F)}_2\text{AsC}_6\text{H}_4\text{As}(\text{o-C}_6\text{H}_4\text{F})_2\}\text{PH}_2\text{C}_6\text{H}_5]\text{BF}_4$ (0.22g, 0.22mmol) in THF (40ml). The reaction was left to stir overnight and filtered. The solvent was removed *in vacuo* to give a yellow solid (M_R 954.28, 0.15g, 71% yield).

Measured	Data
^1H NMR (CDCl_3)	3.74 (s, 5H, Cp), 6.91-7.43 (m, 25H).
$^{13}\text{C}\{^1\text{H}\}$ NMR (CDCl_3)	115.19 (d, $^2J_{\text{C-F}}$ 24.58Hz), 124.88 (s), 128.47-135.05 (m), 144.25 (s), 164.36 (d, $^1J_{\text{C-F}}$ 243.46Hz).
^{31}P NMR (CDCl_3)	112.01 (s, macrocycle)
^{19}F NMR (CDCl_3)	-102.37 (s)
MS (APCI)	867.5 Da/e (M^+).

Preparation of $[\text{Cp}^*\text{Fe}\{\text{(o-C}_6\text{H}_4\text{F)}_2\text{AsC}_6\text{H}_4\text{As}(\text{o-C}_6\text{H}_4\text{F})_2\}\text{AsH}_2\text{C}_6\text{H}_5]\text{[BF}_4\text{]}$

Phenyl arsine (0.8ml, 0.96mmol) was added to a solution of $[\text{Cp}^*\text{Fe}(\text{o-C}_6\text{H}_4\text{F})_2\text{AsC}_6\text{H}_4\text{As}(\text{o-C}_6\text{H}_4\text{F})\text{CH}_3\text{CN}]\text{BF}_4$ (0.90g, 0.97mmol) in THF (30ml). The reaction mixture was heated to 60°C for 16 hours until the colour changed from red to orange. The solvent was removed *in vacuo* and the residue triturated with ether to give an orange powder (M_R 1038.24, 0.88g, 87% yield).

Measured	Data
^1H NMR (CDCl_3)	1.72 (s, 15H, Cp*), 7.01-7.33 (m, 25H)
$^{13}\text{C}\{^1\text{H}\}$ NMR (CDCl_3)	128.90-134.99 (m), 163.99 (d, $^1J_{\text{C-F}}$ 240.01Hz).
^{19}F NMR (CDCl_3)	-101.33 (s)

MS (APCI)	951.44 Da/e (M ⁺).
-----------	--------------------------------

Attempted Preparation of [Cp*Fe(As(C₆H₄F)(C₆H₄)As(C₆H₄F)(C₆H₄)As(C₆H₅)(C₆H₄)] [BF₄]

[Cp*Fe{(o-C₆H₄F)₂AsC₆H₄As(o-C₆H₄F)₂}AsH₂C₆H₅]BF₄ (0.44g, 0.42mmol) was dissolved in THF (40ml), potassium *tert*butoxide (2 mole equivalents, 0.05g, 0.78mol) was added to the solution. The reaction was left to stir overnight and filtered. The solvent was removed *in vacuo* to give a yellow/brown solid (M_R 998.23, 0.12g, 18% yield). The product from this experiment was unstable and decomposed before analysis could take place.

13b Preparation of [CpFe(H₂AsC₆H₄AsH₂)P(C₆H₄F)₃][PF₆]

[CpFe{(H₂AsC₂H₄AsH₂)CH₃CN}][PF₆] (0.38g, 0.85mmol) was dissolved in acetonitrile (35ml). Tri*ortho*fluorophenyl phosphine (0.32g, 1mmol) was added and the reaction mixture heated to 60°C for 10 hours, a colour change from red to yellow was observed. The solvent was removed *in vacuo* and the remaining solid triturated with ether. The solvent was removed to give a yellow powder (M_R 764.10, 0.49g, 76% yield).

Measured	Data
¹ H NMR (CDCl ₃)	3.74 (s, 5H, Cp), 7.02-7.31 (m, 16H).
¹³ C{ ¹ H} NMR (CDCl ₃)	124.87-137.66 (m, 24C), 164.56 (d, ¹ J _{C-F} 309.83Hz).
³¹ P NMR (CDCl ₃)	-143.61 (sept, PF ₆ , ¹ J _{P-F} 714.42), 22.11 [s, co-ordinated P(C ₆ H ₄ F) ₃].
¹⁹ F NMR (CDCl ₃)	-102.89 (s), -73.52 (d, ¹ J _{P-F} 714.42).
MS (APCI)	619.1 Da/e (M ⁺).

13c Preparation of [CpFeAsH(C₆H₄)AsH(C₆H₄)P(C₆H₄)(C₆H₄F)][PF₆]

Potassium *tert*butoxide (catalytic quantity) was added to a solution of [CpFe{(H₂AsC₆H₄AsH₂)P(C₆H₄F)₃][PF₆] (0.49g, 0.65mmol) in THF (30ml), and the

reaction mixture heated to 60°C for 9 hours. The solvent was removed *in vacuo* to give a yellow powder (M_R 724.09, 0.20g, 42% yield).

Measured	Data
^1H NMR (CDCl_3)	3.74 (s, 5H, Cp), 6.89-7.42 (m, 16H).
$^{13}\text{C}\{^1\text{H}\}$ NMR (CDCl_3)	121.97-137.89 (m), 164.43 (d, $^1J_{\text{C-F}}$ 300.68Hz).
^{31}P NMR (CDCl_3)	123.08 (s)
^{19}F NMR (CDCl_3)	-101.64 (s)
MS (APCI)	579.1 Da/e (M^+).

Attempted Preparation of $[\text{Cp}^*\text{Fe}(\text{H}_2\text{As}(\text{C}_6\text{H}_4)\text{AsH}_2)\text{P}(\text{C}_6\text{H}_4\text{F})_3][\text{BF}_4]$

Triorthofluorophenyl phosphine (0.32g, 1mmol) was added to a solution of $[\text{Cp}^*\text{Fe}\{(\text{H}_2\text{AsC}_2\text{H}_4\text{AsH}_2)\text{CH}_3\text{CN}\}]\text{BF}_4$ (0.47g, 0.85mmol) in acetonitrile (35ml). The reaction mixture was heated to 60°C for 10 hours, a colour change from red to orange was observed. The solvent was removed *in vacuo* and the resulting solid triturated with ether to give a dark orange powder. ^{31}P NMR studies indicated decomposition.

14b Preparation of $[\text{Cp}^*\text{Fe}(\text{H}_2\text{PC}_6\text{H}_4\text{PH}_2)\text{As}(\text{C}_2\text{H}_3)_3][\text{PF}_6]$

$[\text{Cp}^*\text{Fe}\{(\text{H}_2\text{PC}_2\text{H}_4\text{PH}_2)\text{CH}_3\text{CN}\}]\text{PF}_6$ (0.40g, 1.00mmol) was dissolved in acetonitrile (30ml). Trivinyl arsine (0.78g, 5mmol) was added and the reaction mixture heated to 60°C for 24 hours, a colour change from red to dark orange was observed. Attempts to remove the solvent *in vacuo* at this stage were unsuccessful and the precursor could not be isolated, a mass spectrum was taken to confirm the presence of the precursor (M_R 634.17, yield unknown).

Measured	Data
MS (APCI)	488.93 (M^+).

14c Preparation of $[\text{Cp}^*\text{FePH}(\text{C}_6\text{H}_4)\text{PH}(\text{C}_2\text{H}_4)\text{As}(\text{C}_2\text{H}_4)(\text{C}_2\text{H}_3)][\text{PF}_6]$

Triethyl amine (0.5ml, 5mmol) was added to a solution of $[\text{Cp}^*\text{Fe}(\text{H}_2\text{PC}_6\text{H}_4\text{PH}_2)\text{As}(\text{C}_2\text{H}_3)_3][\text{PF}_6]$ (made *in situ*, 0.63g, 1.00mmol) in THF (20ml).

The reaction mixture was heated to 70°C for 6 hours. The solvent was removed *in vacuo* to give an orange/yellow powder (M_R 634.17, 0.15g, 24% yield).

Measured	Data
$^1\text{H-NMR}$ (C_6D_6)	1.78 (s, CH_2), 1.93 (s, CH_2), 3.98 (s, 5H, Cp), 4.23 (d, $^1J_{\text{P-H}}$ 323.8Hz, PH), 6.83-7.11 (m, 4H, Ar-H).
$^{31}\text{P-NMR}$ (C_6D_6)	106.40 (s), -144.00 (sept, $^1J_{\text{P-F}}$ 720.13Hz)
MS (APCI)	488.93 (M^+).

Attempted Preparation of $[\text{CpFe}(\text{H}_2\text{PC}_6\text{H}_4\text{PH}_2)\text{Sb}(\text{C}_2\text{H}_3)_3][\text{PF}_6]$

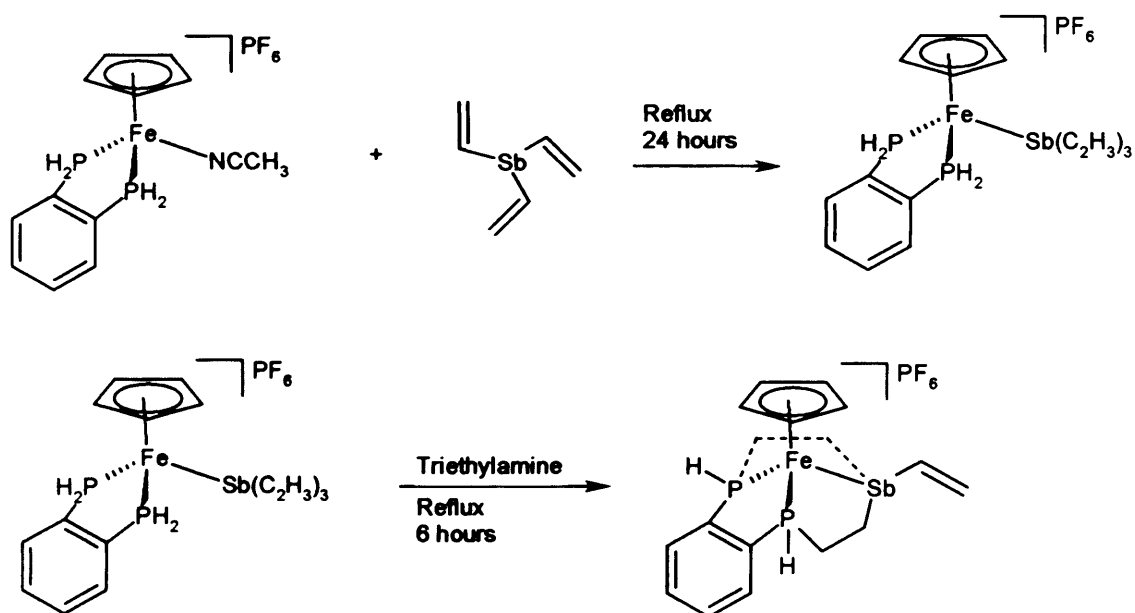
$[\text{CpFe}\{(\text{H}_2\text{PC}_2\text{H}_4\text{PH}_2)\text{CH}_3\text{CN}\}]\text{PF}_6$ (0.40g, 1.00mmol) was dissolved in acetonitrile (30ml). Trivinyl stibine (1.02g, 5mmol) was added and the reaction mixture heated to 60°C for 24 hours, a colour change from red to dark orange was observed. Attempts to remove the solvent *in vacuo* at this stage resulted in decomposition and the precursor could not be isolated, a mass spectrum was taken to confirm the presence of the precursor (M_R 611.12, yield unknown).

Measured	Data
MS (APCI)	466.1 Da/e (M^+).

Attempted Preparation of $[\text{CpFePH}(\text{C}_6\text{H}_4)\text{PH}(\text{C}_2\text{H}_4)\text{Sb}(\text{C}_2\text{H}_4)(\text{C}_2\text{H}_3)][\text{PF}_6]$

Triethylamine (0.5ml, 5mmol) was added to a solution of $[\text{CpFe}(\text{H}_2\text{PC}_6\text{H}_4\text{PH}_2)\text{Sb}(\text{C}_2\text{H}_3)_3]\text{PF}_6$ (made *in situ*, max yield 0.61g, 1.00mmol) in THF (20ml). The reaction mixture was heated to 70°C for 6 hours. The solvent was removed *in vacuo* to give an orange/yellow powder (M_R 611.12, 0.15g, 24% yield). The solid formed in this reaction was exceedingly air sensitive, on mixing with a variety of deuterated solvents decomposition was observed. Mass and infrared spectra could not be obtained from the product due to decomposition.

Measured	Data
$^1\text{H-NMR}$ (C_6D_6)	1.69 (s, CH_2), 2.01 (s, CH_2), 3.99 (s, 5H, Cp), 6.99-7.31 (m, Ar-H).
$^{31}\text{P-NMR}$ (C_6D_6)	-4.47 (s)



Attempted Preparation of $[\text{CpFe}(\text{H}_2\text{PC}_2\text{H}_4\text{PH}_2)\text{Sb}(\text{C}_2\text{H}_3)_3][\text{PF}_6]$

$[\text{CpFe}(\text{H}_2\text{PC}_2\text{H}_4\text{PH}_2)\text{CH}_3\text{CN}]\text{PF}_6$ (0.40g, 1.00mmol) was dissolved in acetonitrile (30ml). Trivinyl stibine (1.02g, 5mmol) was added and the reaction mixture heated to 60°C for 24 hours, a colour change from red to dark orange was observed. Attempts to remove the solvent *in-vacuo* at this stage were unsuccessful and the precursor could not be isolated.

Attempted Preparation of $[\text{CpFePH}(\text{C}_2\text{H}_4)\text{PH}(\text{C}_2\text{H}_4)\text{Sb}(\text{C}_2\text{H}_4)(\text{C}_2\text{H}_3)][\text{PF}_6]$

$[\text{CpFe}(\text{H}_2\text{PC}_2\text{H}_4\text{PH}_2)\text{Sb}(\text{C}_2\text{H}_3)_3]\text{PF}_6$ (from previous method, max yield 0.61g, 1.00mmol) was dissolved in THF (20ml). Triethylamine (0.5ml, 5mmol) was added which resulted in immediate decomposition, the experiment was repeated with potassium *tert*butoxide which also resulted in decomposition.

Preparation of $[\text{Cp}^*\text{Fe}(\text{H}_2\text{PC}_6\text{H}_4\text{PH}_2)\text{Sb}(\text{C}_2\text{H}_3)_3][\text{BF}_4]$

$[\text{Cp}^*\text{Fe}(\text{H}_2\text{PC}_2\text{H}_4\text{PH}_2)\text{CH}_3\text{CN}]\text{BF}_4$ (0.46g, 1.00mmol) was dissolved in acetonitrile (30ml). Trivinyl stibine (1.00g, 5mmol) was added and the reaction mixture heated to 60°C for 24 hours, a colour change from red to dark orange/brown was observed. Attempts to remove the solvent *in-vacuo* at this stage were unsuccessful and the precursor could not be isolated, both NMR's and mass spectra were taken but were inconclusive.

References

- ¹ D. Zhao, J.S. Moore; *Chem. Comm.*; **2003**; 807
- ² R.H.; Crabtree; *The Organometallic Chemistry of the Transition Elements*; Wiley-Interscience; **1989**
- ³ M.J. Atherton, J. Fawcett, J.H. Holloway, E.G. Hope, A. Karaçar, D.R. Russell, G.C. Saunders, *J. Chem. Soc. Dalton Trans.* **1996**; 3215
- ⁴ M.J. Atherton, J. Fawcett, J.H. Holloway, E.G. Hope, D.R. Russell, G.C. Saunders, *J. Organomet. Chem.*, **1999**; **163**; 582
- ⁵ P.C. Cagle, O. Meyer, D. Vichard, K. Weickhardt, A.M. Arif, J.A. Gladysz; *Organometallics*; **1996**; **15**; 194
- ⁶ S. White, B.L. Bennett, D.M. Roddick; *J. Amer. Chem. Soc.* **1998**; **120**; 11020
- ⁷ H.G. Ang, W.L. Kwik, W.K. Leong, B.F.G. Jonson, J. Lewis, P.R. Raithby; *J. Organomet. Chem.*; **1990**; **C43**; 396
- ⁸ P.E. Garou; *Chem. Rev.*; **1985**; **85**; 171
- ⁹ R.M. Bellabarba, M. Nieuwenhuyzen, G.C. Saunders; *Organomet.*; **2002**; **21**; 5726
- ¹⁰ T. Albers; Ph.D. Thesis; Cardiff University; **2000**
- ¹¹ P.G. Edwards, M.L. Whatton, R. Haigh; *Organometallics*; **2000**; **19(14)**; 2652
- ¹² M.L. Whatton; Ph.D. Thesis; Cardiff University; **2002**
- ¹³ E.P. Kyba, S-S.P. Chou; *Chem. Comm.*; **1980**; 449
- ¹⁴ C.S. Slone, D.A. Weinberger, C.A. Mirkin; *Progress in Inorganic Chemistry*; **1999**; **48**; 233-350
- ¹⁵ Determined from a survey of the Cambridge Crystallographic Database September 2004
- ¹⁶ M.A. Fox, K.A. Campbell, E.P. Kyba; *Inorg. Chem.*; **1981**; **20**; 4163
- ¹⁷ C.A. Tolman; *Chem. Rev.*; **1977**; **77**; 313
- ¹⁸ C.W. Smith, G.W. Vanloon, M.C. Baird; *J. Coord. Chem*; In press
- ¹⁹ E.P. Kyba, M.C. Kerby, S.P. Rines; *Organometallics*; **1986**; **5**; 1189
- ²⁰ U. Monkowius, S. Nogai, H. Schmidbaur; *Organometallics*; **2003**; **22**; 145
- ²¹ V.E. Wiberg, K. Mödritzer; *Z. Naturforschg.*; **1956**; **11b**; 750
- ²² V.E. Wiberg, K. Mödritzer; *Z. Naturforschg.*; **1956**; **11b**; 751

Chapter 3

Bimetallic Complexes

Introduction

Bimetallic Complexes

Bimetallic complexes are those which contain two metal ions held together by a ligand structure. Cyclic ligand species which are able to incorporate two metal ions offer the prospect of generating unusual electronic and chemical properties which are a result of the close proximity of the metal centres. There are three main types of binucleating macrocyclic ligands, firstly large ring macrocycles which are capable of incorporating two metal ions in their ring structure, secondly systems with one bridging unit and thirdly, those containing more than one bridging unit. This Chapter provides examples of the second type of binucleating macrocycles with one linker unit. Bimetallic complexes often show characteristic properties including magnetic exchange between the two metal ions and an increased tendency to undergo multi electron redox reactions.

The potential applications of bimetallic dimacrocyclic complexes are widespread. They provide an environment in which two similar metal ions with different alternative ligands can be brought into close proximity. Their proximity could lead to new reactivity between the other ligands attached to the metal ion. The nature of the dimacrocycle could be adjusted to suit different co-ordination environments which could allow the co-ordination of two different metal ions in order to explore more unusual bimetallic complexes and their reactivities.

Previous research has been carried out (see Chapter 2) to synthesise macrocyclic complexes via a novel dehydrofluorinative cyclisation. In this chapter it is aimed to use the precursor complexes containing orthofluorophenyl rings on the bidentate phosphine followed by $\text{H}_2\text{P}(\text{C}_6\text{H}_4)(\text{C}_6\text{H}_4)\text{PH}_2$ as the primary phosphine. It is hoped that both macrocyclic complexes and dimacrocyclic complexes can be synthesised (Figure 3.1).

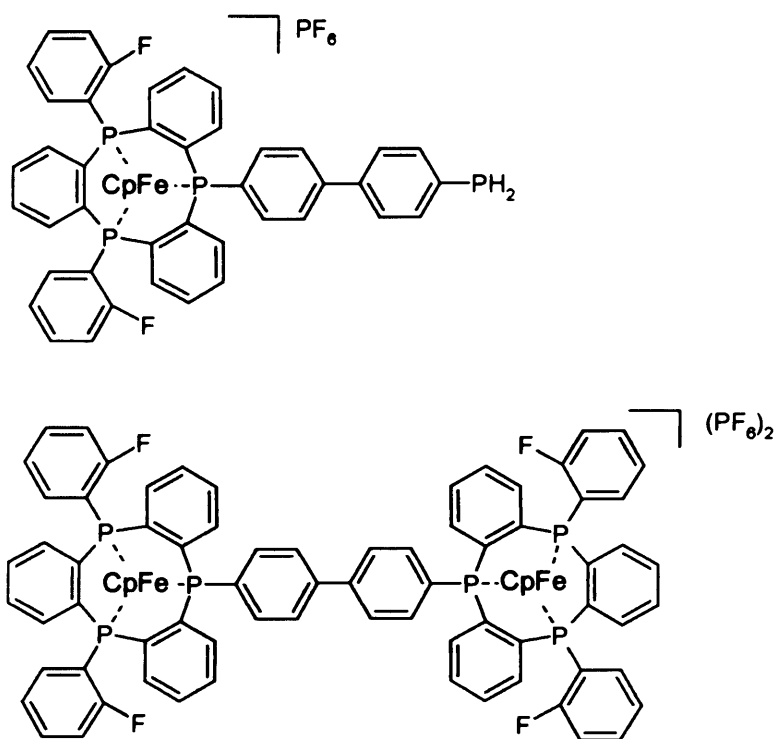


Figure 3.1 Examples of two of the complexes synthesised 15c(1:1) and 15c.

Previous research into bimetallic complexes has focussed on the binucleating properties towards transition metals which has attracted much interest recently, in particular bimetallic copper(II) complexes. These have been widely used in biomimetic chemistry with regard to copper(II) proteins and also in substrate activation by metal centres.¹ Binuclear bimetallic complexes of this type (involving two macrocyclic ligands joined by a linker) are rare but metal co-ordination provides an efficient route to their formation.

Similar research carried out with nitrogen donors and 14[ane] tetra aza macrocycles has resulted in the production of a series of bimetallic complexes (Figure 3.2).² The synthesis of dimacrocyclic complexes by bridging amine groups, or carbon atoms of the ligand backbone is a popular method, by extending this chemistry to bridges between phosphine groups, dimacrocyclic triphosphorus macrocycles can be made by incorporating a primary phosphine linker into the macrocyclic framework.

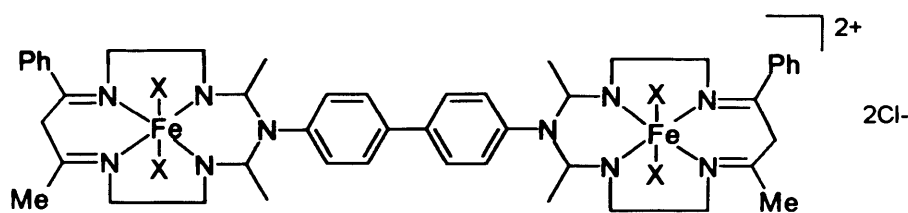


Figure 3.2 An example of a previously synthesised dimacrocylic complex (Singh).²

Shorter bridges between the macrocycles can also be used (Figure 3.3).^{3,4} The length of the bridge between the macrocycles will have an effect on the electronic properties of the dimacrocylic complexes affecting the proximity of the other ligands attached to the metal ion and electronic communication between the metal centres. Aromatic spacer units are especially useful because they provide sites for π stacking and promote hydrophobic interactions within the cavity which increase the crystallinity of the dimacrocylic structure (Figure 3.3).⁴

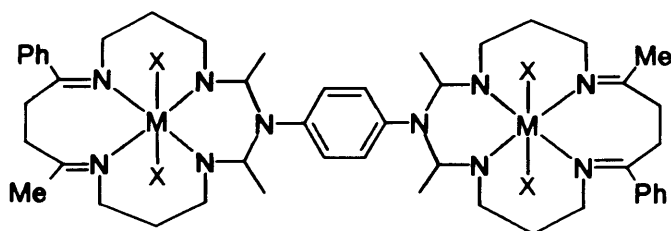


Figure 3.3 An example of a dimacrocylic complex synthesised by Bilyk.⁴

The expansion of the synthesis of dimacrocylic complexes includes the possibility of preparing molecular sieve type structures of defined shape and size with selective recognition properties.⁵

Dimacrocylic 1,4,7-triazacyclononane (TACN) based ligands have been previously synthesised. Sandwich complexes of tacn are well known for their kinetic and thermodynamic stability. N functionalised 9[ane] N_3 macrocycles containing three pendant groups, for example amine groups⁶ give rise to hexadentate ligands which confer additional stability to their metal complexes. Ligands comprising two alkyl bridged 9[ane] moieties have also attracted attention as they form kinetically and thermodynamically stable polynuclear complexes with two or three co-ordination sites on each metal centre available for additional ligands or bridges.^{7,8} A new synthetic technique has been developed by Schröder et al.⁹ to synthesise dimacrocylic 9[ane] N_3 ligands. TACN is reacted with conc. H_2SO_4 and HBr to give $N(C_2H_4)N(C_2H_4)N(C_2H_4)$ with a central CH attached to all of the nitrogen atoms. Reaction with 1,2 dibromoethane leads to the production of 1 (Figure 3.7).

Complex 2 (Figure 3.7) can also be synthesised which is a close analogy to the P_3 dimacrocyclic complexes which have been prepared in this chapter.

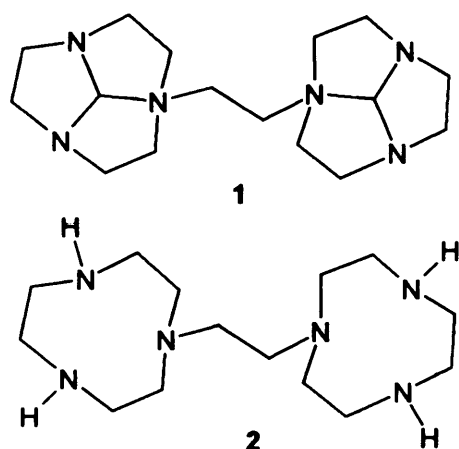


Figure 3.7 Examples of dimacrocyclic complexes synthesised by Schröder.⁹

Phosphorus bimetallic complexes have been previously prepared by the Edwards group to form the following complex (Figure 3.4), yields were not high and the complex could not be fully characterised. Addition of $[\text{CpFe}(\text{C}_3\text{H}_5)_2\text{PC}_2\text{H}_4\text{P}(\text{C}_3\text{H}_5)_2\text{CH}_3\text{CN}][\text{PF}_6]^{12}$ to phenyl phosphine and cyclisation provided both the 11[ane] complex predicted and a 10[ane] complex whereby one of the allyl groups has become an ethyl backbone with an exocyclic methyl group. By heating this reaction mixture to 70°C the following dimacrocyclic complex is proposed as one of the reaction products.¹²

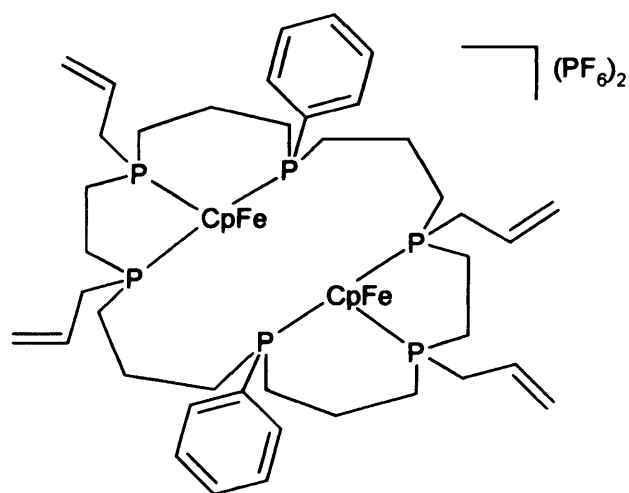


Figure 3.4 This unusual dimacrocyclic complex was synthesised by Haigh¹² as a byproduct of a cyclisation reaction.

It has been demonstrated by Malisch et al.¹⁰ that $\text{Fp}^+\text{P}(\text{RH})$ sub units can be linked using dicarboxylic acid linkers to form bimetallic species, this could be used as an alternative linker unit if the Fp^+PH_2 complex is used with the carbonyl ligands substituted for either $\text{P}(\text{o-C}_6\text{H}_4\text{F})_2$, $(\text{C}_6\text{H}_4)\text{P}(\text{o-C}_6\text{H}_4\text{F})_2$ or TAPC (tetraallylbisphosphinoethane) to form a bimetallic dimacrocylic complex.

If bimetallic dimacrocylic complexes can be synthesised it may be possible to synthesise larger arrays, studying the chemistry within these complexes could lead to the binding of specific metal ions and ligands and lead to selective binding within the structure.

Complexes involving linear triphosphine ligands bridging between either iron and tungsten, or iron and molybdenum have been synthesised and characterised by Baker *et al.*,¹¹ in this chapter it is aimed to investigate the synthesis of bimetallic complexes involving triphosphorus macrocycles to study the feasibility of their synthesis. The complexes synthesised may show unusual properties electrochemically and in terms of unusual electron migrations after oxidation or reduction which could be studied by EPR spectroscopy.

Results and Discussion

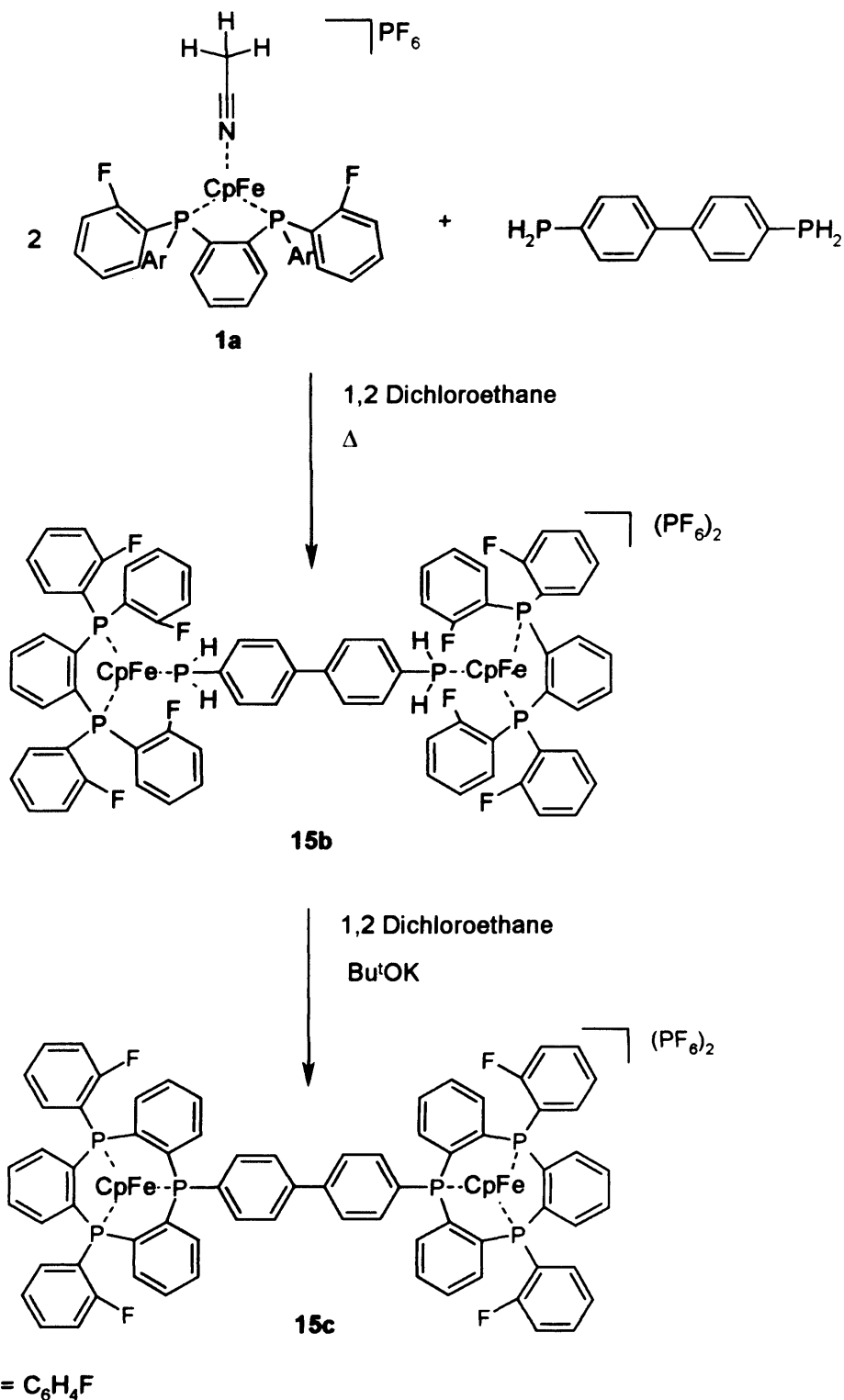


Figure 3.5 The synthetic route used to prepare dimacrocylic complexes.

The first examples of the synthesis of bimetallic dimacrocylic complexes involving triphosphorus macrocycles are described in this Chapter. Figure 3.5 illustrates the synthetic route used to prepare these complexes.

Two similar methods of synthesis were used, the first (Figure 3.5) requires the use of *diortho*fluorophenyl bispnictido precursors followed by the use of $\text{H}_2\text{P}(\text{C}_6\text{H}_4)_2\text{PH}_2$ as a linker unit between the two precursor macrocycles synthesised. Following cyclisation with potassium *tert*butoxide the dimacrocylic complex can be made.

Attempts to make complexes from *diortho*fluorophenyl bisphosphinoethane failed due to decomposition during cyclisation, using triethylamine as a base to cyclise the macrocycles also failed as a result of decomposition.

The dimacrocylic complexes have been described using abbreviated nomenclature describing the nature of the Cp moiety, the nature of the donor atoms and the nature of the backbones. For example, complex 15c $[\text{CpFeP}(\text{C}_6\text{H}_4\text{F})(\text{C}_6\text{H}_4)\text{P}(\text{C}_6\text{H}_4\text{F})(\text{C}_6\text{H}_4)\text{P}(\text{C}_6\text{H}_4)]_2[\text{PF}_6]_2$ is described as $\text{CpP}_3\text{tribenzdimac}$.

Treatment of $[\text{CpFe}\{(\text{C}_6\text{H}_4\text{F})_2\text{P}(\text{C}_6\text{H}_4)\text{P}(\text{C}_6\text{H}_4\text{F})_2\text{CH}_3\text{CN}\}][\text{PF}_6]$ with half a molar equivalent of 4,4'-bisphosphinodiphenyl resulted in the formation of complex 15b, $[\text{CpFeP}(\text{C}_6\text{H}_4\text{F})(\text{C}_6\text{H}_4)\text{P}(\text{C}_6\text{H}_4\text{F})(\text{C}_6\text{H}_4)\text{PH}_2(\text{C}_6\text{H}_4)(\text{C}_6\text{H}_4)]_2[\text{PF}_6]_2$. Characteristic peaks appeared in both the ^1H and $^{13}\text{C}\{^1\text{H}\}$ NMR spectra representing the Cp resonances. The ^{31}P NMR spectrum shows a broad singlet representing the co-ordinated diphosphine at 90.04ppm, a triplet represents the co-ordinated primary phosphine at 81.43ppm ($^1J_{\text{P-H}}$ 347.5Hz). The ^{19}F NMR spectrum shows a singlet at -104.23ppm due to the *ortho*fluorophenyl groups. After cyclisation with base the $\text{CpP}_3\text{tribenzdimac}$ 15c is formed. A complex multiplet was observed in the ^{31}P NMR spectrum from 121.97-126.23ppm representing the macrocyclic phosphorus atoms. Complicated multiplets were observed as a result of the second order nature of the spectrum.

An analogous reaction was carried out with Cp^* replacing Cp to give the $\text{Cp}^*\text{P}_3\text{tribenzdimac}$ as the final product 17c. Characteristic peaks are seen for the Cp^* in the ^1H NMR at 1.69ppm, a multiplet representing the aromatic protons is also seen from 6.89-7.30ppm. The $^{13}\text{C}\{^1\text{H}\}$ NMR spectrum shows characteristic Cp^* peaks at 10.00ppm and 87.02ppm. The *ortho*fluorophenyl resonance can be seen in the ^{19}F NMR spectrum as a singlet at -99.13ppm. Macrocyclic peaks in the ^{31}P NMR spectrum can be seen in ranges from 118.29-119.82ppm and 121.03-122.66ppm as complex multiplets.

In addition to analogous Cp^* complexes, $\text{CpAs}_2\text{Ptribenzdimac}$ 16c and $\text{Cp}^*\text{As}_2\text{Ptribenzdimac}$ 18c were synthesised. For the $\text{CpAs}_2\text{Ptribenzdimac}$ complex 16c a very broad singlet in the ^{31}P NMR is seen between 119.02 and 120.83ppm, no

coupling can be resolved from the spectra as the resolution (due to poor solubility) is poor. The Cp*As₂Ptribenzdimac **18c** was analysed by ³¹P NMR showing macrocyclic phosphorus resonances upfield from its Cp analogue but still poorly resolved as a very broad singlet between 115.98 and 116.04ppm.

Other synthetic strategies were attempted to synthesise single macrocyclic complexes with the 4,4 bisphosphinodibenzene linker unit as part of the macrocyclic structure in order to be able to link dissimilar macrocyclic structures together. The CpP₃tribenz **15c(1:1)** with pendant primary phosphine was synthesised in an identical manner to the synthesis of the dimacrocyclic complexes (Figure 3.5) differing only in the ratio of macrocyclic precursor to linker. Once synthesised both the CpP₃tribenz with pendant primary phosphine **15c(1:1)** and its Cp* analogue **17c(1:1)** are air sensitive and once exposed to air decompose into a variety of signals on the ³¹P NMR spectrum believed to represent phosphine oxides. In the ³¹P NMR spectrum complex **15c(1:1)** shows additional resonances to the CpP₃tribenzdimac at -124.92 (t, ¹J_{P-H} 210.2Hz) indicating the co-ordinated 4,4'-diphenylbisphosphine. Complex **17c(1:1)** shows a characteristic pendant primary phosphine peak at -125.622ppm (t, ¹J_{P-H} 202.5Hz).

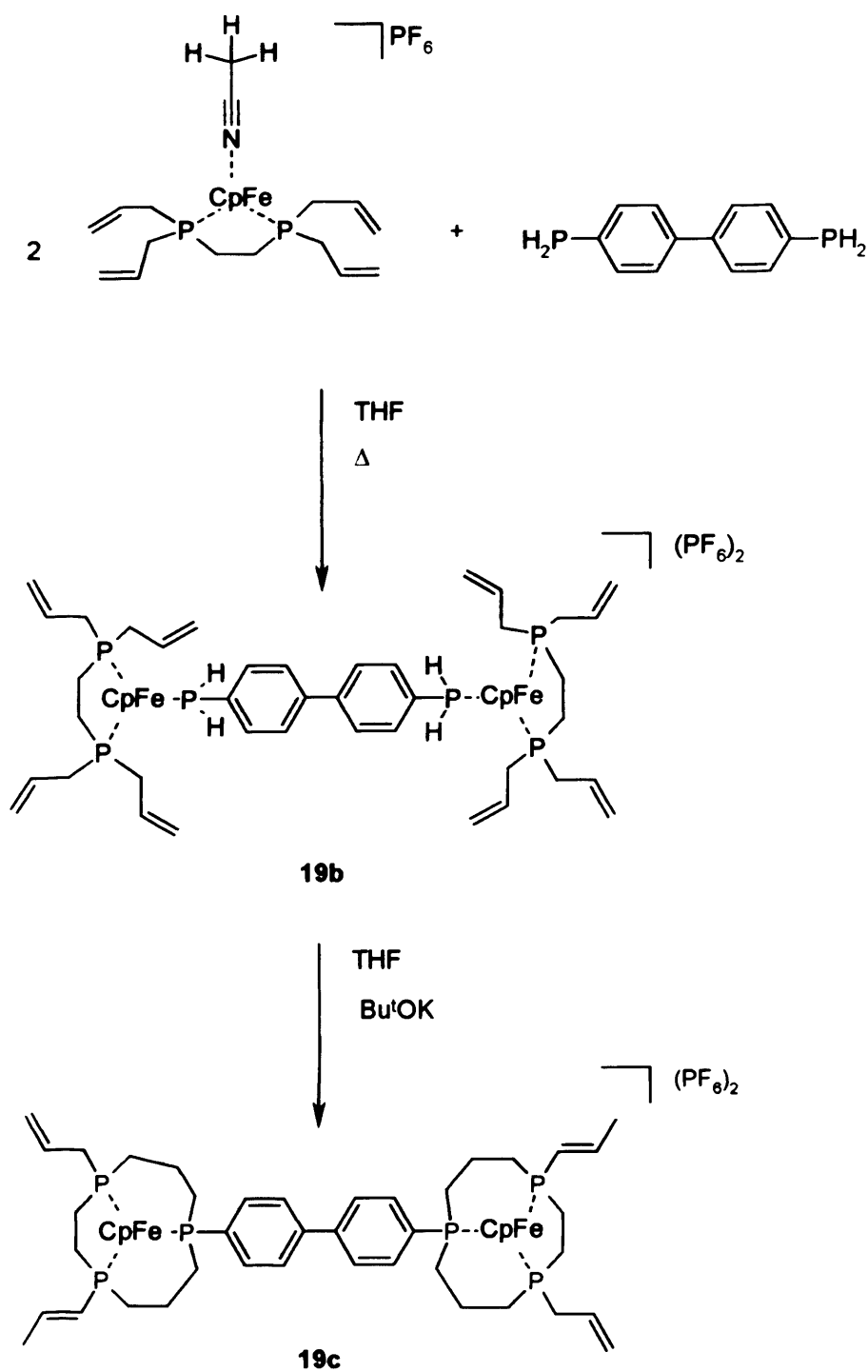


Figure 3.6 Alternative synthetic methodology utilising TAPE.

Alternative phosphines were also used to attempt to synthesise dimacrocyclic ligands. TAPE was used as an alternative to the di*ortho*fluorophenyl bisphosphido ligands to synthesise [CpFe{(C₃H₅)₂PC₆H₄P(C₃H₅)₂}CH₃CN][PF₆] complexes based on previous research.¹² Addition of half an equivalent of 4,4 bisphosphinodibenzene under reflux conditions gave complex 19b

$[\text{CpFe}\{(\text{C}_3\text{H}_5)_2\text{PC}_6\text{H}_4\text{P}(\text{C}_3\text{H}_5)_2\}\text{PH}_2(\text{C}_6\text{H}_4)_2][\text{PF}_6]_2$ characteristic peaks were seen in the ^1H NMR spectrum at 2.91ppm for the ethyl backbone of the TAPE ligand, at 4.02ppm for the Cp ligand and 1.72ppm, 5.31ppm & 5.13ppm for the allyl groups. The ^{31}P NMR spectrum shows a broad singlet (not resolved due to solubility problems) at 69.08ppm ($\text{H}_2\text{P}-$) and a singlet at 89.34ppm representing the TAPE ligand. Addition of potassium *tert*butoxide results in cyclisation to form complex **19c**, $\text{CpP}_3\text{dibenzTAPEdimac}$, as for the precursor complex characteristic peaks were seen in both the ^1H and ^{13}C NMR spectra for Cp and both the ethyl backbone and the allyl groups for the TAPE ligand. ^{31}P NMR resonances were unresolved but appeared as two sets of multiplets from 109.24-109.98ppm and from 110.04-112.58ppm.

Yields for these reactions, especially those involving *ortho*fluorophenyl groups in comparison to the macrocyclic complexes were much lower in most cases due to the complexes lack of solubility, 1,2 dichloroethane solutions often had to be warmed to encourage complexes to fully dissolve.

Conclusions

The novel dimacrocyclic structures which have been synthesised represent an exciting new class of triphosphorus macrocyclic complexes. Opportunities to study unusual reactivities and electron movement along with the redox chemistry of these novel bimetallic dimacrocyclic structures should lead to a better understanding of phosphine and arsine chemistry. Crystallisation was attempted for the complexes but was unsuccessful. NMR and mass spectrum studies were difficult due to the insolubility of the novel complexes in most organic solvents.

In the future different sizes and types of linker groups should be investigated as well as expanding the synthetic possibilities of making compounds containing more than 1 macrocyclic group.

In conclusion the first triphosphorus dimacrocyclic complexes have been synthesised. They will expand the area of phosphorus chemistry and enable new properties formed as a result of their dimacrocyclic nature in the new complexes.

Dimacrocylic Preparation

Most of the macrocylic precursor complexes were prepared as in Chapter 2. TAPE was also used as a ligand attached to both a CpFe^+ and Cp^*Fe^+ template.¹² Only a small proportion of 1:1 (macrocycle:linker) were made, possibly as a route to the synthesis of dimacrocylic complexes containing two different macrocylic fragments.

4,4'-Diphenylbisphosphine was synthesised previously by Albers as part of the Edwards group.¹³

Preparation of $[\text{CpFe}\{(o\text{-C}_6\text{H}_4\text{F})_2\text{PC}_2\text{H}_4\text{P}(o\text{-C}_6\text{H}_4\text{F})_2\}\text{PH}_2(\text{C}_6\text{H}_4)]_2[\text{PF}_6]_2$

$[\text{CpFe}\{(o\text{-C}_6\text{H}_4\text{F})_2\text{PC}_2\text{H}_4\text{P}(o\text{-C}_6\text{H}_4\text{F})_2\}\text{CH}_3\text{CN}][\text{PF}_6]$ (0.50g, 0.64mmol) was dissolved in 1,2-dichloroethane (40ml). $\text{H}_2\text{P}(\text{C}_6\text{H}_4)(\text{C}_6\text{H}_4)\text{PH}_2$ (0.07g, 0.32mmol) in dichloroethane (10ml) was added and the reaction mixture heated to 60°C for 6 hours. The solution changed in colour from red to yellow. The solvent was removed *in vacuo* and the remaining oil triturated with ether to give a yellow powder (M_R 1686.69, 0.34g, 31% yield).

Measured	Data
^1H NMR (CDCl_3)	2.67 (m, CH_2), 3.82 (s, Cp), 6.94-7.28(m).
$^{13}\text{C}\{^1\text{H}\}$ NMR (CDCl_3)	24.81 (CH_2), 82.08 (Cp), 122.96-125.11(m)
^{31}P NMR (CDCl_3)	-14.98 (t, $^1J_{\text{P-H}}$ 321.8Hz), 80.10 (broad singlet)
^{19}F NMR (CDCl_3)	-103.24 (s)
MS (APCI)	698.2 Da/e (M^+)

Attempted Preparation of $[\text{CpFeP}(\text{C}_2\text{H}_4)(o\text{-C}_6\text{H}_4\text{F})\text{P}(\text{C}_6\text{H}_4)(o\text{-C}_6\text{H}_4\text{F})\text{P}(\text{C}_6\text{H}_4)(\text{C}_6\text{H}_4)]_2[\text{PF}_6]$

$[\text{CpFe}\{(o\text{-C}_6\text{H}_4\text{F})_2\text{PC}_2\text{H}_4\text{P}(o\text{-C}_6\text{H}_4\text{F})_2\}\text{PH}_2(\text{C}_6\text{H}_4)]_2[\text{PF}_6]_2$ (0.34g, 0.20mmol) was dissolved in 1,2-dichloroethane (35ml). Potassium *tert*butoxide (0.02g, 0.20mmol) was added and the reaction mixture heated to 60°C for 8 hours. The solution did not change colour and ^{31}P NMR showed no reaction had taken place. The mixture was refluxed for a further 12 hours and a change from yellow to brown was observed. The solvent was removed *in vacuo*, ^{31}P NMR studies showed no recognisable peaks (including PF_6) indicating product decomposition.

15b(1:1) Preparation of [CpFe{(o-C₆H₄F)₂PC₆H₄P(o-C₆H₄F)₂}PH₂(C₆H₄)(C₆H₄)PH₂][PF₆]

H₂P(C₆H₄)(C₆H₄)PH₂ (0.13g, 0.61mmol) in 1,2 dichloroethane (9ml) was added to a solution of [CpFe(o-C₆H₄F)₂PC₆H₄P(o-C₆H₄F)₂CH₃CN][PF₆] (0.50g, 0.61mmol) in 1,2-dichloroethane (40ml). The reaction mixture was heated to 60°C for 8 hours until the colour changed from red to yellow. The solvent was removed *in vacuo* and the residue triturated with ether to give a yellow powder (M_R 1002.49, 0.46g, 76% yield).

Measured	Data
¹ H-NMR (CD ₃ CN)	3.79 (s, Cp), 7.01-7.42 (m).
¹³ C{ ¹ H} NMR (CD ₃ CN)	81.79 (s, Cp), 123.09-129.93 (m), 132.98 (s), 164.92 (dd, ¹ J _{C-F} 240.13Hz, ² J _{C-P} 6.01Hz).
³¹ P-NMR (CD ₃ CN)	-126.8 (t, ¹ J _{P-H} 243.2), -15.02 (t, ¹ J _{P-H} 332.5), 78.29 (t, ¹ J _{P-H} 345.8), 89.99 (d, ³ J _{P-F}).
¹⁹ F-NMR (CD ₃ CN)	-103.98 (s).
MS (APCI)	857.0 Da/e (M ⁺).

15b Preparation of [CpFe{(o-C₆H₄F)₂PC₆H₄P(o-C₆H₄F)₂}PH₂(C₆H₄)₂][PF₆]₂

H₂P(C₆H₄)(C₆H₄)PH₂ (0.08g, 0.37mmol) in 1,2 dichloroethane (6ml) was added to a solution of [CpFe(o-C₆H₄F)₂PC₆H₄P(o-C₆H₄F)₂CH₃CN][PF₆] (0.62g, 0.75mmol) in 1,2-dichloroethane (40ml). The reaction mixture was heated to 60°C for 6 hours until the colour changed from red to yellow. The solvent was removed *in vacuo* and the residue triturated with ether to give a yellow powder (M_R 1782.77, 0.48g, 73% yield).

Measured	Data
¹ H-NMR (CD ₃ CN)	3.76 (s, Cp), 6.91-7.24 (m).
¹³ C{ ¹ H} NMR (CD ₃ CN)	82.04 (s, Cp), 123.99-129.81 (m), 158.14 (dd, ¹ J _{C-F} 232.48Hz, ² J _{C-P} 5.98Hz).
³¹ P-NMR (CD ₃ CN)	-15.41 (t, ¹ J _{P-H} 328.2), 81.43 (t, ¹ J _{P-H} 347.5Hz), 90.04 (d, ³ J _{P-F} 88.2Hz).
¹⁹ F-NMR (CD ₃ CN)	-104.23 (s)
MS (APCI)	746.4 Da/e (M ⁺).

15c(1:1) Preparation of [CpFeP(C₆H₄F)(C₆H₄)P(C₆H₄F)(C₆H₄)(P(C₆H₄)(C₆H₄)PH₂)]₂[PF₆]

Potassium *tert*butoxide (0.05g, 0.46mmol) was added to a solution of [CpFe{(o-C₆H₄F)₂PC₆H₄P(o-C₆H₄F)₂}PH₂(C₆H₄)(C₆H₄)PH₂] [PF₆] (0.46g, 0.46mmol) in warm 1,2 dichlorobenzene (30ml). The reaction was left to stir overnight and filtered. The solvent was removed *in vacuo* and the solid washed with ether to give a yellow powder (M_R 962.47, 0.21g, 47% yield).

Measured	Data
¹ H-NMR (CDCl ₃)	3.78 (s, Cp), 6.70-7.58 (m).
¹³ C{ ¹ H} NMR (CDCl ₃)	82.04 (s, Cp), 123.99-129.81 (m), 160.01 (dd, ¹ J _{C-F} 239.79Hz, ² J _{C-P} 5.32Hz).
³¹ P-NMR (CDCl ₃)	-124.92 (t, ¹ J _{P-H} 210.2Hz), 86.29 (s), 91.11 (s), 116.51-117.21 (m), 120.07-121.01 (m).
¹⁹ F-NMR (CDCl ₃)	-100.89 (s)
MS (APCI)	817.5 Da/e (M ⁺).

15c Preparation of [CpFeP(C₆H₄F)(C₆H₄)P(C₆H₄F)(C₆H₄)P(C₆H₄)(C₆H₄)₂][PF₆]₂

Potassium *tert*butoxide (0.03g, 0.27mol) was added to a solution of [CpFe{(o-C₆H₄F)₂PC₆H₄P(o-C₆H₄F)₂}PH₂(C₆H₄)₂][PF₆]₂ (0.43g, 0.47mmol) in 1,2 dichloroethane (40ml). The reaction was left to stir overnight and filtered. The solvent was removed *in vacuo* and the residue washed with ether to give a yellow solid (M_R 1742.76, 0.30g, 63% yield).

Measured	Data
¹ H-NMR (CDCl ₃)	3.82 (s, Cp), 6.97-7.80 (m).
¹³ C{ ¹ H} NMR (CDCl ₃)	81.69 (s, Cp), 124.38 (s), 125.12-130.19 (m), 160.23 (dd, ¹ J _{C-F} 239.00Hz, ² J _{C-P} 5.54Hz).
³¹ P-NMR (CDCl ₃)	121.97-126.23 (m).
¹⁹ F-NMR (CDCl ₃)	-101.24 (s)
MS (APCI)	708.2 Da/e (M ⁺).
v/cm ⁻¹ (KBr)	2955.33 (s), 2923.42 (s), 2853.38 (w), 2725.85 (m), 2673.51 (w), 1461.6 (s), 1377.18 (s), 1299.91 (w), 1260.59 (m), 1074.04 (w), 1031.95 (w), 800.96 (w), 721.92 (w), 521.40 (w).

16b Preparation of [CpFe((o-C₆H₄F)₂AsC₆H₄As(o-C₆H₄F)₂)PH₂(C₆H₄)₂][PF₆]₂

H₂P(C₆H₄)(C₆H₄)PH₂ (0.03g, 0.24mmol) in 1,2 dichloroethane (3ml) was added to a solution of [CpFe(o-C₆H₄F)₂AsC₆H₄As(o-C₆H₄F)CH₃CN][PF₆] (0.43g, 0.47mmol) in 1,2-dichloroethane (30ml) and the reaction mixture heated to 60°C for 10 hours until the colour changed from blue to orange. The solvent was removed *in vacuo* and the residue triturated with ether to give an orange powder (M_R 1958.47, 0.13g, 28% yield).

Measured	Data
¹ H-NMR (CDCl ₃)	3.96 (s, Cp), 7.00-7.13 (m).
¹³ C{ ¹ H} NMR (CDCl ₃)	80.99 (s, Cp), 126.82-132.91 (m).
³¹ P-NMR (CDCl ₃)	76.18 (t, ¹ J _{P-H} 333.1Hz)
¹⁹ F-NMR (CDCl ₃)	-104.20 (s)
MS (APCI)	834.4 Da/e (M ⁺).

16c Preparation of [CpFe(As(C₆H₄F)(C₆H₄)As(C₆H₄F)(C₆H₄)P(C₆H₄))₂][PF₆]₂

[CpFe((o-C₆H₄F)₂AsC₆H₄As(o-C₆H₄F)₂)PH₂(C₆H₄)₂][PF₆]₂ (0.13g, 0.07mmol) was dissolved in 1,2 dichlorobenzene (40ml), potassium *tert*butoxide (0.01g) was added to the solution. The reaction was left to stir overnight and filtered. The solvent was removed *in vacuo* and the residue washed to give a yellow solid (M_R 1918.46, 0.09g, 68% yield).

Measured	Data
¹ H-NMR (CDCl ₃)	3.92 (s, Cp), 7.01-7.26 (m).
¹³ C{ ¹ H} NMR (CDCl ₃)	81.02 (s, Cp), 125.96-132.28 (m)
³¹ P-NMR (CDCl ₃)	119.02-120.83 (m).
¹⁹ F-NMR (CDCl ₃)	-105.32 (s).
MS (APCI)	814.3Da/e (M ⁺).

Preparation of [Cp*Fe((o-C₆H₄F)₂PC₂H₄P(o-C₆H₄F)₂)PH₂(C₆H₄)(C₆H₄)PH₂][BF₄]

{Cp*Fe((o-C₆H₄F)₂PC₂H₄P(o-C₆H₄F)₂)CH₃CN}BF₄ (0.41g, 0.48mmol) was dissolved in 1,2-dichloroethane (35ml). H₂P(C₆H₄)(C₆H₄)PH₂ (0.03g, 0.24mmol) in

1,2 dichloroethane was added and the reaction mixture heated to 60°C for 18 hours. The solution changed in colour from red to orange. The solvent was removed *in vacuo* and the oily solid triturated with ether to give an orange powder (M_R 1826.99, 0.10g, 23% yield).

Measured	Data
$^1\text{H-NMR}$ (CDCl_3)	1.71 (s, Cp*), 6.89-7.23 (m).
$^{13}\text{C}\{^1\text{H}\}$ NMR (CDCl_3)	9.79 (s, Cp*), 87.69 (s, Cp*), 123.48-130.23 (m), 163.29 (dd, $^1J_{\text{C-F}}233.98\text{Hz}$, $^2J_{\text{C-P}}7.82\text{Hz}$).
$^{31}\text{P-NMR}$ (CDCl_3)	80.01 (broad singlet).
$^{19}\text{F-NMR}$ (CDCl_3)	-104.98 (s).
MS (APCI)	755.4 Da/e (M^+).

Attempted Preparation of $[\text{Cp}^*\text{Fe}\{(\text{o-C}_6\text{H}_4\text{F})_2\text{PC}_2\text{H}_4\text{P}(\text{o-C}_6\text{H}_4\text{F})_2\}\text{P}(\text{C}_6\text{H}_4)(\text{C}_6\text{H}_4)\text{PH}_2][\text{BF}_4]$

$[\text{Cp}^*\text{Fe}\{(\text{o-C}_6\text{H}_4\text{F})_2\text{PC}_2\text{H}_4\text{P}(\text{o-C}_6\text{H}_4\text{F})_2\}\text{PH}_2(\text{C}_6\text{H}_4)(\text{C}_6\text{H}_4)\text{PH}_2][\text{BF}_4]$ (0.10g, 0.05mmol) was dissolved in 1,2 dichloroethane (30ml), potassium *tert*butoxide (0.01g, 0.09mmol) was added to the solution. The reaction was heated to 60°C for 10 hours. After filtration, the majority of the solvent was removed *in vacuo* to give a brown/yellow oily mixture ^{31}P NMR studies (in $\delta\text{CH}_3\text{CN}$) showed decomposition had taken place.

17b (1:1) Preparation of $[\text{Cp}^*\text{Fe}\{(\text{o-C}_6\text{H}_4\text{F})_2\text{PC}_6\text{H}_4\text{P}(\text{o-C}_6\text{H}_4\text{F})_2\}\text{PH}_2(\text{C}_6\text{H}_4)(\text{C}_6\text{H}_4)\text{PH}_2][\text{BF}_4]$

$[\text{Cp}^*\text{Fe}(\text{o-C}_6\text{H}_4\text{F})_2\text{PC}_6\text{H}_4\text{P}(\text{o-C}_6\text{H}_4\text{F})_2\text{CH}_3\text{CN}][\text{BF}_4]$ (0.46g, 0.51mmol) was dissolved in 1,2-dichloroethane (40ml). $\text{H}_2\text{P}(\text{C}_6\text{H}_4)(\text{C}_6\text{H}_4)\text{PH}_2$ (0.05g, 0.51mmol) was added and the reaction mixture heated to 60°C for 8 hours until the colour changed from red to yellow. The solvent was removed *in vacuo* and the residue triturated with ether to give a yellow powder (M_R 1069.27, 0.42g, 77% yield).

Measured	Data
$^1\text{H-NMR}$ (CDCl_3)	1.69 (s, Cp*), 6.97-7.13 (m).
$^{13}\text{C}\{^1\text{H}\}$ NMR (CDCl_3)	9.81 (s, Cp*), 86.98 (s, Cp*), 121.98 (s), 122.99-125.79 (m), 163.42 (dd, $^1J_{\text{C-F}}234.34\text{Hz}$, $^2J_{\text{C-P}}8.13\text{Hz}$).

³¹ P-NMR (CDCl ₃)	-125.03 (t, ¹ J _{P-H} 213.10Hz), -15.01 (t, ¹ J _{P-H} 344.6Hz), 81.02-81.33 (m).
¹⁹ F-NMR (CDCl ₃)	-97.62 (s)

17b Preparation of [Cp*Fe{(o-C₆H₄F)₂PC₆H₄P(o-C₆H₄F)₂}PH₂(C₆H₄)₂][BF₄]₂

[Cp*Fe(o-C₆H₄F)₂PC₆H₄P(o-C₆H₄F)₂CH₃CN][BF₄] (0.46g, 0.51mmol) was dissolved in 1,2-dichloroethane (40ml). H₂P(C₆H₄)(C₆H₄)PH₂ (0.03g, 0.26mmol) was added and the reaction mixture heated to 60°C for 8 hours until the colour changed from red to yellow. The solvent was removed *in vacuo* and the residue triturated with ether to give a yellow powder (M_R 1922.33, 0.33g, 67% yield).

Measured	Data
¹ H-NMR (CDCl ₃)	1.73 (s, Cp*), 6.87-7.39 (m).
¹³ C{ ¹ H} NMR (CDCl ₃)	9.98 (s, Cp*), 86.99 (s, Cp*), 124.38-131.88 (m), 163.84 (dd, ¹ J _{C-F} 234.82Hz, ² J _{C-P} 6.09Hz).
³¹ P-NMR (CDCl ₃)	-14.02 (t, ¹ J _{P-H} 327.8), 80.98-81.32 (m).
¹⁹ F-NMR (CDCl ₃)	-98.02 (s).

17c(1:1) Preparation of [Cp*Fe(P(C₆H₄F)(C₆H₄)P(C₆H₄F)(C₆H₄)P(C₆H₄)₂PH₂(C₆H₄))][BF₄]

[Cp*Fe{(o-C₆H₄F)₂PC₆H₄P(o-C₆H₄F)₂}PH₂(C₆H₄)(C₆H₄)PH₂][BF₄] (0.42g, 0.39mmol) was dissolved in THF (30ml), potassium *tert*butoxide (0.04g, 0.39mmol) was added to the solution. The reaction was heated to 60°C for 16 hours. After filtration, the solvent was removed *in vacuo* and the solid washed with ether to give a yellow solid (M_R 1029.26, 0.20g, 51% yield).

Measured	Data
¹ H-NMR (CDCl ₃)	1.68 (s, Cp*), 7.00-7.31 (m).
¹³ C{ ¹ H} NMR (CDCl ₃)	9.88 (s, Cp*), 86.12 (s, Cp*), 121.67 (s), 125.55 (s), 125.77-132.36 (m), 136.41 (s).
³¹ P-NMR (CDCl ₃)	-125.62 (t, ¹ J _{P-H} 212.5), 119.47-120.40 (m), 126.28 -127.94 (m).
¹⁹ F-NMR (CDCl ₃)	-98.02 (s)
MS (APCI)	942.4 Da/e (M ⁺).

17c Preparation of $[\text{Cp}^*\text{Fe}(\text{P}(\text{C}_6\text{H}_4\text{F})(\text{C}_6\text{H}_4)\text{P}(\text{C}_6\text{H}_4\text{F})(\text{C}_6\text{H}_4)\text{P}(\text{C}_6\text{H}_4)(\text{C}_6\text{H}_4))_2[\text{BF}_4]_2$

$[\text{Cp}^*\text{Fe}\{\text{(o-C}_6\text{H}_4\text{F)}_2\text{PC}_6\text{H}_4\text{P}(\text{o-C}_6\text{H}_4\text{F})_2\}\text{PH}_2(\text{C}_6\text{H}_4)]_2[\text{BF}_4]_2$ (0.33g, 0.17mmol) was dissolved in 1,2 dichlorobenzene (30ml), potassium *tert*butoxide (0.02g, 0.17mmol) was added to the solution. The reaction was heated to 60°C for 16 hours. After filtration, the solvent was removed *in vacuo* and washed with THF to give a yellow solid (M_R 1882.32, 0.20g, 62% yield).

Measured	Data
$^1\text{H-NMR}$ (CDCl_3)	1.69 (s, Cp*), 6.89-7.30 (m).
$^{13}\text{C}\{^1\text{H}\}$ NMR (CDCl_3)	10.00 (s, Cp*), 87.02 (s, Cp*), 123.82-131.81 (m)
$^{31}\text{P-NMR}$ (CDCl_3)	118.29-119.82 (m), 121.03-122.66 (m).
$^{19}\text{F-NMR}$ (CDCl_3)	-99.13 (s).
MS (APCI)	854.2 Da/e (M^+).

18b Preparation of $[\text{Cp}^*\text{Fe}\{\text{(o-C}_6\text{H}_4\text{F)}_2\text{AsC}_6\text{H}_4\text{As}(\text{o-C}_6\text{H}_4\text{F})_2\}\text{PH}_2(\text{C}_6\text{H}_4)]_2[\text{PF}_6]_2$

$\text{H}_2\text{P}(\text{C}_6\text{H}_4)(\text{C}_6\text{H}_4)\text{PH}_2$ (0.01g, 0.13mmol) in 1,2 dichloroethane (5ml) was added to a solution of $[\text{Cp}^*\text{Fe}(\text{o-C}_6\text{H}_4\text{F})_2\text{AsC}_6\text{H}_4\text{As}(\text{o-C}_6\text{H}_4\text{F})\text{CH}_3\text{CN}][\text{PF}_6]$ (0.25g, 0.25mmol) in 1,2-dichloroethane (30ml) and the reaction mixture heated to 60°C for 12 hours until the colour changed from red to orange. The solvent was removed *in vacuo* and the residue triturated with ether to give an orange powder (M_R 2028.60, 0.08g, 32% yield).

Measured	Data
$^1\text{H-NMR}$ (CDCl_3)	1.62 (s, Cp*), 7.01-7.60 (m).
$^{13}\text{C}\{^1\text{H}\}$ NMR (CDCl_3)	9.95 (s, Cp*), 87.05 (s, Cp*), 121.98 (s), 123.68-129.82 (m), 134.68 (s).
$^{19}\text{F-NMR}$ (CDCl_3)	-103.26 (s).
$^{31}\text{P-NMR}$ (CDCl_3)	-14.02 (unresolved)
MS (APCI)	891.2 Da/e (M^+).

18c Preparation of $[\text{Cp}^*\text{Fe}(\text{As}(\text{C}_6\text{H}_4\text{F})(\text{C}_6\text{H}_4)\text{As}(\text{C}_6\text{H}_4\text{F})(\text{C}_6\text{H}_4)\text{P}(\text{C}_6\text{H}_4))_2[\text{BF}_4]_2$

$[\text{Cp}^*\text{Fe}\{\text{(o-C}_6\text{H}_4\text{F)}_2\text{AsC}_6\text{H}_4\text{As}(\text{o-C}_6\text{H}_4\text{F})_2\}\text{PH}_2(\text{C}_6\text{H}_4)]_2[\text{PF}_6]_2$ (0.08g, 0.04mmol) was dissolved in 1,2 dichlorobenzene (40ml), potassium *tert*butoxide (XS 0.01g) was

added to the solution. The reaction was left to stir overnight and filtered. The solvent was removed *in vacuo* and the solid was washed with THF to remove excess potassium *tert*butoxide to give a yellow solid (M_R 1988.59, 0.06g, 78% yield).

Measured	Data
$^1\text{H-NMR}$ (CDCl_3)	1.64 (s, Cp*), 6.98-7.56 (m).
$^{13}\text{C}\{^1\text{H}\}$ NMR (CDCl_3)	9.20 (s, Cp*), 87.24 (s, Cp*), 122.09 (s), 124.03-131.53 (m), 163.58 (dd, $^1J_{\text{C-F}}243.22\text{Hz}$, $^2J_{\text{C-P}}7.02\text{Hz}$).
$^{31}\text{P-NMR}$ (CDCl_3)	115.98-116.04 (m).
$^{19}\text{F-NMR}$ (CDCl_3)	-103.82
MS (APCI)	907.6 Da/e (M^+).

19b Preparation of $[\text{CpFe}\{(\text{C}_3\text{H}_5)_2\text{PC}_2\text{H}_4\text{P}(\text{C}_3\text{H}_5)_2\}\text{PH}_2(\text{C}_6\text{H}_4)_2][\text{PF}_6]_2$

$\text{H}_2\text{P}(\text{C}_6\text{H}_4)(\text{C}_6\text{H}_4)\text{PH}_2$ (0.21g, 0.97mmol) in THF (10ml) was added to a solution of $[\text{CpFe}(\text{o-C}_6\text{H}_4\text{F})_2\text{PC}_2\text{H}_4\text{P}(\text{o-C}_6\text{H}_4\text{F})_2\text{CH}_3\text{CN}][\text{PF}_6]$ (1.18g, 1.94mmol) in THF (30ml). The reaction mixture was heated to 60°C for 8 hours resulting in a colour changed from red to orange. The solvent was removed *in vacuo* and the residue triturated with ether to give a brown/orange powder (M_R 738.36, 0.18g, 25% yield).

Measured	Data
$^1\text{H-NMR}$ (CD_3CN)	1.72 (s, $\text{PCH}_2\text{CHCH}_2$), 2.91 (s, $\text{PCH}_2\text{CH}_2\text{P}$), 4.02 (s, Cp), 5.13 ($\text{PCH}_2\text{CHCH}_2$), 5.31 ($\text{PCH}_2\text{CHCH}_2$), 6.69-6.98 (m).
$^{13}\text{C}\{^1\text{H}\}$ NMR (CD_3CN)	22.42 (s, $\text{PCH}_2\text{CH}_2\text{P}$), 30.19 ($\text{PCH}_2\text{CHCH}_2$), 33.10 ($\text{PCH}_2\text{CHCH}_2$), 79.90 (s, Cp), 130.24 ($\text{PCH}_2\text{CHCH}_2$).
$^{31}\text{P-NMR}$ (CD_3CN)	69.08 (broad s, co-ordinated $\text{H}_2\text{P-}$), 89.34 (s).

19c Preparation of $[\text{CpFe}(\text{C}_3\text{H}_5)\text{PC}_2\text{H}_4\text{P}(\text{C}_3\text{H}_5)\{\text{P}(\text{C}_6\text{H}_4)(\text{C}_6\text{H}_4)\text{PH}_2\}(\text{C}_3\text{H}_6)][\text{PF}_6]$

Potassium *tert*butoxide (2 mole equivalents, 0.03g, 0.23mol) was added to a solution of $[\text{CpFe}\{(\text{C}_3\text{H}_5)_2\text{PC}_2\text{H}_4\text{P}(\text{C}_3\text{H}_5)_2\}\text{PH}_2(\text{C}_6\text{H}_4)_2][\text{PF}_6]_2$ (0.18g, 0.23mmol) in THF (40ml). The reaction was left to stir overnight and filtered. The solvent was removed *in vacuo* to give a brown/orange solid (M_R 786.40, 0.14g, 75% yield).

Measured	Data
^1H -NMR (CDCl_3)	1.69 (s, $\text{PCH}_2\text{CHCH}_2$), 2.92 (s, $\text{PCH}_2\text{CH}_2\text{P}$), 3.98 (s, Cp), 5.11 ($\text{PCH}_2\text{CHCH}_2$), 5.40 ($\text{PCH}_2\text{CHCH}_2$), 6.70-7.04 (m).
$^{13}\text{C}\{^1\text{H}\}$ NMR (CDCl_3)	19.42 (s, $\text{PCH}_2\text{CH}_2\text{P}$), 30.24 ($\text{PCH}_2\text{CHCH}_2$), 32.18 ($\text{PCH}_2\text{CHCH}_2$), 78.98 (s, Cp), 131.00 ($\text{PCH}_2\text{CHCH}_2$).
^{31}P -NMR (CDCl_3)	109.24-109.98 (m), 110.04-112.58 (m).

References

- ¹ R.N. Patel, N. Singh, K.K. Shukla, U.K. Chauhan, J. Niclos-Gutierrez, A. Castineiras; *Inorg. Chim. Acta*; **2004**; 357(9); 2469
- ² A.K. Singh, A. Panwar, R. Singh, S. Baniwal; *Trans. Met. Chem.*; **2003**; 28; 160
- ³ T.A. Khan, M. Shagufta; *Trans. Met. Chem.*; **1999**; 24; 669
- ⁴ A. Bilyk, M.M. Harding; *J. Chem. Soc., Dalton Trans.*; **1994**; 77
- ⁵ L.F. Lindoy; *The Chemistry of Macrocyclic Ligand Complexes*; Cambridge University Press; **1989**
- ⁶ K. Weighardt, E. Scoeffmann, B. Naber, J. Weiss; *Polyhedron*; **1993**; 12; 1
- ⁷ K. Weighardt, I. Tolksdorf, W. Herrmann; *Inorg. Chem.*; **1985**; 24; 1230
- ⁸ R. Haider, M. Ipek, B. DasGupta, M. Yousaf, L.J. Zompa; *Inorg. Chem.*; **1997**; 36; 3125
- ⁹ A.J. Blake, J.P. Danks, W-S. Li, V. Lippolis, M. Schröder; *J. Chem. Soc., Dalton Trans.*; **2000**; 3034
- ¹⁰ W. Malisch, B. Klupfel, D. Schumacher, M. Nieger; *J. Organomet. Chem.*; **2002**; 661; 95
- ¹¹ P. Baker, M.M. Meehan; *Inorg. Chim. Acta*; **2000**; 303; 17
- ¹² R. Haigh; Ph.D. Thesis; Cardiff University; **2002**
- ¹³ T. Albers; Ph.D. Thesis; Cardiff University; **2000**

Appendix

General Experimental Information

All reactions were carried out in an atmosphere of dry nitrogen using standard Schlenk techniques or in a Vacuum Atmospheres glove box. All solvents were dried by refluxing over standard drying agents and distilled immediately prior to use. The petroleum ether (petrol) used had a boiling point of 40-60 °C. All other chemicals were obtained from commercial sources and where appropriate, dried over molecular sieves and deoxygenated by repeated freeze-thaw degassing. UV photolyses were carried out using a Hanovia 125 W mercury discharge lamp (254 nm). The NMR spectra were recorded on a Bruker DPX-400 instrument at 400 MHz (¹H) and 100 MHz (¹³C) or a Jeol Lamda Eclipse 300 at 121.65 MHz (³¹P), 300.52 MHz (¹H), 75.57 MHz (¹³C), 96.42 MHz (¹¹B) and 282.78 MHz (¹⁹F). All chemical shifts are quoted in units of δ ppm. ¹H and ¹³C NMR chemical shifts are relative to solvent resonance, ³¹P chemical shifts are relative to 85% external H₃PO₄ (δ = 0 ppm), ¹¹B chemical shifts are relative to external BF₃.OEt₂ (δ = 0 ppm), ¹⁹F chemical shifts are relative to external CFC₃ (δ = 0 ppm). Mass spectra (E.I. and APCI) were recorded on a VG Platform II Fisons mass spectrometer. Infrared spectra were recorded on a Perkin Elmer 1600 or a Nicolet 510 FT-IR spectrometer as a nujol mull between CsI plates or in solution using KBr solution cells or as KBr disks.

Abbreviations used in this Thesis.

APCI – atmospheric pressure chemical ionisation

ⁿBu – *n*-butyl

^tBu – *tert*-butyl

Bz – benzyl

Cp – cyclopentadienyl (C₅H₅)

Cp⁺ – pentamethylcyclopentadienyl (C₅Me₅)

CV – Cyclic voltammetry

edta – ethylenediaminetetra-acetic acid

en – ethylenediamine

Et - ethyl

IR – Infrared spectroscopy

(s) – strong

(m) – medium

(w) – weak

Me – methyl

M.S. – mass spectroscopy

NMR – Nuclear magnetic resonance

(s) – singlet

(d) – doublet

(t) – triplet

(q) – quartet

(m) – multiplet

(dt) – doublet of triplets

(dd) – doublet of doublets

(tt) – triplet of triplets

(br) - broad

${}^nJ_{xy}$ – n-bond coupling between atoms X and Y

Ph – phenyl

R – alkyl or aryl group

TAPE - Tetraallylbisphosphinoethane

THF - tetrahydrofuran

Tp – tris(hydropyrazolyl)borate

VT NMR – Variable temperature NMR

Crystal Structure Data

Table 1. Crystal data and structure refinement for $P(C_6H_4F)_3$

Empirical formula	C18 H12 F3 P
Formula weight	316.25
Temperature	150(2) K
Wavelength	0.71073 Å
Crystal system	Monoclinic
Space group	P2(1)/n
Unit cell dimensions	a = 8.4912(2) Å alpha = 90 deg. b = 11.2757(3) Å beta = 93.0477(16) deg. c = 15.5481(4) Å gamma = 90 deg.
Volume	1486.54(7) Å ³
Z	4
Density (calculated)	1.413 Mg/m ³

Absorption coefficient	0.210 mm ⁻¹
F(000)	648
Crystal size	0.18 x 0.16 x 0.15 mm
Theta range for data collection	3.01 to 27.47 deg.
Index ranges	-11<=h<=11, -14<=k<=14, -19<=l<=20
Reflections collected	19181
Independent reflections	3386 [R(int) = 0.0829]
Max. and min. transmission	0.9692 and 0.9632
Refinement method	Full-matrix least-squares on F ²
Data / restraints / parameters	3386 / 0 / 199
Goodness-of-fit on F ²	1.035
Final R indices [I>2sigma(I)]	R1 = 0.0432, wR2 = 0.1006
R indices (all data)	R1 = 0.0593, wR2 = 0.1084
Diff. peak and hole	0.233 and -0.345 e.A ⁻³

Table 3. Bond lengths [Å] and angles [deg] for P(C₆H₄F)₃

P(1)-C(13)	1.836(2)	P(1)-C(7)	1.836(2)
P(1)-C(1)	1.839(2)	F(1)-C(2)	1.364(2)
F(2)-C(8)	1.366(2)	F(3)-C(14)	1.358(2)
C(1)-C(2)	1.389(2)	C(1)-C(6)	1.395(3)
C(2)-C(3)	1.375(3)	C(3)-C(4)	1.379(3)
C(4)-C(5)	1.382(3)	C(5)-C(6)	1.388(3)
C(7)-C(8)	1.387(2)	C(7)-C(12)	1.392(3)
C(8)-C(9)	1.375(3)	C(9)-C(10)	1.387(3)
C(10)-C(11)	1.383(3)	C(11)-C(12)	1.389(3)
C(13)-C(14)	1.387(2)	C(13)-C(18)	1.396(2)
C(14)-C(15)	1.374(3)	C(15)-C(16)	1.380(3)
C(16)-C(17)	1.385(3)	C(17)-C(18)	1.390(3)
C(13)-P(1)-C(7)	101.23(7)	C(13)-P(1)-C(1)	99.96(7)
C(7)-P(1)-C(1)	101.09(8)	C(2)-C(1)-C(6)	116.01(16)
C(2)-C(1)-P(1)	119.20(14)	C(6)-C(1)-P(1)	124.76(13)
F(1)-C(2)-C(3)	117.92(16)	F(1)-C(2)-C(1)	118.31(16)
C(3)-C(2)-C(1)	123.76(18)	C(2)-C(3)-C(4)	118.69(17)
C(3)-C(4)-C(5)	120.01(18)	C(4)-C(5)-C(6)	120.04(19)
C(5)-C(6)-C(1)	121.50(17)	C(8)-C(7)-C(12)	116.06(16)
C(8)-C(7)-P(1)	118.30(13)	C(12)-C(7)-P(1)	125.46(14)
F(2)-C(8)-C(9)	117.95(16)	F(2)-C(8)-C(7)	117.56(15)
C(9)-C(8)-C(7)	124.50(17)	C(8)-C(9)-C(10)	117.67(18)
C(11)-C(10)-C(9)	120.39(18)	C(10)-C(11)-C(12)	120.03(19)
C(11)-C(12)-C(7)	121.34(17)	C(14)-C(13)-C(18)	116.26(16)
C(14)-C(13)-P(1)	117.28(13)	C(18)-C(13)-P(1)	126.45(14)
F(3)-C(14)-C(15)	118.12(17)	F(3)-C(14)-C(13)	117.48(15)
C(15)-C(14)-C(13)	124.38(18)	C(14)-C(15)-C(16)	117.86(19)
C(15)-C(16)-C(17)	120.38(18)	C(16)-C(17)-C(18)	120.28(18)
C(17)-C(18)-C(13)	120.84(18)		

Table 1. Crystal data and structure refinement for**[CpFeP(C₆H₄F)(C₆H₄)P(C₆H₄F)(C₆H₄)P(C₆H₅)(C₆H₄)] [PF₆]**

Identification code	s92
Empirical formula	C73 H62 B F2 Fe N4 P3
Formula weight	1192.84
Temperature	150(2) K
Wavelength	0.71073 Å
Crystal system	Monoclinic
Space group	P2(1)/c
Unit cell dimensions	a = 15.6204(3) Å alpha = 90 deg. b = 14.7050(3) Å beta = 102.6900(10) deg.

c = 27.0880(6) Å gamma = 90 deg.

Volume 6070.1(2) Å³
Z 4
Density (calculated) 1.305 Mg/m³
Absorption coefficient 0.381 mm⁻¹
F(000) 2488
Crystal size 0.05 x 0.04 x 0.02 mm
Theta range for data collection 2.96 to 26.01 deg.
Index ranges -17 ≤ h ≤ 19, -15 ≤ k ≤ 18, -33 ≤ l ≤ 33
Reflections collected 37113
Independent reflections 11801 [R(int) = 0.1505]
Max. and min. transmission 0.9943 and 0.9812
Refinement method Full-matrix least-squares on F²
Data / restraints / parameters 11801 / 60 / 791
Goodness-of-fit on F² 0.970
Final R indices [I > 2σ(I)] R1 = 0.0784, wR2 = 0.1615
R indices (all data) R1 = 0.1707, wR2 = 0.1946
Largest diff. peak and hole 1.602 and -0.709 e.Å⁻³

Table 2. Atomic coordinates (× 10⁴) and equivalent isotropic displacement parameters (Å² × 10³) for S92. U(eq) is defined as one third of the trace of the orthogonalized Uij tensor.

	x	y	z	U(eq)
Fe(1)	1918(1)	3586(1)	256(1)	21(1)
P(1)	2655(1)	3514(1)	-328(1)	20(1)
P(2)	2752(1)	4713(1)	557(1)	21(1)
P(3)	2908(1)	2730(1)	697(1)	20(1)
F(1)	1637(3)	4761(3)	-1115(2)	56(1)
F(2)	1834(3)	6315(3)	-27(2)	41(1)
F(3)	2525(4)	2648(4)	1747(2)	75(2)

B(1)	7271(4)	1244(4)	1735(2)	24(1)
C(1)	3297(3)	4552(3)	-330(2)	20(1)
C(2)	3737(3)	4794(3)	-705(2)	22(1)
C(3)	4225(3)	5587(3)	-655(2)	26(1)
C(4)	4284(3)	6133(3)	-239(2)	26(1)
C(5)	3856(3)	5900(3)	147(2)	22(1)
C(6)	3356(3)	5110(3)	90(2)	21(1)
C(7)	3614(3)	4336(3)	1090(2)	21(1)
C(8)	4207(3)	4908(3)	1404(2)	24(1)
C(9)	4855(3)	4534(3)	1779(2)	26(1)
C(10)	4916(3)	3610(4)	1845(2)	28(1)
C(11)	4344(3)	3031(3)	1537(2)	24(1)
C(12)	3686(3)	3403(3)	1153(2)	22(1)
C(13)	3615(3)	2258(3)	301(2)	20(1)
C(14)	4271(3)	1617(3)	465(2)	23(1)
C(15)	4807(3)	1352(3)	149(2)	27(1)
C(16)	4687(3)	1718(3)	-332(2)	27(1)
C(17)	4047(3)	2368(3)	-498(2)	23(1)
C(18)	3508(3)	2631(3)	-176(2)	21(1)
C(19)	2095(3)	3282(3)	-977(2)	23(1)
C(20)	1681(3)	3949(4)	-1293(2)	35(1)
C(21)	1163(4)	3766(4)	-1765(2)	43(2)
C(22)	1064(4)	2881(4)	-1931(2)	44(2)
C(23)	1472(4)	2188(4)	-1620(2)	47(2)
C(24)	1967(4)	2389(4)	-1143(2)	41(2)
C(25)	2288(3)	5718(3)	786(2)	23(1)
C(26)	1898(3)	6397(3)	460(2)	28(1)
C(27)	1460(3)	7120(3)	620(2)	36(1)
C(28)	1384(3)	7149(4)	1115(2)	38(1)
C(29)	1753(4)	6484(4)	1454(2)	43(2)
C(30)	2207(3)	5771(4)	1286(2)	32(1)
C(31)	2589(3)	1775(3)	1039(2)	23(1)
C(32)	2454(3)	1839(4)	1523(2)	30(1)
C(33)	2093(3)	1155(4)	1756(2)	36(1)
C(34)	1854(3)	360(4)	1495(2)	38(1)
C(35)	1978(4)	264(4)	1011(2)	41(1)
C(36)	2331(3)	969(4)	783(2)	39(1)
C(37)	888(5)	3856(6)	613(2)	27(3)
C(38)	773(5)	4368(4)	159(3)	31(3)
C(39)	704(6)	3748(6)	-250(2)	29(3)
C(40)	775(6)	2853(4)	-49(3)	26(3)
C(41)	889(6)	2919(5)	485(3)	33(4)
C(37')	817(3)	4176(4)	421(2)	27(3)
C(38')	717(3)	4111(4)	-112(2)	22(3)
C(39')	755(3)	3177(5)	-238(2)	25(3)
C(40')	880(2)	2664(3)	216(2)	23(3)
C(41')	918(2)	3282(4)	624(2)	20(3)
C(42)	6289(2)	1032(3)	1844(1)	24(1)
C(43)	6060(2)	1364(3)	2279(1)	29(1)
C(44)	5242(3)	1218(3)	2396(2)	32(1)
C(45)	4616(3)	694(3)	2068(2)	29(1)
C(46)	4824(3)	340(3)	1641(2)	31(1)
C(47)	5641(3)	499(3)	1533(2)	29(1)
C(48)	7546(3)	2275(3)	1931(2)	22(1)
C(49)	7006(3)	3026(3)	1758(2)	23(1)

C(50)	7205(3)	3905(3)	1916(2)	27(1)
C(51)	7966(3)	4087(3)	2278(2)	29(1)
C(52)	8515(3)	3368(3)	2465(2)	30(1)
C(53)	8308(3)	2490(3)	2295(2)	21(1)
C(54)	7229(3)	1109(3)	1127(2)	20(1)
C(55)	7156(3)	1809(3)	766(2)	26(1)
C(56)	7063(3)	1647(4)	259(2)	29(1)
C(57)	7035(3)	773(3)	73(2)	27(1)
C(58)	7102(3)	57(3)	410(2)	28(1)
C(59)	7207(3)	228(3)	923(2)	27(1)
C(60)	7990(3)	515(3)	2051(2)	24(1)
C(61)	7867(3)	-51(3)	2436(2)	29(1)
C(62)	8525(4)	-601(4)	2708(2)	34(1)
C(63)	9358(3)	-591(4)	2603(2)	34(1)
C(64)	9511(3)	-40(4)	2220(2)	31(1)
C(65)	8843(3)	497(3)	1949(2)	27(1)
N(1)	33(4)	937(5)	-605(3)	85(2)
C(66)	276(4)	220(5)	-626(2)	51(2)
C(67)	561(4)	-713(4)	-642(2)	53(2)
N(2)	253(4)	2270(4)	1675(2)	59(2)
C(68)	-286(4)	2738(4)	1465(2)	39(1)
C(69)	-982(4)	3339(5)	1201(2)	53(2)
N(3)	3499(3)	3629(4)	-1918(2)	52(1)
C(70)	3566(4)	2867(5)	-1967(2)	40(2)
C(71)	3650(4)	1895(4)	-2024(3)	62(2)
N(4)	5843(4)	2539(4)	-1270(2)	64(2)
C(72)	6225(4)	2126(4)	-1506(2)	40(2)
C(73)	6701(4)	1597(4)	-1804(2)	46(2)

Table 3. Bond lengths [Å] and angles [deg] for
 $[\text{CpFeP}(\text{C}_6\text{H}_5\text{F})(\text{C}_6\text{H}_4)\text{P}(\text{C}_6\text{H}_4)\text{P}(\text{C}_6\text{H}_4)\text{P}(\text{C}_6\text{H}_5)(\text{C}_6\text{H}_4)]\text{PF}_6$

Fe(1)-C(37')	2.060(5)
Fe(1)-C(38')	2.070(3)
Fe(1)-C(41')	2.078(5)
Fe(1)-C(41)	2.090(8)
Fe(1)-C(37)	2.090(8)
Fe(1)-C(40)	2.093(8)
Fe(1)-C(38)	2.093(8)
Fe(1)-C(39')	2.094(4)
Fe(1)-C(39)	2.095(8)
Fe(1)-C(40')	2.098(5)
Fe(1)-P(3)	2.1421(13)
Fe(1)-P(1)	2.1522(14)
P(1)-C(19)	1.816(5)
P(1)-C(1)	1.826(5)
P(1)-C(18)	1.841(5)
P(2)-C(25)	1.814(5)
P(2)-C(7)	1.831(4)
P(2)-C(6)	1.831(5)
P(3)-C(31)	1.812(5)
P(3)-C(12)	1.824(5)

P(3)-C(13)	1.836(5)
F(1)-C(20)	1.297(7)
F(2)-C(26)	1.306(6)
F(3)-C(32)	1.329(7)
B(1)-C(48)	1.633(7)
B(1)-C(54)	1.645(7)
B(1)-C(60)	1.649(7)
B(1)-C(42)	1.655(7)
C(1)-C(6)	1.390(6)
C(1)-C(2)	1.392(6)
C(2)-C(3)	1.384(7)
C(3)-C(4)	1.369(7)
C(4)-C(5)	1.401(7)
C(5)-C(6)	1.389(6)
C(7)-C(12)	1.384(6)
C(7)-C(8)	1.393(6)
C(8)-C(9)	1.382(6)
C(9)-C(10)	1.372(7)
C(10)-C(11)	1.374(7)
C(11)-C(12)	1.402(6)
C(13)-C(18)	1.380(6)
C(13)-C(14)	1.391(6)
C(14)-C(15)	1.380(7)
C(15)-C(16)	1.383(7)
C(16)-C(17)	1.385(7)
C(17)-C(18)	1.394(7)
C(19)-C(20)	1.369(7)
C(19)-C(24)	1.388(7)
C(20)-C(21)	1.380(7)
C(21)-C(22)	1.374(8)
C(22)-C(23)	1.386(8)
C(23)-C(24)	1.383(7)
C(25)-C(26)	1.383(7)
C(25)-C(30)	1.391(7)
C(26)-C(27)	1.383(7)
C(27)-C(28)	1.373(8)
C(28)-C(29)	1.378(8)
C(29)-C(30)	1.397(7)
C(31)-C(32)	1.377(7)
C(31)-C(36)	1.387(7)
C(32)-C(33)	1.372(7)
C(33)-C(34)	1.375(8)
C(34)-C(35)	1.376(8)
C(35)-C(36)	1.380(7)
C(37)-C(38)	1.4200
C(37)-C(41)	1.4200
C(38)-C(39)	1.4200
C(39)-C(40)	1.4200
C(40)-C(41)	1.4200
C(37)-C(38)	1.4200
C(37)-C(41)	1.4200
C(38)-C(39)	1.4200
C(39)-C(40)	1.4200
C(40)-C(41)	1.4200
C(42)-C(43)	1.3943

C(42)-C(47)	1.404(6)
C(43)-C(44)	1.398(6)
C(44)-C(45)	1.399(7)
C(45)-C(46)	1.371(7)
C(46)-C(47)	1.390(7)
C(48)-C(53)	1.405(6)
C(48)-C(49)	1.406(6)
C(49)-C(50)	1.375(7)
C(50)-C(51)	1.390(7)
C(51)-C(52)	1.385(7)
C(52)-C(53)	1.385(7)
C(54)-C(55)	1.406(7)
C(54)-C(59)	1.406(6)
C(55)-C(56)	1.372(7)
C(56)-C(57)	1.378(7)
C(57)-C(58)	1.381(7)
C(58)-C(59)	1.384(7)
C(60)-C(61)	1.380(7)
C(60)-C(65)	1.420(7)
C(61)-C(62)	1.386(7)
C(62)-C(63)	1.392(8)
C(63)-C(64)	1.377(8)
C(64)-C(65)	1.384(7)
N(1)-C(66)	1.126(8)
C(66)-C(67)	1.445(9)
N(2)-C(68)	1.138(7)
C(68)-C(69)	1.459(9)
N(3)-C(70)	1.136(7)
C(70)-C(71)	1.446(9)
N(4)-C(72)	1.140(8)
C(72)-C(73)	1.441(9)

C(37')-Fe(1)-C(38')	40.21(7)
C(37')-Fe(1)-C(41')	40.14(9)
C(38')-Fe(1)-C(41')	67.27(12)
C(37')-Fe(1)-C(41)	53.1(2)
C(38')-Fe(1)-C(41)	69.1(2)
C(41')-Fe(1)-C(41)	17.9(2)
C(37')-Fe(1)-C(37)	19.2(2)
C(38')-Fe(1)-C(37)	56.2(2)
C(41')-Fe(1)-C(37)	23.4(2)
C(41)-Fe(1)-C(37)	39.72(13)
C(37')-Fe(1)-C(40)	67.8(2)
C(38')-Fe(1)-C(40)	53.0(2)
C(41')-Fe(1)-C(40)	54.0(2)
C(41)-Fe(1)-C(40)	39.70(14)
C(37)-Fe(1)-C(40)	66.64(17)
C(37')-Fe(1)-C(38)	20.9(2)
C(38')-Fe(1)-C(38)	22.5(2)
C(41')-Fe(1)-C(38)	57.8(2)
C(41)-Fe(1)-C(38)	66.64(16)
C(37)-Fe(1)-C(38)	39.69(13)
C(40)-Fe(1)-C(38)	66.58(16)
C(37')-Fe(1)-C(39')	67.15(11)
C(38')-Fe(1)-C(39')	39.87(6)

C(41')-Fe(1)-C(39')	66.84(13)
C(41)-Fe(1)-C(39')	55.9(2)
C(37)-Fe(1)-C(39')	72.7(2)
C(40)-Fe(1)-C(39')	19.2(2)
C(38)-Fe(1)-C(39')	58.7(2)
C(37')-Fe(1)-C(39)	54.2(2)
C(38')-Fe(1)-C(39)	17.9(2)
C(41')-Fe(1)-C(39)	70.7(2)
C(41)-Fe(1)-C(39)	66.61(17)
C(37)-Fe(1)-C(39)	66.60(16)
C(40)-Fe(1)-C(39)	39.65(14)
C(38)-Fe(1)-C(39)	39.64(13)
C(39')-Fe(1)-C(39)	23.3(2)
C(37')-Fe(1)-C(40')	67.07(13)
C(38')-Fe(1)-C(40')	66.89(12)
C(41')-Fe(1)-C(40')	39.76(9)
C(41)-Fe(1)-C(40')	22.5(2)
C(37)-Fe(1)-C(40')	58.7(2)
C(40)-Fe(1)-C(40')	20.7(2)
C(38)-Fe(1)-C(40')	73.7(2)
C(39')-Fe(1)-C(40')	39.60(9)
C(39)-Fe(1)-C(40')	57.4(2)
C(37')-Fe(1)-P(3)	131.34(17)
C(38')-Fe(1)-P(3)	162.53(16)
C(41')-Fe(1)-P(3)	97.61(11)
C(41)-Fe(1)-P(3)	93.8(2)
C(37)-Fe(1)-P(3)	112.8(2)
C(40)-Fe(1)-P(3)	111.4(2)
C(38)-Fe(1)-P(3)	152.2(2)
C(39')-Fe(1)-P(3)	127.30(17)
C(39)-Fe(1)-P(3)	150.5(2)
C(40')-Fe(1)-P(3)	95.97(11)
C(37')-Fe(1)-P(1)	141.87(17)
C(38')-Fe(1)-P(1)	103.88(19)
C(41')-Fe(1)-P(1)	157.12(17)
C(41)-Fe(1)-P(1)	139.9(2)
C(37)-Fe(1)-P(1)	160.0(2)
C(40)-Fe(1)-P(1)	103.5(2)
C(38)-Fe(1)-P(1)	121.0(2)
C(39')-Fe(1)-P(1)	92.62(17)
C(39)-Fe(1)-P(1)	94.5(2)
C(40')-Fe(1)-P(1)	117.59(18)
P(3)-Fe(1)-P(1)	86.75(5)
C(19)-P(1)-C(1)	107.6(2)
C(19)-P(1)-C(18)	104.7(2)
C(1)-P(1)-C(18)	102.7(2)
C(19)-P(1)-Fe(1)	119.87(16)
C(1)-P(1)-Fe(1)	110.12(16)
C(18)-P(1)-Fe(1)	110.42(17)
C(25)-P(2)-C(7)	104.9(2)
C(25)-P(2)-C(6)	106.3(2)
C(7)-P(2)-C(6)	103.8(2)
C(25)-P(2)-Fe(1)	120.19(15)
C(7)-P(2)-Fe(1)	110.17(16)
C(6)-P(2)-Fe(1)	110.19(16)

C(31)-P(3)-C(12) 106.9(2)
C(31)-P(3)-C(13) 105.9(2)
C(12)-P(3)-C(13) 101.8(2)
C(31)-P(3)-Fe(1) 119.67(15)
C(12)-P(3)-Fe(1) 110.56(16)
C(13)-P(3)-Fe(1) 110.49(15)
C(48)-B(1)-C(54) 112.9(4)
C(48)-B(1)-C(60) 109.5(4)
C(54)-B(1)-C(60) 108.3(4)
C(48)-B(1)-C(42) 107.7(4)
C(54)-B(1)-C(42) 108.7(4)
C(60)-B(1)-C(42) 109.7(4)
C(6)-C(1)-C(2) 119.4(4)
C(6)-C(1)-P(1) 115.4(3)
C(2)-C(1)-P(1) 125.1(4)
C(3)-C(2)-C(1) 119.6(4)
C(4)-C(3)-C(2) 120.7(5)
C(3)-C(4)-C(5) 120.9(5)
C(6)-C(5)-C(4) 118.0(5)
C(5)-C(6)-C(1) 121.3(4)
C(5)-C(6)-P(2) 123.6(4)
C(1)-C(6)-P(2) 115.1(3)
C(12)-C(7)-C(8) 119.8(4)
C(12)-C(7)-P(2) 115.1(3)
C(8)-C(7)-P(2) 125.0(4)
C(9)-C(8)-C(7) 119.4(5)
C(10)-C(9)-C(8) 120.5(4)
C(9)-C(10)-C(11) 121.2(4)
C(10)-C(11)-C(12) 118.7(5)
C(7)-C(12)-C(11) 120.4(4)
C(7)-C(12)-P(3) 115.4(3)
C(11)-C(12)-P(3) 124.2(4)
C(18)-C(13)-C(14) 119.9(4)
C(18)-C(13)-P(3) 115.6(3)
C(14)-C(13)-P(3) 124.4(4)
C(15)-C(14)-C(13) 119.8(5)
C(14)-C(15)-C(16) 120.0(4)
C(15)-C(16)-C(17) 120.9(5)
C(16)-C(17)-C(18) 118.6(5)
C(13)-C(18)-C(17) 120.7(4)
C(13)-C(18)-P(1) 114.9(4)
C(17)-C(18)-P(1) 124.3(4)
C(20)-C(19)-C(24) 117.4(4)
C(20)-C(19)-P(1) 122.2(4)
C(24)-C(19)-P(1) 119.8(4)
F(1)-C(20)-C(19) 118.8(5)
F(1)-C(20)-C(21) 117.2(5)
C(19)-C(20)-C(21) 122.7(5)
C(22)-C(21)-C(20) 119.2(5)
C(21)-C(22)-C(23) 119.6(5)
C(24)-C(23)-C(22) 119.9(5)
C(23)-C(24)-C(19) 121.1(5)
C(26)-C(25)-C(30) 117.4(5)
C(26)-C(25)-P(2) 121.6(4)
C(30)-C(25)-P(2) 120.5(4)

F(2)-C(26)-C(25)	120.1(5)
F(2)-C(26)-C(27)	117.0(5)
C(25)-C(26)-C(27)	122.3(5)
C(28)-C(27)-C(26)	119.0(5)
C(27)-C(28)-C(29)	121.0(5)
C(28)-C(29)-C(30)	118.9(5)
C(25)-C(30)-C(29)	121.4(5)
C(32)-C(31)-C(36)	116.5(5)
C(32)-C(31)-P(3)	123.4(4)
C(36)-C(31)-P(3)	119.3(4)
F(3)-C(32)-C(33)	116.6(5)
F(3)-C(32)-C(31)	118.9(5)
C(33)-C(32)-C(31)	123.4(5)
C(32)-C(33)-C(34)	118.7(5)
C(33)-C(34)-C(35)	119.8(5)
C(34)-C(35)-C(36)	120.1(5)
C(35)-C(36)-C(31)	121.3(5)
C(38)-C(37)-C(41)	108.0
C(38)-C(37)-Fe(1)	70.3(3)
C(41)-C(37)-Fe(1)	70.1(3)
C(39)-C(38)-C(37)	108.0
C(39)-C(38)-Fe(1)	70.2(3)
C(37)-C(38)-Fe(1)	70.0(3)
C(40)-C(39)-C(38)	108.0
C(40)-C(39)-Fe(1)	70.1(3)
C(38)-C(39)-Fe(1)	70.1(3)
C(41)-C(40)-C(39)	108.0
C(41)-C(40)-Fe(1)	70.0(3)
C(39)-C(40)-Fe(1)	70.3(3)
C(40)-C(41)-C(37)	108.0
C(40)-C(41)-Fe(1)	70.3(3)
C(37)-C(41)-Fe(1)	70.2(3)
C(38')-C(37')-C(41')	108.0
C(38')-C(37')-Fe(1)	70.28(13)
C(41')-C(37')-Fe(1)	70.59(12)
C(37')-C(38')-C(39')	108.0
C(37')-C(38')-Fe(1)	69.51(17)
C(39')-C(38')-Fe(1)	70.95(17)
C(40')-C(39')-C(38')	108.0
C(40')-C(39')-Fe(1)	70.37(12)
C(38')-C(39')-Fe(1)	69.18(14)
C(41')-C(40')-C(39')	108.0
C(41')-C(40')-Fe(1)	69.34(17)
C(39')-C(40')-Fe(1)	70.03(10)
C(40')-C(41')-C(37')	108.0
C(40')-C(41')-Fe(1)	70.90(18)
C(37')-C(41')-Fe(1)	69.28(12)
C(43)-C(42)-C(47)	114.7(3)
C(43)-C(42)-B(1)	120.4(3)
C(47)-C(42)-B(1)	124.9(4)
C(42)-C(43)-C(44)	123.6(3)
C(43)-C(44)-C(45)	119.2(5)
C(46)-C(45)-C(44)	118.8(5)
C(45)-C(46)-C(47)	120.8(5)
C(46)-C(47)-C(42)	122.8(5)

C(53)-C(48)-C(49) 114.2(4)
 C(53)-C(48)-B(1) 124.0(4)
 C(49)-C(48)-B(1) 121.7(4)
 C(50)-C(49)-C(48) 123.8(4)
 C(49)-C(50)-C(51) 120.0(4)
 C(52)-C(51)-C(50) 118.4(5)
 C(51)-C(52)-C(53) 120.6(4)
 C(52)-C(53)-C(48) 122.9(4)
 C(55)-C(54)-C(59) 114.2(4)
 C(55)-C(54)-B(1) 125.9(4)
 C(59)-C(54)-B(1) 119.8(4)
 C(56)-C(55)-C(54) 123.0(5)
 C(55)-C(56)-C(57) 120.9(5)
 C(56)-C(57)-C(58) 118.6(5)
 C(57)-C(58)-C(59) 119.9(5)
 C(58)-C(59)-C(54) 123.3(5)
 C(61)-C(60)-C(65) 115.3(4)
 C(61)-C(60)-B(1) 126.4(4)
 C(65)-C(60)-B(1) 118.2(4)
 C(60)-C(61)-C(62) 123.0(5)
 C(61)-C(62)-C(63) 120.1(5)
 C(64)-C(63)-C(62) 119.0(5)
 C(63)-C(64)-C(65) 120.1(5)
 C(64)-C(65)-C(60) 122.5(5)
 N(1)-C(66)-C(67) 177.7(8)
 N(2)-C(68)-C(69) 179.2(7)
 N(3)-C(70)-C(71) 179.3(7)
 N(4)-C(72)-C(73) 179.4(7)

Symmetry transformations used to generate equivalent atoms:

Table 4. Anisotropic displacement parameters ($\text{\AA}^2 \times 10^3$) for S92.
 The anisotropic displacement factor exponent takes the form:
 $-2 \pi^2 [h^2 a^{*2} U_{11} + \dots + 2 h k a^* b^* U_{12}]$

	U11	U22	U33	U23	U13	U12
Fe(1)	14(1)	25(1)	24(1)	2(1)	6(1)	1(1)
P(1)	17(1)	23(1)	20(1)	0(1)	5(1)	0(1)
P(2)	18(1)	23(1)	21(1)	1(1)	7(1)	1(1)
P(3)	18(1)	23(1)	20(1)	1(1)	6(1)	1(1)
F(1)	58(3)	47(3)	54(3)	9(3)	-5(3)	6(3)
F(2)	44(3)	48(3)	34(3)	12(2)	12(2)	11(2)
F(3)	75(4)	88(5)	68(4)	-10(4)	31(3)	-18(3)
B(1)	24(3)	27(3)	23(3)	5(3)	8(2)	1(2)

C(1)	17(3)	21(3)	19(2)	5(2)	1(2)	0(2)
C(2)	24(3)	21(3)	23(3)	-3(2)	9(2)	2(2)
C(3)	24(3)	34(3)	20(3)	6(2)	9(2)	2(2)
C(4)	21(3)	25(3)	30(3)	4(2)	5(2)	-3(2)
C(5)	20(3)	24(3)	21(3)	-1(2)	1(2)	1(2)
C(6)	17(2)	23(3)	21(3)	9(2)	1(2)	4(2)
C(7)	18(3)	25(3)	21(3)	-3(2)	8(2)	2(2)
C(8)	23(3)	26(3)	23(3)	-3(2)	9(2)	2(2)
C(9)	25(3)	33(3)	19(3)	-10(2)	3(2)	2(2)
C(10)	19(3)	39(3)	24(3)	-3(2)	1(2)	7(2)
C(11)	20(3)	30(3)	21(3)	4(2)	5(2)	5(2)
C(12)	19(3)	30(3)	18(2)	0(2)	9(2)	-3(2)
C(13)	15(2)	26(3)	21(3)	2(2)	6(2)	-1(2)
C(14)	21(3)	23(3)	22(3)	3(2)	0(2)	0(2)
C(15)	21(3)	22(3)	37(3)	-4(2)	3(2)	3(2)
C(16)	23(3)	31(3)	30(3)	-8(2)	13(2)	1(2)
C(17)	23(3)	21(3)	25(3)	-2(2)	5(2)	-6(2)
C(18)	14(2)	19(3)	30(3)	-6(2)	6(2)	-4(2)
C(19)	14(3)	27(3)	29(3)	1(2)	5(2)	0(2)
C(20)	37(3)	29(3)	36(3)	-1(3)	4(3)	7(3)
C(21)	47(4)	50(4)	28(3)	11(3)	4(3)	8(3)
C(22)	39(3)	61(4)	28(3)	-2(3)	0(3)	-10(3)
C(23)	55(4)	42(4)	38(4)	-6(3)	-6(3)	-13(3)
C(24)	40(3)	39(4)	38(3)	-8(3)	-4(3)	-6(3)
C(25)	16(3)	27(3)	26(3)	-1(2)	3(2)	0(2)
C(26)	28(3)	29(3)	27(3)	-2(2)	3(2)	0(2)
C(27)	35(3)	20(3)	48(4)	2(3)	-1(3)	6(2)
C(28)	32(3)	35(3)	48(4)	-13(3)	13(3)	5(3)
C(29)	48(4)	47(4)	37(3)	-2(3)	19(3)	11(3)
C(30)	33(3)	33(3)	34(3)	4(2)	16(2)	4(2)
C(31)	17(3)	26(3)	25(3)	5(2)	2(2)	5(2)
C(32)	35(3)	25(3)	34(3)	-1(3)	18(2)	1(2)
C(33)	40(3)	37(3)	35(3)	9(3)	19(3)	5(3)
C(34)	29(3)	38(4)	48(4)	14(3)	13(3)	1(2)
C(35)	51(4)	34(3)	40(4)	4(3)	11(3)	-5(3)
C(36)	44(3)	34(3)	41(3)	4(3)	16(3)	-6(3)
C(37)	12(5)	44(7)	31(6)	-10(6)	15(4)	-10(5)
C(38)	22(5)	27(6)	42(6)	0(5)	1(5)	-1(4)
C(39)	15(5)	35(7)	32(6)	-4(6)	-4(4)	3(5)
C(40)	18(5)	28(6)	31(6)	3(5)	7(5)	-3(4)
C(41)	26(5)	33(6)	42(7)	3(6)	10(5)	-2(5)
C(37')	21(5)	29(6)	31(6)	6(5)	9(5)	4(4)
C(38')	18(5)	24(6)	26(6)	4(5)	6(4)	0(4)
C(39')	13(5)	33(6)	31(6)	4(5)	10(4)	-5(5)
C(40')	17(5)	23(5)	28(6)	-5(5)	2(5)	-6(4)
C(41')	10(5)	26(6)	28(5)	6(5)	14(4)	1(5)
C(42)	21(3)	22(3)	27(3)	7(2)	2(2)	5(2)
C(43)	29(3)	26(3)	35(3)	3(2)	9(2)	-4(2)
C(44)	33(3)	35(3)	33(3)	8(2)	18(2)	9(2)
C(45)	19(3)	34(3)	36(3)	16(3)	11(2)	-1(2)
C(46)	24(3)	35(3)	29(3)	12(3)	-5(2)	-4(2)
C(47)	28(3)	38(3)	19(3)	0(2)	4(2)	-7(2)
C(48)	22(3)	27(3)	19(2)	0(2)	11(2)	-4(2)
C(49)	21(3)	25(3)	24(3)	1(2)	9(2)	2(2)
C(50)	36(3)	26(3)	24(3)	2(2)	15(2)	8(2)

C(51)	39(3)	23(3)	27(3)	-1(2)	13(2)	-6(2)
C(52)	23(3)	39(3)	27(3)	1(2)	6(2)	-10(2)
C(53)	19(3)	28(3)	18(3)	4(2)	8(2)	0(2)
C(54)	16(2)	21(3)	24(3)	-1(2)	6(2)	-1(2)
C(55)	26(3)	24(3)	30(3)	-4(2)	8(2)	2(2)
C(56)	25(3)	32(3)	33(3)	5(2)	12(2)	-3(2)
C(57)	25(3)	36(3)	19(3)	-2(2)	6(2)	5(2)
C(58)	25(3)	27(3)	31(3)	-5(2)	5(2)	2(2)
C(59)	23(3)	30(3)	29(3)	3(2)	7(2)	-2(2)
C(60)	29(3)	19(3)	23(3)	-7(2)	6(2)	-5(2)
C(61)	28(3)	27(3)	30(3)	-3(2)	7(2)	-1(2)
C(62)	47(4)	30(3)	25(3)	5(2)	7(2)	3(3)
C(63)	30(3)	33(3)	35(3)	-5(3)	-4(2)	13(2)
C(64)	20(3)	37(3)	35(3)	-3(3)	3(2)	4(2)
C(65)	28(3)	25(3)	29(3)	-3(2)	9(2)	-3(2)
N(1)	90(5)	51(4)	117(6)	-17(4)	25(4)	-10(4)
C(66)	47(4)	46(4)	60(4)	-15(4)	14(3)	-7(3)
C(67)	36(3)	68(5)	58(4)	-9(4)	19(3)	-3(3)
N(2)	52(4)	63(4)	65(4)	-4(3)	18(3)	2(3)
C(68)	38(4)	49(4)	34(3)	-4(3)	18(3)	-17(3)
C(69)	29(3)	90(5)	43(4)	10(3)	16(3)	-5(3)
N(3)	59(4)	53(4)	51(3)	-1(3)	27(3)	-5(3)
C(70)	40(4)	47(4)	38(4)	-4(3)	18(3)	-14(3)
C(71)	64(5)	54(4)	71(5)	-11(4)	22(4)	-11(3)
N(4)	75(4)	55(4)	68(4)	-11(3)	31(3)	-1(3)
C(72)	49(4)	30(3)	39(4)	1(3)	5(3)	-8(3)
C(73)	51(4)	44(4)	44(4)	4(3)	15(3)	7(3)

Table 5. Hydrogen coordinates ($\times 10^4$) and isotropic displacement parameters ($\text{\AA}^2 \times 10^3$) for $[\text{CpFeP}(\text{C}_6\text{H}_4\text{F})(\text{C}_6\text{H}_4)\text{P}(\text{C}_6\text{H}_4\text{F})(\text{C}_6\text{H}_4)\text{P}(\text{C}_6\text{H}_5)(\text{C}_6\text{H}_4)][\text{PF}_6]$

	x	y	z	U(eq)
H(2)	3703	4416	-993	27
H(3)	4522	5756	-911	31
H(4)	4619	6676	-211	31
H(5)	3906	6272	439	27
H(8)	4166	5548	1360	28
H(9)	5263	4921	1993	31
H(10)	5360	3365	2108	34
H(11)	4393	2391	1583	28
H(14)	4349	1363	795	27
H(15)	5258	918	261	33
H(16)	5049	1521	-551	32
H(17)	3977	2629	-826	28

H(21)	879	4246	-1973	51
H(22)	717	2746	-2257	53
H(23)	1411	1575	-1733	57
H(24)	2224	1908	-926	49
H(27)	1216	7589	390	43
H(28)	1072	7635	1226	46
H(29)	1699	6510	1796	51
H(30)	2466	5312	1518	38
H(33)	2010	1230	2090	43
H(34)	1605	-123	1650	45
H(35)	1821	-288	832	50
H(36)	2398	901	445	46
H(37)	952	4097	945	33
H(38)	747	5012	133	37
H(39)	623	3905	-597	35
H(40)	752	2306	-237	31
H(41)	955	2424	716	40
H(37')	817	4721	609	32
H(38')	637	4606	-343	26
H(39')	706	2937	-569	29
H(40')	928	2021	243	28
H(41')	997	3124	971	24
H(43)	6483	1710	2510	35
H(44)	5113	1471	2694	38
H(45)	4057	585	2140	35
H(46)	4405	-17	1415	37
H(47)	5767	236	1237	34
H(49)	6474	2921	1517	27
H(50)	6821	4387	1779	33
H(51)	8107	4690	2393	35
H(52)	9037	3479	2713	35
H(53)	8699	2013	2431	25
H(55)	7172	2421	880	32
H(56)	7018	2146	31	35
H(57)	6971	664	-279	32
H(58)	7075	-552	290	33
H(59)	7268	-275	1148	33
H(61)	7306	-65	2518	34
H(62)	8407	-985	2968	41
H(63)	9814	-960	2792	41
H(64)	10075	-29	2143	37
H(65)	8961	868	1684	32
H(67A)	504	-1026	-332	79
H(67B)	1176	-725	-671	79
H(67C)	196	-1019	-936	79
H(69A)	-1396	3457	1417	79
H(69B)	-1291	3048	886	79
H(69C)	-725	3914	1122	79
H(71A)	4059	1651	-1726	93
H(71B)	3873	1769	-2328	93
H(71C)	3074	1607	-2055	93
H(73A)	7179	1270	-1579	68
H(73B)	6945	2001	-2026	68
H(73C)	6303	1158	-2010	68

Table 1. Crystal data and structure refinement for
[CpFeAs(C₆H₄F)(C₆H₄)As(C₆H₄F)(C₆H₄)As(C₆H₅)(C₆H₄)] [PF₆]

Identification code	02SRC311
Empirical formula	C73 H62 As3 B F2 Fe N4 [Fe(C ₅ H ₅)(C ₃₆ H ₂₅ F ₂ As ₃), B(C ₆ H ₅) ₄ , 4(CH ₃ CN)]
Formula weight	1324.69
Temperature	120(2) K
Wavelength	0.71073 Å
Crystal system	Monoclinic
Space group	P 21/c
Unit cell dimensions	a = 15.6500(3) Å alpha = 90 deg. b = 14.7771(4) Å beta = 102.417(2) deg. c = 27.3245(5) Å gamma = 90 deg.
Volume	6171.3(2) Å ³
Z	4
Density (calculated)	1.426 Mg/m ³
Absorption coefficient	1.894 mm ⁻¹
F(000)	2704
Crystal size	0.16 x 0.10 x 0.01 mm
Theta range for data collection	2.95 to 25.00 deg.
Index ranges	-18 ≤ h ≤ 18, -16 ≤ k ≤ 17, 0 ≤ l ≤ 32
Reflections collected	17757
Independent reflections	10828 [R(int) = 0.0451]
Absorption correction	Semi-empirical from equivalents
Max. and min. transmission	0.9813 and 0.7515
Refinement method	Full-matrix least-squares on F ²
Data / restraints / parameters	10828 / 36 / 761

Goodness-of-fit on F^2 0.990
Final R indices [$I > 2\sigma(I)$] $R1 = 0.0707$, $wR2 = 0.2097$
R indices (all data) $R1 = 0.1101$, $wR2 = 0.2360$
Largest diff. peak and hole 1.864 and -1.803 e.A⁻³

Table 3. Bond lengths [Å] and angles [deg] for
CpFeAs(C₆H₄F)(C₆H₄)As(C₆H₄F)(C₆H₄)As(C₆H₅)(C₆H₄)][PF₆]

Fe(1)-C(2)	2.025(7)	Fe(1)-C(3)	2.059(7)
Fe(1)-C(1)	2.068(7)	Fe(1)-C(4)	2.120(8)
Fe(1)-C(5)	2.126(8)	Fe(1)-As(3)	2.2095(14)
Fe(1)-As(1)	2.2251(13)	Fe(1)-As(2)	2.2339(12)
As(1)-C(6)	1.902(7)	As(1)-C(41)	1.911(7)
As(1)-C(12)	1.928(6)	As(2)-C(18)	1.890(7)
As(2)-C(24)	1.918(7)	As(2)-C(17)	1.925(7)
As(3)-C(30)	1.874(7)	As(3)-C(36)	1.901(7)
As(3)-C(29)	1.910(7)	F(1)-C(11)	1.300(9)
F(2)-C(19)	1.279(11)	F(3)-C(35)	1.287(11)
C(1)-C(2)	1.4200	C(1)-C(5)	1.4200
C(2)-C(3)	1.4200	C(3)-C(4)	1.4200
C(4)-C(5)	1.4200	C(6)-C(11)	1.373(11)
C(6)-C(7)	1.386(10)	C(7)-C(8)	1.384(11)
C(8)-C(9)	1.368(12)	C(9)-C(10)	1.363(11)
C(10)-C(11)	1.372(12)	C(12)-C(17)	1.383(9)
C(12)-C(13)	1.396(10)	C(13)-C(14)	1.371(10)
C(14)-C(15)	1.400(10)	C(15)-C(16)	1.354(10)
C(16)-C(17)	1.401(9)	C(18)-C(19)	1.357(11)
C(18)-C(23)	1.407(11)	C(19)-C(20)	1.411(12)
C(20)-C(21)	1.379(13)	C(21)-C(22)	1.385(13)
C(22)-C(23)	1.378(11)	C(24)-C(25)	1.397(9)
C(24)-C(29)	1.416(9)	C(25)-C(26)	1.372(10)
C(26)-C(27)	1.397(10)	C(27)-C(28)	1.395(10)
C(28)-C(29)	1.375(10)	C(30)-C(35)	1.382(10)
C(30)-C(31)	1.384(11)	C(31)-C(32)	1.395(11)
C(32)-C(33)	1.392(11)	C(33)-C(34)	1.375(12)
C(34)-C(35)	1.380(12)	C(36)-C(41)	1.391(10)
C(36)-C(37)	1.397(10)	C(37)-C(38)	1.398(11)
C(38)-C(39)	1.383(11)	C(39)-C(40)	1.398(10)
C(40)-C(41)	1.411(10)	B(1)-C(60)	1.628(11)
B(1)-C(42)	1.644(11)	B(1)-C(54)	1.650(11)
B(1)-C(48)	1.656(9)	C(42)-C(47)	1.414(10)
C(42)-C(43)	1.422(10)	C(43)-C(44)	1.366(11)
C(44)-C(45)	1.396(11)	C(45)-C(46)	1.378(11)
C(46)-C(47)	1.396(11)	C(48)-C(53)	1.385(10)
C(48)-C(49)	1.401(10)	C(49)-C(50)	1.395(10)
C(50)-C(51)	1.383(11)	C(51)-C(52)	1.369(11)
C(52)-C(53)	1.421(10)	C(54)-C(55)	1.373(10)
C(54)-C(59)	1.412(10)	C(55)-C(56)	1.399(10)
C(56)-C(57)	1.399(11)	C(57)-C(58)	1.372(11)
C(58)-C(59)	1.394(11)	C(60)-C(65)	1.408(10)
C(60)-C(61)	1.409(10)	C(61)-C(62)	1.375(11)
C(62)-C(63)	1.409(11)	C(63)-C(64)	1.383(11)
C(64)-C(65)	1.368(11)	N(1)-C(67)	1.119(11)
C(66)-C(67)	1.472(12)	N(2)-C(69)	1.128(12)
C(68)-C(69)	1.489(14)	N(3)-C(71)	1.115(11)
C(70)-C(71)	1.445(13)	N(4)-C(73)	1.138(13)
C(72)-C(73)	1.433(14)		
C(2)-Fe(1)-C(3)	40.69(13)	C(2)-Fe(1)-C(1)	40.58(13)

C(3)-Fe(1)-C(1)	67.67(16)	C(2)-Fe(1)-C(4)	67.27(16)
C(3)-Fe(1)-C(4)	39.70(13)	C(1)-Fe(1)-C(4)	66.53(17)
C(2)-Fe(1)-C(5)	67.17(16)	C(3)-Fe(1)-C(5)	66.59(17)
C(1)-Fe(1)-C(5)	39.56(13)	C(4)-Fe(1)-C(5)	39.08(13)
C(2)-Fe(1)-As(3)	132.1(2)	C(3)-Fe(1)-As(3)	161.2(2)
C(1)-Fe(1)-As(3)	97.3(2)	C(4)-Fe(1)-As(3)	125.0(2)
C(5)-Fe(1)-As(3)	94.7(2)	C(2)-Fe(1)-As(1)	93.9(2)
C(3)-Fe(1)-As(1)	109.5(2)	C(1)-Fe(1)-As(1)	116.1(2)
C(4)-Fe(1)-As(1)	148.0(2)	C(5)-Fe(1)-As(1)	155.6(2)
As(3)-Fe(1)-As(1)	86.86(5)	C(2)-Fe(1)-As(2)	140.6(2)
C(3)-Fe(1)-As(2)	102.4(2)	C(1)-Fe(1)-As(2)	156.8(2)
C(4)-Fe(1)-As(2)	92.22(19)	C(5)-Fe(1)-As(2)	117.6(2)
As(3)-Fe(1)-As(2)	87.22(5)	As(1)-Fe(1)-As(2)	86.78(4)
C(6)-As(1)-C(4)	104.5(3)	C(6)-As(1)-C(12)	106.8(3)
C(4)-As(1)-C(12)	103.2(3)	C(6)-As(1)-Fe(1)	121.7(2)
C(4)-As(1)-Fe(1)	109.4(2)	C(12)-As(1)-Fe(1)	109.7(2)
C(18)-As(2)-C(24)	104.4(3)	C(18)-As(2)-C(17)	108.2(3)
C(24)-As(2)-C(17)	102.2(3)	C(18)-As(2)-Fe(1)	121.2(2)
C(24)-As(2)-Fe(1)	109.45(19)	C(17)-As(2)-Fe(1)	109.6(2)
C(30)-As(3)-C(36)	107.4(3)	C(30)-As(3)-C(29)	105.6(3)
C(36)-As(3)-C(29)	101.3(3)	C(30)-As(3)-Fe(1)	120.1(2)
C(36)-As(3)-Fe(1)	110.1(2)	C(29)-As(3)-Fe(1)	110.6(2)
C(2)-C(1)-C(5)	108.0	C(2)-C(1)-Fe(1)	68.1(3)
C(5)-C(1)-Fe(1)	72.4(3)	C(3)-C(2)-C(1)	108.0
C(3)-C(2)-Fe(1)	70.9(3)	C(1)-C(2)-Fe(1)	71.3(3)
C(4)-C(3)-C(2)	108.0	C(4)-C(3)-Fe(1)	72.5(3)
C(2)-C(3)-Fe(1)	68.4(3)	C(5)-C(4)-C(3)	108.0
C(5)-C(4)-Fe(1)	70.7(3)	C(3)-C(4)-Fe(1)	67.8(3)
C(4)-C(5)-C(1)	108.0	C(4)-C(5)-Fe(1)	70.3(3)
C(1)-C(5)-Fe(1)	68.0(3)	C(11)-C(6)-C(7)	118.2(7)
C(11)-C(6)-As(1)	121.1(5)	C(7)-C(6)-As(1)	120.2(6)
C(8)-C(7)-C(6)	120.1(8)	C(9)-C(8)-C(7)	120.0(7)
C(10)-C(9)-C(8)	120.5(8)	C(9)-C(10)-C(11)	119.3(8)
F(1)-C(11)-C(10)	116.8(7)	F(1)-C(11)-C(6)	120.8(7)
C(10)-C(11)-C(6)	121.9(7)	C(17)-C(12)-C(13)	120.8(6)
C(17)-C(12)-As(1)	116.1(5)	C(13)-C(12)-As(1)	123.1(5)
C(14)-C(13)-C(12)	119.0(6)	C(13)-C(14)-C(15)	120.0(7)
C(16)-C(15)-C(14)	121.3(6)	C(15)-C(16)-C(17)	119.3(6)
C(12)-C(17)-C(16)	119.6(6)	C(12)-C(17)-As(2)	115.6(5)
C(16)-C(17)-As(2)	124.8(5)	C(19)-C(18)-C(23)	117.7(7)
C(19)-C(18)-As(2)	121.9(6)	C(23)-C(18)-As(2)	119.8(5)
F(2)-C(19)-C(18)	120.1(7)	F(2)-C(19)-C(20)	116.0(8)
C(18)-C(19)-C(20)	122.3(8)	C(21)-C(20)-C(19)	119.3(8)
C(20)-C(21)-C(22)	118.8(8)	C(23)-C(22)-C(21)	121.3(9)
C(22)-C(23)-C(18)	120.5(8)	C(25)-C(24)-C(29)	118.7(6)
C(25)-C(24)-As(2)	125.5(5)	C(29)-C(24)-As(2)	115.8(5)
C(26)-C(25)-C(24)	120.4(6)	C(25)-C(26)-C(27)	121.0(7)
C(28)-C(27)-C(26)	119.0(7)	C(29)-C(28)-C(27)	120.5(6)
C(28)-C(29)-C(24)	120.4(6)	C(28)-C(29)-As(3)	124.3(5)
C(24)-C(29)-As(3)	115.2(5)	C(35)-C(30)-C(31)	118.5(7)
C(35)-C(30)-As(3)	121.5(6)	C(31)-C(30)-As(3)	119.1(5)
C(30)-C(31)-C(32)	121.1(7)	C(33)-C(32)-C(31)	118.9(8)
C(34)-C(33)-C(32)	120.4(8)	C(33)-C(34)-C(35)	119.7(7)
F(3)-C(35)-C(34)	115.3(7)	F(3)-C(35)-C(30)	123.0(8)
C(34)-C(35)-C(30)	121.4(7)	C(41)-C(36)-C(37)	121.6(7)

C(41)-C(36)-As(3)	115.8(5)	C(37)-C(36)-As(3)	122.6(6)
C(36)-C(37)-C(38)	117.9(7)	C(39)-C(38)-C(37)	121.3(7)
C(38)-C(39)-C(40)	120.7(7)	C(39)-C(40)-C(41)	118.7(7)
C(36)-C(41)-C(40)	119.7(6)	C(36)-C(41)-As(1)	115.8(5)
C(40)-C(41)-As(1)	124.4(5)	C(60)-B(1)-C(42)	108.8(6)
C(60)-B(1)-C(54)	110.8(6)	C(42)-B(1)-C(54)	108.4(6)
C(60)-B(1)-C(48)	108.4(6)	C(42)-B(1)-C(48)	112.1(6)
C(54)-B(1)-C(48)	108.3(6)	C(47)-C(42)-C(43)	114.5(7)
C(47)-C(42)-B(1)	123.7(6)	C(43)-C(42)-B(1)	121.7(6)
C(44)-C(43)-C(42)	123.1(7)	C(43)-C(44)-C(45)	120.8(7)
C(46)-C(45)-C(44)	118.3(7)	C(45)-C(46)-C(47)	121.0(7)
C(46)-C(47)-C(42)	122.1(7)	C(53)-C(48)-C(49)	115.2(6)
C(53)-C(48)-B(1)	125.3(6)	C(49)-C(48)-B(1)	119.4(6)
C(50)-C(49)-C(48)	122.8(7)	C(51)-C(50)-C(49)	120.2(7)
C(52)-C(51)-C(50)	119.2(7)	C(51)-C(52)-C(53)	119.7(7)
C(48)-C(53)-C(52)	122.8(7)	C(55)-C(54)-C(59)	115.4(7)
C(55)-C(54)-B(1)	125.4(6)	C(59)-C(54)-B(1)	119.2(6)
C(54)-C(55)-C(56)	123.4(7)	C(55)-C(56)-C(57)	119.6(7)
C(58)-C(57)-C(56)	118.7(7)	C(57)-C(58)-C(59)	120.4(7)
C(58)-C(59)-C(54)	122.4(7)	C(65)-C(60)-C(61)	113.4(7)
C(65)-C(60)-B(1)	121.0(6)	C(61)-C(60)-B(1)	125.4(6)
C(62)-C(61)-C(60)	124.1(7)	C(61)-C(62)-C(63)	119.1(7)
C(64)-C(63)-C(62)	119.1(7)	C(65)-C(64)-C(63)	119.6(8)
C(64)-C(65)-C(60)	124.6(7)	N(1)-C(67)-C(66)	178.0(11)
N(2)-C(69)-C(68)	179.5(13)	N(3)-C(71)-C(70)	179.3(11)
N(4)-C(73)-C(72)	178.2(11)		

